# CHEMICAL ENGINEERING SCIENCE
## GENIE CHIMIQUE

VOL. 5 FEBRUARY 1956 No. 1




## The effect of a surface-active agent on mass transfer in falling drop extraction*


K. P. LINDLAND and S. G. TERJESEN

The Technical University of Norway, Chemical Engineering Laboratory, Trondheim, Norway



**Abstract**—The effect of small additions of sodium oleyl-*p*-anisidinesulphonate on the rate of extraction of iodine from aqueous solutions with 4·2 to 22·3 $mm^3$ falling droplets of carbon tetrachloride has been determined. The droplets were formed in a section of the column containing water and surface-active agent only, thus eliminating extraction during drop formation and securing a stationary adsorption state before the droplets entered the extraction column proper.

A maximum reduction in the overall mass transfer coefficient of 67 to 68% was observed for all droplet-sizes, with an addition of about $6 \times 10^{-5}$ g surface-active agent per 100 ml aqueous solution, whereas much larger additions were practically without further effect.

The results have been analysed in terms of an interfacial resistance coefficient $R_i$ sec/cm, which was found to be independent of the droplet size, and to obey the equation $C_S = 5{\cdot}4 \times 10^{-9} \frac{R_i}{\left(1 - \frac{R_i}{7400}\right)^{0{\cdot}1}}$ where $C_S$ is the aqueous concentration of surface-active agent in g/100 ml, and $R_i$ is calculated on a solvent basis. The equation is derived on the assumptions that the interfacial resistance is proportional to the interfacial concentration of surface-active agent, and that the adsorbed film is of the "vapour expanded" type. An adsorption isotherm for a "vapour expanded" film is given.

It is concluded that the results cannot easily be explained in terms of interfacial turbulence or transfer of turbulence, but that there is some kind of interaction between the adsorbed film and the diffusing solute, as postulated by HUTCHINSON [2] and GARNER and HALE [3].

The rate of fall of the droplets was also found to decrease sharply on the addition of small amounts of surface-active agent, the reduction amounting to 7 to 10% for all droplet sizes at about 2 to $3 \times 10^{-5}$ g per 100 ml. Much larger additions resulted in a more gradual decrease.

**Résumé**—Les auteurs ont étudié l'influence de petites additions d'oleyl-*p* anisidine sulfonate de sodium sur la vitesse d'extraction de l'iode à partir de solutions aqueuses dans lesquelles tombent des gouttelettes de $CCl_4$ de 4,2 à 22,3 mm 3 formées dans une section de la colonne contenant uniquement de l'eau et l'agent tensio-actif. On élimine ainsi toute extraction pendant leur formation et l'on assure dans la colonne d'extraction proprement dite état stationnaire avant que les gouttelettes n'y entrent.

Dans le cas d'une addition d'environ $6{\cdot}10^{-5}$ g. d'agent tensio-actif pour 100 moles de solution aqueuse, la réduction maximum du coefficient global de transfert de masse est de 67 à 68% quelles que soient les dimensions des gouttelettes ; des additions plus importantes n'ont pratiquement pas d'effet supplémentaire.

Le coefficient de résistance à l'interface $R_i$/sec/cm est indépendant de la dimension des gouttes et obéit à l'équation

$$C_S = 5.4 \times 10^{-9} \frac{R_i}{\left(1 - \frac{R_i}{7400}\right)^{0{\cdot}1}}$$


* A summary of this paper has appeared elsewhere [1].

où $C_S$ est la concentration aqueuse de l'agent tensio-actif en g/100 ml et $R_i$ est calculé sur la base du solvant.

Les auteurs supposent qu'à l'interface la résistance est proportionnelle à la concentration en agent tensio-actif et que le film adsorbé est du type " vapeur détendue." Ils donnent pour ce cas, un isotherme d'adsorption.

Ils concluent que les résultats s'expliquent difficilement par une turbulence à l'interface ou un transfert de turbulence mais qu'il y a plusieurs types d'interaction entre le film adsorbé et le soluté qui diffuse comme l'ont supposé Hutchinson, Garner et Hale.

La vitesse de chute des gouttes décroit nettement par addition de petites quantités d'agent tensio-actif, de 7 à 10%, quelles que soient leurs dimensions, pour environ 2 à 3 $\times$ $10^{-5}$ g/100 ml d'agent tensio-actif. Des additions plus importantes entrainent une diminution plus lente.

## INTRODUCTION

Increasing attention is being devoted to interfacial resistance to mass transfer processes, and the evidence collected indicates that in liquid-liquid extraction the Lewis and Whitman two-film concept (which forms the basis of conventional design methods) is not universally applicable. In addition to molecular and eddy diffusion, there is apparently in some cases a further resistance closely associated with the interface itself. This contention has been supported mainly by observations that additions of surface-active agents in some cases materially reduce the rate of extraction. Some investigators, however, have failed to find this effect, and HUTCHINSON [2] has reported that adsorbed films which retarded some species of diffusing molecules did not retard others. The most important papers on the effect of surface-active agents on the rate of extraction have been reviewed recently by GARNER and HALE [3], who have themselves provided strong evidence for the existence of interfacial resistance. MURDOCH and PRATT [4] have shown that the rate of transfer of uranyl nitrate from aqueous solutions to methyl-i-butyl ketone and dibutoxy-diethyl ether is partly determined by an interfacial resistance caused by a slow chemical reaction with the solvent molecules at the interface. The recent work of LEWIS [14] with a new type of transfer cell will be discussed later.

STUKE [6] has reported that some surface-active substances greatly reduce the rate of rise of oxygen bubbles through water. With increasing equivalent diameter of the bubbles, the rate of rise normally goes through a maximum at about 1·7 mm at 18°C, but with an addition of 5·2 $\times$ $10^{-3}$ g caproic acid per 100 ml this maximum disappears, and the rate of rise is reduced to less than half for this bubble diameter. Formic acid, on the other hand, had no such effect, even in concentrations which caused a twenty times greater reduction in surface tension.

In a previous paper HOLM and TERJESEN [1, 5] have shown that additions of 8 $\times$ $10^{-5}$ g per 100 ml of sodium oleyl-*p*-anisidinesulphonate reduced by about 40% the rate of transfer of iodine from an aqueous solution to carbon tetrachloride in a stirred extractor. These results pointed clearly to a surface resistance, but they were not susceptible to quantitative treatment, because the observed changes in the rates of extraction resulted from two opposing effects. The surface-active agent caused an increase in the interfacial area as well as a retardation of the rate of mass transfer per unit area, the latter effect predominating at concentrations below 8 $\times$ $10^{-5}$ g per 100 ml, and the former above.

In the present investigation, falling drops of carbon tetrachloride of known size were used. With the extremely low concentrations of surface-active agent, it is not safe to assume that a stationary adsorption state is rapidly established, and methods of correction for extraction during drop formation would be particularly uncertain. These difficulties have been overcome by forming the drops in a separate section of the column equipped with a rod type stirrer, and containing water and surface-active agent only. The drops were allowed to descend in a spiral path through this liquid under the action of the agitator before reaching the extraction section. It was also considered essential to prevent the liquids from coming into contact with rubber or similar materials. The rate of fall of the droplets in the extraction section was also noted in order to

ascertain any correlation between the effect of the surface-active agent on the rate of mass transfer and on the rate of fall.

In aqueous solutions of iodine, the surface-active agent was found to add two atoms of iodine, presumably at the double bond. It is therefore the effect of this iodinated compound which has been observed in these investigations.

## Apparatus and Procedure

The apparatus is shown diagrammatically in Fig. 1. The upper section, called the adsorption column, was provided with a rotating glass rod,

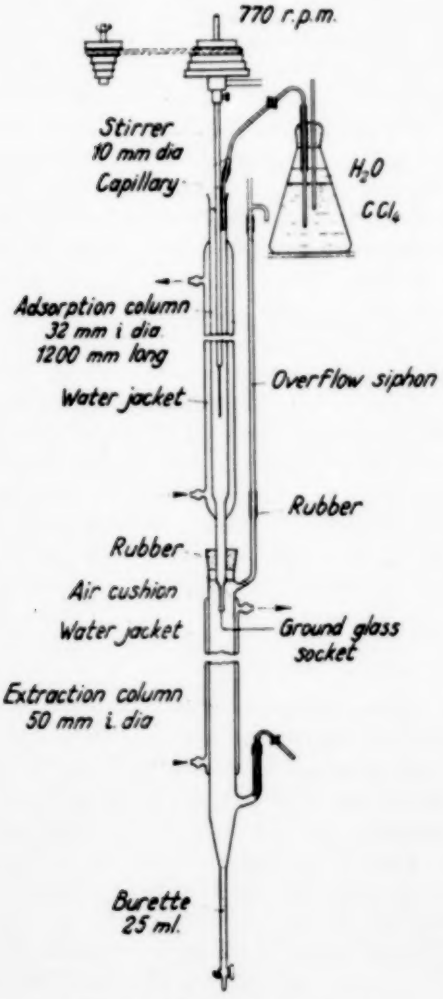


Fig. 1. Extraction apparatus.

and contained an aqueous solution of surface-active agent of the same concentration as used in the extraction column underneath. The bottom end of the adsorption column was gradually narrowed down to an internal diameter of 7 mm, and ended in a Pyrex 10/30 ground-glass joint fitted with a hollow plug. This plug could be pushed out by carefully lowering the glass rod, and would then float on the liquid in the extraction column. When the glass rod again was raised, an equivalent volume of water containing surface-active agent was added from a burette at the top, to prevent the iodine solution in the extraction column from penetrating into the adsorption column. The extraction column, which had an internal diameter of 50 mm, was available in three lengths, giving alternative extraction paths of 1430-1310, 940-830 and 580-440 mm, the ranges being due to the varying liquid level in the 25 ml burettes attached to the bottom of these columns. Both columns were provided with jackets for circulating water which was thermostatically controlled at 25·0°C. Accurate temperature control was essential for preventing thermal convection currents, which would cause mixing of the liquids in the two columns. One hour was allowed for establishing thermal equilibrium before the plug separating the two liquids was pushed out.

All rubber connections were so arranged that a cushion of air prevented the liquids from coming into contact with the rubber. The stop-cock on the burette was lubricated with glycerol and bentonite, whereas the one in the carbon tetrachloride feed line was not lubricated at all.

The arrangement for producing the drops can also been seen in Fig. 1. Carbon tetrachloride saturated with water was run from a constant head flask through a capillary which dipped into the liquid in the adsorption column. By adjusting the effective difference in level, and by using capillaries from 0·1 to 3 mm in diameter, the rate of formation of the drops was varied between 1 and 3 per sec, and the size of the drops between 4·2 and 22·3 $mm^3$. Some difficulties were, however, experienced in maintaining a constant drop size from one experiment to another.

During an experiment the drops were finally collected in the burette at the bottom of the

extraction column, and the liquid withdrawn for analysis. The aqueous phase remained stationary in the column during each experiment, and was sampled before and after. Only a very small fraction of the solute was extracted.

The drop volume was determined by counting the number of drops required to give a volume of 1 to 5 ml in the burette. The rate of fall of the drops was obtained by measuring with a stop-watch the time for a fall of 1,000 mm, and the average of 10 observations taken. With varying rates of drop formation the distance between the drops varied from 70 to 500 mm, but this did not noticeably affect the rate of fall.

## MATERIALS

The aqueous phase was not saturated with solvent before the experiments, as this was not found to influence the results. The solvent was, however, saturated with water.

The iodine used was "B.D.H. Laboratory Reagent, Resublimed." For each experiment a small amount was ground in a mortar, and dissolved in water under vigorous stirring to give a concentration between 180 and 210 mg iodine per litre, and finally filtered.

Carbon tetrachloride "Merck Puriss" was distilled in a packed column of 5-10 theoretical stages at a reflux ratio of about 10 : 1. The fraction boiling between 76·5 and 76·8°C was collected. Used solvent was regenerated by treatment with sodium thiosulphate followed by simple distillation.

Sodium oleyl-*p*-anisidinesulphonate was purified and dissolved in water, together with sodium sulphate and sodium chloride, as described previously [5].

## METHODS OF ANALYSIS

Solutions of iodine in water and carbon tetrachloride were analysed photometrically using a Beckman DU Quartz Spectrophotometer, the readings being taken at the absorption maxima, which were found to be located at 4,600 and 5,150 Å respectively. The calibration curves giving optical density as a function of concentration were straight lines through the origin for both solvents. Samples were kept in glass-stoppered bottles, and analysed as quickly as possible to avoid loss by evaporation. The formation of a compound between the iodine and the surface-active agent previously mentioned did not interfere with the analysis, due to the extremely low concentrations of surface-active agent used.

## END EFFECTS

Although the technique of forming the drops in solute-free aqueous phase eliminated the need to correct for extraction during the formation of the drops, the need to correct for extraction at the interface in the burette still remained. To determine the magnitude of this correction, it was not considered sufficient to observe the uptake of iodine by a stagnant volume of solvent in the burette, because the turbulence caused by the drops striking the interface would entail a higher rate of transfer during actual opertaing conditions. As the nearest approach to determining true correction factors, a series of experiments was carried out with drops of equal size but with differing frequencies of formation. By comparing the observed mass transfers with the values extrapolated to an infinitely high frequency of formation, it was found that an average of 2·4 mg of iodine per minute were transferred at the interface. With the longest column the correction amounted to less than 1% with drops of 22 $mm^3$ volume formed at a rate of 3 per second. Most of the experiments reported in this paper were carried out under conditions where this correction was insignificant.

## RESULTS

The effect of additions of surface-active agent on the rate of extraction was determined for three different droplet sizes, using the largest column where the droplets travelled an average distance of 137 cm. The experimental results have been summarized in Table 1. During a run, only between one and two per cent of the iodine in the aqueous phase was extracted, and it was sufficiently accurate to use an average concentration for the calculation of the approach to equilibrium, $p = \frac{C_E \times 100}{m \times C_{RA}}$. PEARCE and EVER-

*Table* 1. *Results with* 187 *cm average extraction length.*

| $C_S$ g/100 ml $\cdot 10^5$ | $v$ cm/sec | $C_R 0$ mg/ml | $C_R$ mg/ml | $C_E$ mg/ml | $p = \frac{C_E \cdot 100}{m \cdot C_{R_A}}$ | $f$ | $K_{E(h)} \cdot 10^5$ Dimensionless | $K_{E(t)} \cdot 10^{-5}$ cm/sec | $R_{i(h)} \cdot 10^{-5}$ Dimensionless | $R_{i(t)}\ 10^{-5}$ sec/cm |
|---|---|---|---|---|---|---|---|---|---|---|
| | Droplet volume : 22·8 mm³ ± 0·1, equivalent radius : 1·75 mm ± 0·005 | | | | | | | | | |
| 0 | 21·5 | 0·180 | 0·177 | 0·408 | 2·54 | 0·992 | 1·087 | 23·4 | 0 | 0 |
| 1 | 19·7 | 0·221 | 0·218 | 0·332 | 1·68 | 0·992 | 0·715 | 14·1 | 0·48 | 0·028 |
| 2 | 20·0 | 0·200 | 0·188 | 0·247 | 1·42 | 0·992 | 0·604 | 12·1 | 0·74 | 0·040 |
| 3 | 19·7 | 0·198 | 0·196 | 0·235 | 1·33 | 0·992 | 0·565 | 11·1 | 0·85 | 0·047 |
| 5 | 19·7 | 0·190 | 0·188 | 0·179 | 1·05 | 0·992 | 0·445 | 8·76 | 1·33 | 0·071 |
| 6 | 19·7 | 0·203 | 0·200 | 0·179 | 0·99 | 0·991 | 0·420 | 8·27 | 1·46 | 0·078 |
| 7 | 19·7 | 0·203 | 0·202 | 0·183 | 1·01 | 0·991 | 0·428 | 8·34 | 1·42 | 0·077 |
| 10 | 19·7 | 0·206 | 0·204 | 0·190 | 1·03 | 0·991 | 0·437 | 8·60 | 1·37 | 0·074 |
| 20 | 19·2 | 0·214 | 0·212 | 0·199 | 1·04 | 0·990 | 0·445 | 8·55 | 1·33 | 0·074 |
| 50 | 16·6 | 0·216 | 0·214 | 0·204 | 1·06 | 0·968 | 0·447 | 7·42 | 1·32 | 0·092 |
| 80 | 15·8 | 0·206 | 0·205 | 0·211 | 1·14 | 0·978 | 0·476 | 7·52 | 1·18 | 0·090 |
| | Droplet volume : 9·5 mm³ ± 0·1, equivalent radius : 1·32 mm ± 0·01 | | | | | | | | | |
| 0 | 19·3 | 0·200 | 0·199 | 0·822 | 4·58 | 0·996 | 1·504 | 29·0 | 0 | 0 |
| 1 | 18·4 | 0·186 | 0·183 | 0·534 | 3·22 | 0·996 | 1·048 | 19·2 | 0·29 | 0·018 |
| 2 | 17·9 | 0·192 | 0·190 | 0·423 | 2·46 | 0·996 | 0·799 | 14·3 | 0·59 | 0·035 |
| 5 | 17·4 | 0·206 | 0·205 | 0·314 | 1·70 | 0·996 | 0·549 | 9·55 | 1·16 | 0·070 |
| 10 | 17·9 | 0·181 | 0·178 | 0·262 | 1·625 | 0·996 | 0·525 | 9·40 | 1·24 | 0·072 |
| 25 | 17·4 | 0·184 | 0·183 | 0·270 | 1·64 | 0·995 | 0·529 | 9·20 | 1·28 | 0·072 |
| 50 | 16·4 | 0·177 | 0·175 | 0·271 | 1·715 | 0·993 | 0·552 | 9·05 | 1·15 | 0·076 |
| 50 | 16·4 | 0·181 | 0·177 | 0·263 | 1·635 | 0·993 | 0·527 | 8·63 | 1·23 | 0·081 |
| 80 | 15·3 | 0·206 | 0·205 | 0·314 | 1·70 | 0·984 | 0·542 | 8·29 | 1·18 | 0·086 |
| | Droplet volume : 4·2 mm³ ± 0·2, equivalent radius : 1·00 mm ± 0·02 | | | | | | | | | |
| 0 | 16·6 | 0·183 | 0·188 | 1·160 | 6·95 | 0·999 | 1·751 | 29·1 | 0 | 0 |
| 0 | 17·1 | 0·205 | 0·204 | 1·117 | 6·07 | 0·999 | 1·522 | 26·0 | – | – |
| 2 | 16·0 | 0·192 | 0·190 | 0·643 | 3·75 | 0·999 | 0·927 | 14·9 | 0·51 | 0·033 |
| 5 | 16·0 | 0·200 | 0·198 | 0·454 | 2·54 | 0·998 | 0·625 | 10·0 | 1·03 | 0·066 |
| 10 | 15·7 | 0·202 | 0·200 | 0·448 | 2·48 | 0·998 | 0·610 | 9·58 | 1·07 | 0·070 |
| 25 | 15·3 | 0·203 | 0·202 | 0·445 | 2·44 | 0·997 | 0·600 | 9·18 | 1·10 | 0·075 |
| 50 | 14·8 | 0·189 | 0·186 | 0·428 | 2·54 | 0·995 | 0·623 | 9·22 | 1·03 | 0·074 |
| 80 | 14·8 | 0·211 | 0·211 | 0·486 | 2·56 | 0·988 | 0·624 | 8·92 | 1·03 | 0·078 |

SOLE [7] have found that the partition coefficient for iodine between water and carbon tetrachloride is independent of the iodine concentration up to 0·248 g per 1,000 g of aqueous phase. They give the value of $m = 88{\cdot}7 \frac{\text{mg iodine per ml of solvent phase}}{\text{mg iodine per ml of aqueous phase}}$ at 25°C. Recently DAVIES and GWYNNE [8] have reported the value of 89·9 at this temperature, and this value has been used in the present calculations.

The overall mass-transfer coefficients can be expressed either on the basis of the distance travelled by the droplets, or on the basis of the time of contact :

$$dN = K_{E(h)} (C^*_E - C_E) \cdot A \cdot dh = \\ = K_{E(t)} (C^*_E - C_E) \cdot A \cdot dt \quad (1)$$

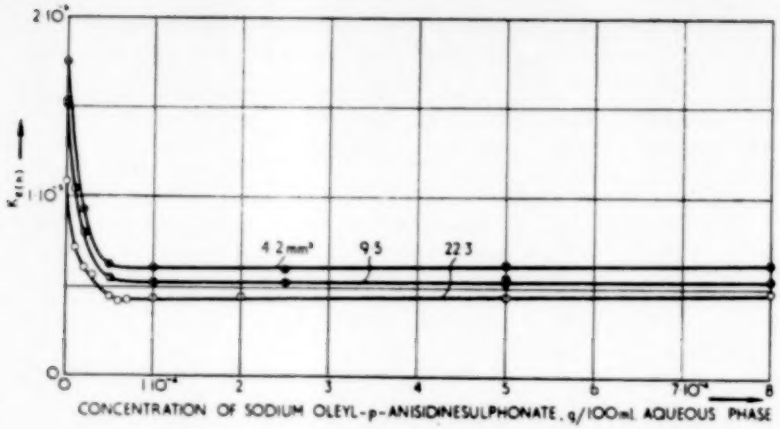


FIG. 2. Overall extraction coefficients on a height and solvent basis, plotted against concentration of surface-active agent for 3 droplet sizes.

or integrated :

$$K_{E(h)} = -\frac{V}{A \cdot h} \ln\left(1 - \frac{p}{100}\right) \qquad (2)$$

$$K_{E(t)} = -\frac{V}{A \cdot t} \ln\left(1 - \frac{p}{100}\right) \qquad (3)$$

It is seen that

$$K_{E(t)} = v\, K_{E(h)} \qquad (4)$$

where $v$ is the droplet velocity. The droplets are assumed to have the form of an oblate ellipsoid, and it is convenient to express the ratio of droplet volume to surface by means of the radius of a sphere of volume $V$, multiplied by a correction factor which allows for the departure from the spherical form :

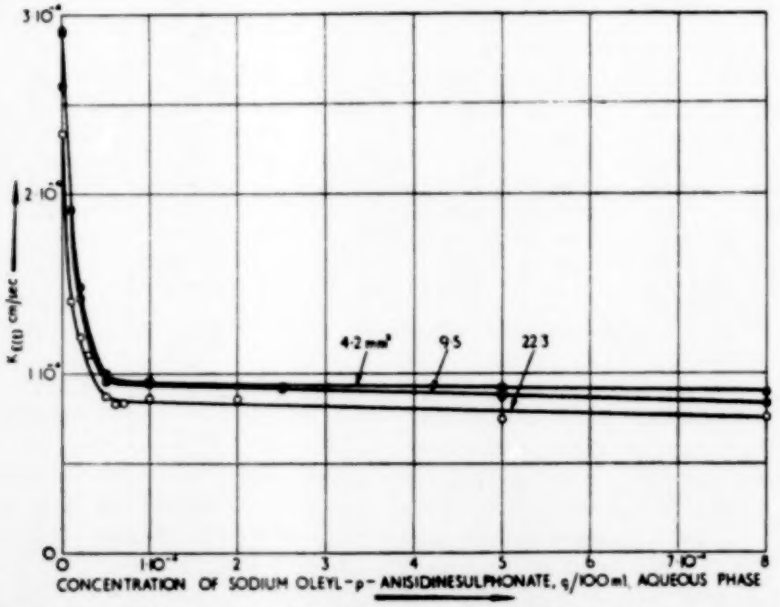


FIG. 3. Overall extraction coefficients on a time and solvent basis, plotted against concentration of surface-active agent for 3 droplet sizes.

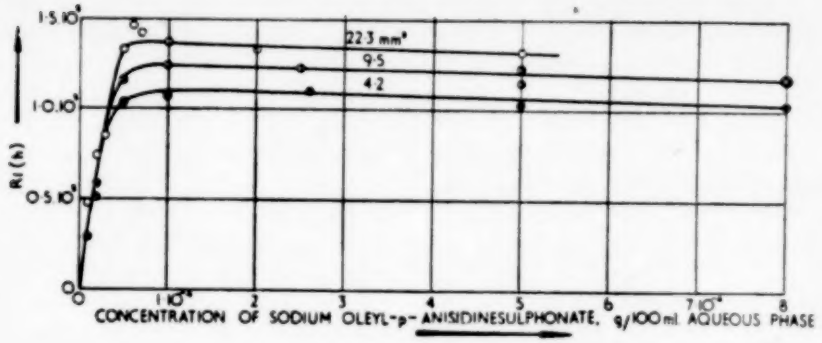


FIG. 4. Interfacial resistances on a height and solvent basis, plotted against concentration of surface-active agent for 3 droplet sizes.

$$K_{E(h)} = -\frac{r \cdot f}{3 \cdot k} \ln\left(1 - \frac{p}{100}\right) \quad (5)$$

$$K_{E(t)} = -\frac{r \cdot f}{3t} \ln\left(1 - \frac{p}{100}\right) \quad (6)$$

where

$$f = \frac{2\sqrt[3]{\frac{b}{a}}}{1 + \left(\frac{b}{a}\right)^2 \frac{1}{\sqrt{1 - \left(\frac{b}{a}\right)^2}} \ln \frac{1 + \sqrt{1 - \left(\frac{b}{a}\right)^2}}{\left(\frac{b}{a}\right)}} \quad (7)$$

where $a$ and $b$ are the long and short axis of the ellipsoid. The droplets were photographed and $a$ and $b$ measured [9]. The resulting correction factors given in column 7 in Table 1 differ from unity by less than 1% in most cases. Correction for droplet deformation has been reported also by HEERTJES, HOLVE and TALSMA [11].

In the presence of the surface-active agent the rate of mass transfer is reduced considerably. It is mathematically convenient to define an interfacial resistance which is additional to the diffusional resistances in the two liquid phases. On an extract basis the equations are :

$$dN = \frac{1}{R_{i(h)}} (mC_{Ri} - C_{Ei}) \cdot A \cdot dh$$

$$= \frac{1}{R_{i(t)}} (mC_{Ri} - C_{Ei}) \cdot A \cdot dt \quad (8)$$

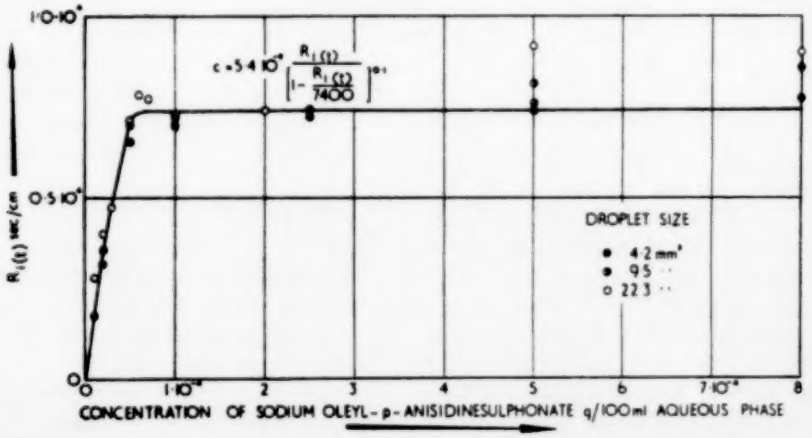


FIG. 5. Interfacial resistances on a time and solvent basis, plotted against concentration of surface-active agent for 3 droplet sizes.

The interfacial resistance as defined by equation (8) includes any interfacial resistance that may be present in the absence of the surface-active agent, whereas the resistance calculated from (9), below, as a difference between the overall resistances, measured with and without the addition, expresses the contribution made by the surface-active agent only.

$$R_i = \frac{1}{K_{E(\text{with})}} - \frac{1}{K_{E(\text{without})}} \qquad (9)$$

The overall coefficients as well as the interfacial resistances are given in Table 1 both on a height and time basis, and are plotted against concentration of surface-active agent in Figs. 2, 3, 4 and 5. In Fig. 6 the velocity of the falling droplets is plotted, also against concentration of surface-active agent.

The reason for using the distance travelled by the droplets as a basis for the results, as well as the actual extraction time, is the somewhat irregular behaviour of the latter observed at high concentrations of surface-active agent. As pointed out by COULSON and SKINNER [10] however, the actual time of fall must be expected to be more important than the height.

It will be noted that the coefficients are all given on an extract (solvent) basis, and that the extraction and resistance coefficients on a raffinate basis can be obtained by respectively multiplying and dividing by the partition coefficient. Of the two liquid films, the aqueous will offer by far the greatest resistance to the transfer of iodine due to the magnitude of the partition coefficient.

## DISCUSSION

The results show that an addition of surface-active agent of $10^{-4}$ g/100 ml of the aqueous phase has reduced the overall extraction coefficient to a value which is only 32 to 38% of the original. The percentage reduction appears to be practically independent of droplet size within the range investigated. Further additions of surface-active agent exerted only a very small effect on the extraction coefficient, giving a slight increase if calculated on a height basis, and a slight decrease on a time basis. Up to about $6 \cdot 10^{-5}$ g/100 ml there is a rapid fall.

The results obtained are similar to those of GARNER and HALE [3], who found that $1 \cdot 5 \times 10^{-2}$ ml/100 ml of the surface-active agent *Teepol* reduced the rate of extraction of diethylamine from toluene drops by water to 45% of the original value. The present results differ from those of GARNER and HALE [3] in three respects: the maximum reduction in the rate of extraction occurred with a concentration of surface-active agent which is about 250 times smaller than theirs, the reduction was 67 to 68% against their 55%, and further additions of surface-active agent were practically without effect, whereas they found a marked increase in the rate of extraction.

In the present investigation it has been possible to analyse the results in terms of an interfacial resistance coefficient $R_i$, which is given in Fig. 4 on a height basis and in Fig. 5 on a time basis. For not too high concentrations of surface-active agent, a single curve was obtained when the resistance coefficient based on the extraction time was plotted in Fig. 5 against the concentration of the surface active agent for the three droplet sizes 4·2, 9·5 and 22·3 $mm^3$. This result indicates that the interfacial resistance is independent of droplet size within the range investigated. It can be seen from Fig. 5 that at about $6 \times 10^{-5}$ g/100 ml the interfacial resistance reaches a constant value of 7,400 sec/cm (82 sec/cm), the figure in brackets indicating the corresponding value on a raffinate, i.e., aqueous basis. This compares with an overall resistance, without addition of surface-active agent, of 10,600 (118) and 11,900 (182) sec/cm for the smallest and largest drops respectively. The interfacial resistance thus amounts to 69 and 62% of the resistance without the addition for the smallest and largest droplets.

### *A theory of interfacial resistance*

GARNER and HALE [3] have shown that the maximum reduction in the rate of extraction occurred at a concentration of surface-active agent which produced only a comparatively small reduction in the interfacial tension. They concluded that there was no direct connection between the two phenomena. For the present system, MELHUS and TERJESEN [9] have also failed to find any direct correspondence between

interfacial resistance and reduction in surface tension.

The increase in the resistance to mass transfer on the addition of the surface-active agent occurred at very low concentrations, and it is inconceivable that this effect can be caused by anything but a layer of surface-active molecules adsorbed at the interface. The sharp rise in interfacial resistance followed by an almost perfect levelling off, as shown in Fig. 5, strongly suggests that the interfacial layer of surface-active molecules was almost completed when the bulk concentration reached about $6 \times 10^{-5}$ g/100 ml. This conclusion is at variance with that of GARNER and HALE [3], who state that the resistance to transfer reached a maximum when the interfacial concentration was far less than required for saturation.

A theory of interfacial resistance will be developed on the basis of the assumption that the resistance is proportional to the interfacial concentration of surface-active molecules. This point of view differs radically from that adopted by HUTCHINSON [2], and by GARNER and HALE [3].

The following assumptions are made with regard to the adsorption of surface-active molecules at the interface :

1. The adsorbed film is of the " vapour – expanded " type with strong cohesive forces.
2. The rate of adsorption on the free interfacial area is proportional to that area and to the bulk concentration :

$$k_c C_s (1 - A_0\Gamma)$$

3. Some of the surface-active molecules striking the covered areas are also adsorbed, and they find a place at the interface through adjustments in the film. The accommodation coefficient for the covered areas depends on the ease of this adjustment, and decreases rapidly with decreasing free interfacial area. This leads to the following expression for this contribution to the rate of adsorption :

$$k_c C_s (A_0\Gamma) (1 - A_0\Gamma)^n$$

4. Desorption can only take place at the covered areas, and the rate increases rapidly with the tension of the film. For an expanded film the tension increases slowly with surface cocentration when the free area is large, but very rapidly when the free area approaches zero. This leads to the following expression for the rate of desorption :

$$k_e (A_0\Gamma) (1 - A_0\Gamma)^{-m}$$

The concept of " vapour-expanded " films has been dealt with by ADAM [12], whereas MOILLIET and COLLIE [13] have stated that surface-active agents, such as efficient emulsifying agents, usually form films of a somewhat condensed nature.

The expressions given above for the rate of adsorption and desorption lead to the following adsorption isotherm :

$$C_s = \frac{k_e}{k_c} \frac{A_0\Gamma}{(1-A_0\Gamma)^{n+m}} \frac{1}{A_0\Gamma + (1-A_0\Gamma)^{1-n}} \quad (10)$$

It will be seen that this equation gives the Langmuir isotherm for $n = \infty$ and $m = 0$. To fit the data appertaining to expanded films, the values of $n$ and $m$ must be small, and the equation can be simplified to

$$C_s = \frac{k_e}{k_c} \cdot \frac{A_0\Gamma}{(1-A_0\Gamma)^{n+m}} \quad (11)$$

It has not been proved that a true adsorption equilibrium is always established on the surface of a falling droplet, and it is possible that the isotherm describes a stationary state rather than an equilibrium.

Assuming that the interfacial resistance is proportional to the covered fraction of the interface :

$$R_{i(t)} = (A_0\Gamma) R^1_{i(t)} \quad (12)$$

the following relation between interfacial resistance and bulk concentration of surface-active agent results :

$$C_s = K \frac{R_{i(t)}}{\left(1 - \frac{R_{i(t)}}{R^1_{i(t)}}\right)^{n+m}} \quad (13)$$

In this equation, $R^1_{i(t)}$ is the limiting value of the interfacial resistance, and equal to $7{\cdot}4 \times 10^3$

sec/cm, and $K$ the initial slope of the curve in Fig. 5, and equal to $5{\cdot}4 \times 10^{-9}$. The exponent was determined from a logarithmic plot of $\left(1 - \frac{R_{i(l)}}{R^1_{i(l)}}\right)$ against $K \frac{R_{i(l)}}{C_s}$, and found to be 0·1. The final equation :

$$C_s = 5{\cdot}4 \times 10^{-9} \frac{R_{i(l)}}{\left(1 - \frac{R_{i(l)}}{7400}\right)^{0{\cdot}1}}$$

is shown as the fully drawn curve in Fig. 5, and is seen to fit the experimental data very well.

*Interfacial resistance and the transfer of turbulence*

LEWIS [14] has recently reported an extensive study of individual coefficients with a new type of transfer cell with agitation in both liquid phases. He found that transfer took place by eddy, not molecular diffusion, and that the transfer coefficients for all phases except furfural could be correlated on one curve by plotting $\frac{k_1}{v_1}$ against $N_{Re\,1} + N_{Re\,2} \frac{n_2}{n_1}$. The turbulence on each side of the interface contributes to the coefficient, whereas the Schmidt number, which is characteristic of molecular diffusion, does not enter at all. LEWIS found that, while mobile films adsorbed at the interface had little effect, rigid protein films caused a retardation of transfer. He explained this as a result of suppression of the transfer of turbulence from one phase to the other, so that the term in the correlation involving the Reynolds number of the other phase drops out.

This explanation of the effect of interfacial films does not appear to apply to the present results. GARNER and SKELLAND [15] have shown that there is no internal circulation in droplets of carbon tetrachloride which fall through water when the Reynolds number is of the order encountered in the present investigation. But if there is no form of motion within the droplet, there can be no basis for the idea that the absorbed film suppresses the transfer of turbulence from one phase to another. Further evidence is obtained by calculating the droplet side-resistance on the assumption that the interior is stagnant. The curves given by HEERTJES, HOLVE and TALSMA [11], based on the equation of NEWMAN [16], were used, and the diffusion coefficient for iodine in carbon tetrachloride was estimated to be $1{\cdot}4 \times 10^{-5}$ cm$^2$/sec by the method of WILKE [17]. The resistance was calculated to be 0·6 to 0·7 sec/cm as compared with an observed interfacial resistance of 8 to $9 \times 10^3$ sec/cm. This result shows that even if complete transfer of turbulence to the droplets took place in the absence of surface-active agent, and the addition inhibited completely this transfer, the resulting reduction in the rate of mass-transfer would only be a small fraction of that actually observed.

These considerations show that the observed effect cannot be explained by assuming that the solvent side mass-transfer coefficient is reduced due to suppression of transfer of turbulence from the aqueous to the solvent phase. They do not, however, rule out the possibility that the adsorbed surface-active agent can give to the interface a certain rigidity, which could suppress the development of turbulence in the aqueous phase close to the interface, and thus reduce the mass-transfer coefficient on the aqueous side. On the other hand, the observation of GARNER and HALE [8] that surface-active agents can reduce the rate of mass-transfer, even if there is no original internal circulation in the droplets, indicates that there is no appreciable transfer of momentum across the interface, even in the absence of the surface-active agent. The evidence on this point is still inconclusive.

The spontaneous interfacial turbulence described by LEWIS and PRATT [18] still remains to be considered. When the transfer of material from one liquid phase to another was accompanied by evolution of heat, they observed vigorous turbulence and pulsations at the interface. This interfacial turbulence would undoubtedly greatly increase the rate of mass transfer, and it is conceivable that an adsorbed interfacial film might reduce or eliminate this turbulence. According to DAVIES and GWYNNE [8] however, the transfer of iodine from water to carbon tetrachloride is endothermic, and in such cases interfacial turbulence has not been reported. This explanation therefore does not seem to apply.

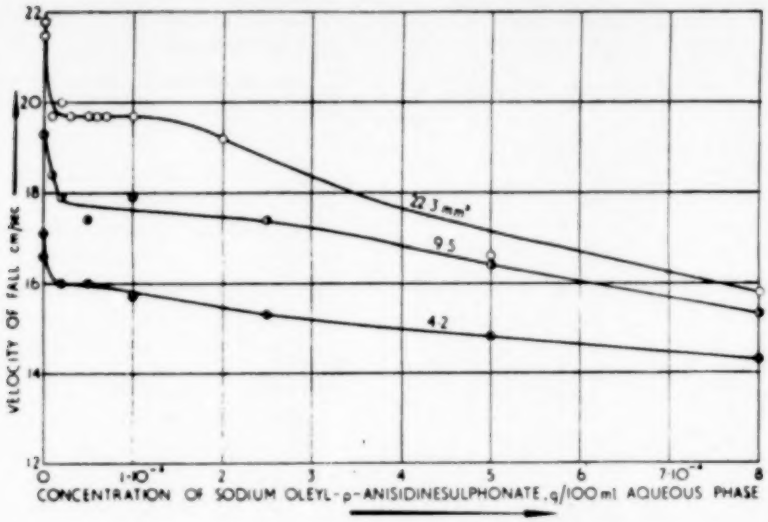


FIG. 6. Velocity of fall for 3 droplet sizes, plotted against concentration of surface-active agent.

*The nature of the interfacial resistance*

The preceding discussion indicates that the interfacial resistance may not be caused primarily by changes in the hydrodynamical conditions such as transfer of turbulence or interfacial turbulence. Some kind of interaction seems to occur between the adsorbed film of surface-active agent and the diffusing molecules. This interaction could be purely mechanical, or more specific, involving forces of a chemical or physical nature. HUTCHINSON [2] and GARNER and HALE [8] favour the latter hypothesis, but further work is required before a final conclusion can be drawn. A comparative study of the action of the same surface-active agent on different diffusing solutes is in progress in this laboratory. The present system is particularly suitable for such studies, because the interfacial resistance reaches a practically constant value after the addition of very small quantities of the surface-active agent. Although the mechanism of the retardation phenomenon is not yet known, the results of the present work show that the effect can be described in terms of an interfacial resistance proportional to the interfacial concentration of the surface-active agent.

*Retardation of the rate of droplet fall*

The retardation of the falling droplets caused by the addition of the surface-active agent is shown in Fig. 6, and is analogous to that reported by STUKE [6] for rising gas bubbles. The sharp primary retardation appears to reach its maximum value at a concentration of surface-active agent about one-third to one-half of that for the interfacial resistance. The present results throw no light on the nature of this effect, and no explanations can be offered in addition to that already put forward by STUKE.

**Acknowledgement**—The authors are indebted to the Royal Norwegian Council for Scientific and Industrial Research for a grant which has made this work possible.

NOTATION

$A$ = Interfacial area, cm²
$A_0$ = Effective cross-sectional area of adsorbed surface active molecules, cm²/g mol
$b/a$ = Ratio of short to long axis of ellipsoid
$C_E$ = Concentration of iodine in solvent phase, mg/cm³
$C_E^*$ = Equilibrium concentration in solvent phase, mg/cm³
$C_R$ = Concentration of iodine in aqueous phase, mg/cm³

$C_R'$ = Original concentration in aqueous phase mg/cm³
$C_{RA}$ = Average of initial and final concentration in aqueous phase mg/cm³
$C_S$ = Concentration of surface-active agent in aqueous phase g/100 ml
$f$ = Correction factor given by equation (7)
$h$ = Average effective column height cm
$K_{E(h)}$ = Overall transfer coefficient on a solvent and height basis dimensionless
$K_{E(t)}$ = Overall transfer coefficient on a solvent and time basis cm/sec
$k_e$ = Constant
$k_c$ = Constant
$m$ = Distribution coefficient : $\frac{\text{mg iodine per ml solvent phase}}{\text{mg iodine per ml aqueous phase}}$
$n$ = Constant
$N$ = Amount extracted mg
$N_{Re}$ = Reynolds number dimensionless
$p$ = Approach to equilibrium $\frac{C_E \cdot 100}{m \cdot C_{RA}}$ %
$R_{i(h)}$ = Interfacial resistance on a solvent and height basis dimensionless
$R_{i(t)}$ = Interfacial resistance on a solvent and time basis sec/cm
$R_i^1$ = Limiting value of interfacial resistance sec/cm
$r$ = Equivalent radius of droplet cm
$V$ = Droplet volume cm³
$v$ = Droplet velocity cm/sec
$\Gamma$ = Surface concentration of surface active agent g mol/cm²
$\eta$ = Absolute viscosity poise
$\nu$ = Kinematic viscosity cm²/sec

## REFERENCES


[1] HOLM, A., LINDLAND, K. and TERJESEN, S. G.; *Ber. 8. Nordiske Kjemikermøte*, Oslo, 14-17 June 1953.
[2] HUTCHINSON, E.; *J. Phys. Coll. Chem.* 1948 **52** 897.
[3] GARNER, F. H. and HALE, A. R.; *Chem. Eng. Sci.* 1953 **2** 157.
[4] MURDOCH, R. and PRATT, H. R. C.; *Trans. Inst. Chem. Engrs.* 1953 **31** 807.
[5] HOLM, A. and TERJESEN, S. G.; *Chem. Eng. Sci.* 1955 **6** 265.
[6] STUKE, B.; *Naturwiss enschaften.* 1952 **39** 325.
[7] PEARCE, J. N. and EVERSOLE, W. G.; *J. Phys. Chem.* 1924 **28** 245.
[8] DAVIES, M. and GWYNNE, E.; *J. Amer. Chem. Soc.* 1952 **74** 2748.
[9] MELHUS, B. J and TERJESEN, S. G.; Not yet published.
[10] COULSON, J. M. and SKINNER, S. J.; *Chem. Eng. Sci.* 1952 **1** 197.
[11] HEERTJES, P. M., HOLVE, W. A. and TALSMA, H.; *Chem. Eng. Sci.* 1954 **3** 122.
[12] ADAM, N. K.; *The Physics and Chemistry of Surfaces*, Third Ed., Oxford University Press, London, 1941, p. 61.
[13] MOILLIET, J. L. and COLLIE, B.; *Surface Activity*, Spon. London, 1951, p. 6.
[14] LEWIS, J. B.; *Chem. Eng. Sci.* 1954 **3** 248 and 260.
[15] GARNER, F. H. and SKELLAND, A. H. P.; *Trans. Inst. Chem. Engrs.* 1950 **28** 88.
[16] NEWMAN, A. B.; *Trans. Amer. Inst. Chem. Engrs.* 1931 **27** 310.
[17] WILKE, C. R.; *Chem. Eng. Progress* 1949 **45** 218.
[18] LEWIS, J. B. and PRATT, H. R. C.; *Nature* 1953 **171** 1133.

Chemical Engineering Science, 1956, Vol. 5, pp. 13 to 19. Pergamon Press Ltd.

# Forced heat convection in cylindrical channels: Some problems involving potential and parabolic velocity distribution

LEONARD TOPPER*
The Johns Hopkins University, Baltimore 18, Maryland

(*Received* 5 *April*, 1955)

**Abstract**—Analytical solutions are presented for two kinds of problem in the convection of heat by a fluid. The first problem is that of the uniform and constant generation of heat within the fluid; the second is that of temperature equalization when the inlet temperature has one constant value for part of the radius and another value for the rest of the radius. Steady-state solutions are developed for both plug flow and laminar flow; the wall of the tube is assumed to be isothermal.

**Résumé**—L'auteur présente des solutions analytiques de deux sortes de problèmes sur la convection thermique par un fluide : le premier relatif à la production constante et uniforme de chaleur au sein du fluide ; le second concernant l'égalisation des températures quand la température interne a une valeur constante pour une partie du rayon et une autre valeur pour le reste. Il donne des solutions à l'état stationnaire soit pour l'écoulement en piston soit pour l'écoulement laminaire, en supposant que la paroi du tube est isotherme.

THE merit of the analytical approach to problems in convective heat transfer has been demonstrated in the sixty-five years that have elapsed since the pioneer theoretical studies by GRAETZ and by L. LORENZ. The design of equipment, the prediction of its performance, and the planning and interpretation of experimental research are often conducted more effectively when the implications of the heat equation in the particular problem are clearly stated.

Two different kinds of problem in forced convection are solved here. In both of them, a fluid flows through a cylindrical tube. The tube wall is isothermal, the properties of the fluid are independent of temperature, and we assume the fluid velocity to be entirely in the axial direction and to be steady. In the first problem, the fluid inlet temperature is uniform and there is a constant heat generation per unit volume; in the second, the inlet temperature is uniform at one value for part of the radius and at another value for the rest of the radius. Both constant and parabolic velocity distributions are considered in each of the problems. The steady-state local temperatures are calculated and presented analytically and also graphically. The solution of the first problem should be helpful in estimating temperatures developed in chemical and nuclear reactors, and that of the second problem in estimating the average life of non-uniformities of the temperature in such streams.

## I. UNIFORM HEAT GENERATION

The differential equation of heat conduction in a moving medium is

$$\frac{dT}{d\tau_\tau} = \frac{\partial T}{\partial \tau_\tau} + V_x \frac{\partial T}{\partial x} + V_y \frac{\partial T}{\partial y} + V_z \frac{\partial T}{\partial z} = q/\rho c + \alpha \Delta^2 T. \quad (1)$$

Assuming symmetry about the axis of the cylinder, neglecting axial conduction of heat $\left(\text{assuming } \frac{\partial^2 T}{\partial x} \ll \frac{\partial^2 T}{\partial r} + \frac{1}{r}\frac{\partial T}{\partial r}\right)$, at the steady-state (1) becomes

$$V_x \frac{\partial T}{\partial x} = \alpha \left(\frac{\partial^2 T}{\partial r^2} + \frac{1}{r}\frac{\partial T}{\partial r}\right) + A. \quad (2)$$

The fluid enters at $x = 0$, at the uniform tem-

* Present Address: Esso Research and Engineering Co., P.O. Box 121, Linden, New Jersey.

perature $T_0$, and the wall ($r = s$) is at the constant temperature $T_s$. Define $\theta$ as $T - T_s$. Then the boundary conditions are :

$$\text{at } x = 0,\ \theta = \theta_0 = T_0 - T_s \tag{3}$$

$$\text{at } r = s,\quad \theta = 0. \tag{4}$$

*A. Potential Flow*

Here $V_x$ is a constant, $V_m$, and (2) becomes

$$V_m \frac{\partial \theta}{\partial x} = \alpha \left( \frac{\partial^2 \theta}{\partial r^2} + \frac{1}{r} \frac{\partial \theta}{\partial r} \right) + A. \tag{5}$$

The homogeneous equation ($A = 0$) has the solution [references 1, 2]

$$\frac{\theta}{\theta_0} = \sum_{n=1}^{\infty} \frac{2}{\beta_n J_1(\beta_n)} J_0(\beta_n w) \exp\left( - \beta_n^2 \frac{\alpha}{s V_m} \frac{x}{s} \right) \tag{6}$$

The values of $\beta_n$ are the positive roots of $J_0(\beta_n) = 0$, $w = (r/s)$; $J_0$ and $J_1$ are Bessel functions of the first kind and zero and first order respectively.

The solution of (5) has the form

$$\theta = \sum_{n=1}^{\infty} N_n J_0(\beta_n w) \exp\left( - \beta_n^2 \frac{\alpha}{s V_m} \frac{x}{s} \right) + \frac{A s^2}{4\alpha} (1 - w^2). \tag{7}$$

This automatically satisfies (4); $N_n$ must be computed from boundary condition (3) :

$$\theta = \theta_0 = \sum_{n=1}^{\infty} N_n J_0(\beta_n w) + \frac{A s^2}{4\alpha} (1 - w^2) \tag{8}$$

Multiply (8) by $J_0(\beta_m w)\, w\, dw$ where $\beta_m$ need not be the same eigen value as $\beta_n$, and integrate from $w = 0$ to $w = 1$.

For each $n$, we have the result

$$\theta_0 \int_0^1 J_0(\beta_m w)\, w\, dw = N_n \int_0^1 J_0(\beta_m w)\, J_0(\beta_n w)\, w\, dw - \frac{A s^2}{4\alpha} \left[ \int_0^1 J_0(\beta_m w)\, w^3\, dw - \int_0^1 J_0(\beta_m w)\, w\, dw \right] \tag{9}$$

The following properties of $J_0$ are introduced in (9) to produce (14) :

$$\int_0^1 J_0(\beta_n w)\, w\, dw = \frac{J_1(\beta_n)}{\beta_n} \tag{10}$$

$$\int_0^1 J_0(\beta_n w)\, J_0(\beta_m w)\, w\, dw = 0, \quad m \neq n \tag{11}$$

$$\int_0^1 [J_0(\beta_n w)]^2\, w\, dw = \frac{1}{2} [J_1(\beta_n)]^2 \tag{12}$$

$$\int_0^1 J_0(\beta_n w)\, w^3\, dw = \frac{J_1(\beta_n)}{\beta_n} - \frac{4 J_1(\beta_n)}{\beta_n^3} \tag{13}$$

$$\frac{\theta_0 J_1(\beta_n)}{\beta_n} = \frac{N_n}{2} [J_1(\beta_n)]^2 + \frac{A s^2}{\alpha} \frac{J_1(\beta_n)}{\beta_n^2} \tag{14}$$

and

$$\frac{N_n}{\theta_0} = \frac{2}{\beta_n J_1(\beta_n)} \left[ 1 - \frac{A s^2}{\alpha \theta_0} \frac{1}{\beta_n^2} \right] \tag{15}$$

and finally, from (7),

$$\frac{\theta}{\theta_0} = \sum_{n=1}^{\infty} \frac{2}{\beta_n J_1(\beta_n)} \left[ 1 - \frac{A s^2}{\alpha \theta_0} \frac{1}{\beta_n^2} \right] J_0(\beta_n w) \exp\left( - \beta_n^2 \frac{\alpha}{s V_m} \frac{x}{s} \right) + \frac{A s^2}{4 \alpha \theta_0} (1 - w^2). \tag{16}$$

The table below is for use in computing the first three terms of (16).

| $n$ | $\beta_n$ | $J_1(\beta_n)$ |
|---|---|---|
| 1 | 2·40 | 0·520 |
| 2 | 5·52 | − 0·340 |
| 3 | 8·65 | 0·272 |

Fig. 1 is a plot of axial temperature ($w = 0$), from equation (16), using appropriate dimensionless groups. The average (or bulk) temperature at any axial station is another important quantity. It is defined as

$$\theta_m = \frac{\int_0^1 \theta\, 2\pi\, w\, V_x\, dw}{\int_0^1 2\, \pi\, w\, V_x\, dw} \tag{17}$$

Fig. 2 expresses the difference between the axial temperature and the mean temperature.

*B. Laminar Flow*

In laminar flow, $V_x$ is a function of $w$ :

$$V_x = 2\, V_m (1 - w^2) \tag{18}$$

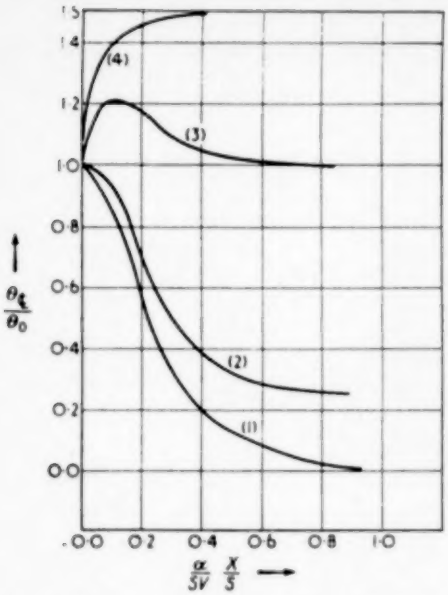


FIG. 1. Axial temperature in a tube. Potential flow, uniform heat generation, isothermal wall.

(1) $\frac{As^2}{\alpha\theta_0} = 0$; (2) $\frac{As^2}{\alpha\theta_0} = 1$; (3) $\frac{As^2}{\alpha\theta_0} = 4$; (4) $\frac{As^2}{\alpha\theta_0} = 6$.

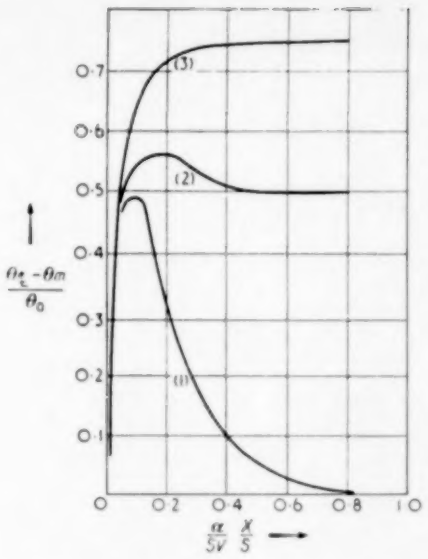


FIG. 2. Difference between axial and mean temperature. Potential flow, uniform heat generation, isothermal wall:

(1) $\frac{As^2}{\alpha\theta_0} = 0$; (2) $\frac{As^2}{\alpha\theta_0} = 4$; (3) $\frac{As^2}{\alpha\theta_0} = 6$.

The differential equation here is

$$2\,V_m(1-w^2)\frac{\partial\theta}{\partial x} = \frac{\alpha}{s^2}\left(\frac{\partial^2\theta}{\partial w^2} + \frac{1}{w}\frac{\partial\theta}{\partial w}\right) + A \quad (19)$$

with the boundary conditions of eqs. (3) and (4). The homogeneous form of eq. (19) was solved by GRAETZ [2] discussed in the modern literature, [1], [3], [4]), who also presented equation (6).

GRAETZ found the solution of the homogeneous form to be

$$\frac{\theta}{\theta_0} = \sum_{n=0}^{\infty} \frac{2}{\beta_n\left(\frac{\partial R}{\partial\beta}\right)_{n,\,w=1}} R(w,\beta_n) \exp\left(-\frac{\beta_n^2}{2}\frac{\alpha}{s\,V_m}\frac{x}{s}\right) \quad (20)$$

$$R(w,\beta_n) = \sum_{n=0}^{\infty} Bzn\,(w\,\beta_n)^{2n} \quad (21)$$

where $B_0 = 1$, $B_2 = -\frac{1}{2^2}$, $B_{2n} = \frac{1}{(2n)^2}\left[\frac{1}{\beta^2}B_{2n-4} - B_{2n-2}\right]$ and the $\beta_n$ are the roots of $R(1,\beta_n) = 0$. This function was studied by GRAETZ, and a table of its numerical values follows. The first three zeros are (4): $\beta_0 = 2{\cdot}704$, $\beta_1 = 6{\cdot}68$, $\beta_2 = 10{\cdot}67$.

A solution of eq. (19) is

$$\theta = \sum_{n=0}^{\infty} N_n R(w,\beta_n) \exp\left(-\frac{\beta_n^2}{2}\frac{\alpha}{s\,V_m}\frac{x}{s}\right) + \frac{As^2}{4\alpha}(1-w^2) \quad (22)$$

The $N_n$ of eq. (22) are calculated from eq. (3), since boundary condition (4) is automatically satisfied by (22). At $x = 0$,

$$\theta = \theta_0 = \sum_{n=0}^{\infty} N_n R(w,\beta_n) + \frac{As^2}{4\alpha}(1-w^2) \quad (23)$$

Multiply eq. (23) by $R_m\,w\,(1-w^2)\,dw$, where $m$ need not be equal to $n$. By $R_m$ or $R_m$ we will mean $R(w,\beta_m)$ or $R(w,\beta_n)$ respectively. Integrate from $w = 0$ to $w = 1$,
For each $n$,

$$\left.\begin{aligned}\theta_0 \int_0^1 R_m\, w\,(1-w^2)\,dw &= N_n \int_0^1 R_n\, R_m\, w\,(1-w^2)\,dw \\ &+ \frac{As^2}{4\alpha}\left[\int_0^1 R_m\, w\,(1-w^2)\,dw - \int_0^1 R_m\, w^3\,(1-w^2)\,dw\right]\end{aligned}\right\} \quad (24)$$

These properties of $R$ are used in (24):

$$\int_0^1 R_n\, R_m\, w\,(1-w^2)\,dw = 0, \quad m \neq n \qquad (25)$$

$$\int_0^1 R_n^2\, w\,(1-w^2)\,dw = \frac{1}{2\,\beta_n}\left[\left(\frac{\partial R}{\partial \beta}\right)_n \frac{dR_n}{dw}\right]_{w=1} \qquad (26)$$

$$\int_0^1 R_n^2\, w\,(1-w^2)\,dw = \frac{1}{\beta_n^2}\left(\frac{dR_n}{dw}\right)_{w=1} \qquad (27)$$

$$\int_0^1 R_n\, w^3\,(1-w^2)\,dw = \frac{-1}{\beta_n^2}\left(\frac{d\,R_n}{dw}\right)_{w=1} + \frac{2}{\beta_n^2}\int_{w=0}^{w=1} w^2\, d\,R_n \qquad (28)$$

Equations (25) to (28) are due to GRAETZ; (28) follows from an integration by parts. These lead to

$$N_n = \frac{-2\,\theta_0}{\beta_n\left(\dfrac{\partial R}{\partial \beta}\right)_{n,\,w=1}} + \frac{As^2}{\beta_n\,\alpha}\,\frac{\displaystyle\int_{w=0}^{w=1} w^2\, dR_n}{\left[\left(\dfrac{\partial R}{\partial \beta}\right)_n \dfrac{dR_n}{dw}\right]_{w=1}} \qquad (29)$$

The first terms of the series solution of (22) are then



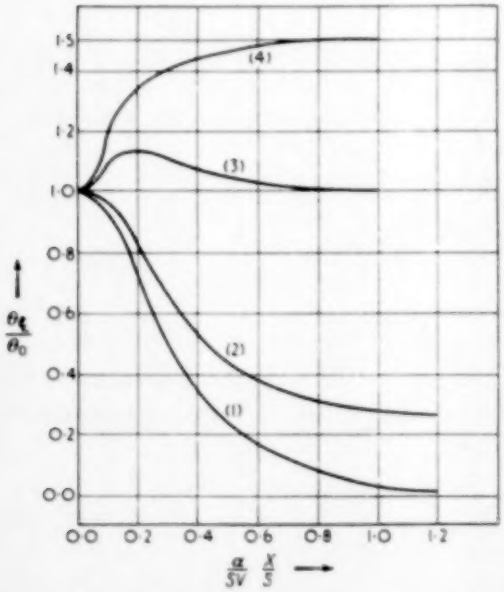


FIG. 3. Axial temperature in a tube. Laminar flow, uniform heat generation, isothermal wall:

(1) $\frac{As^2}{\alpha\theta_0} = 0$; (2) $\frac{As^2}{\alpha\theta_0} = 1$; (3) $\frac{As^2}{\alpha\theta_0} = 4$; (4) $\frac{As^2}{\alpha\theta_0} = 6$.

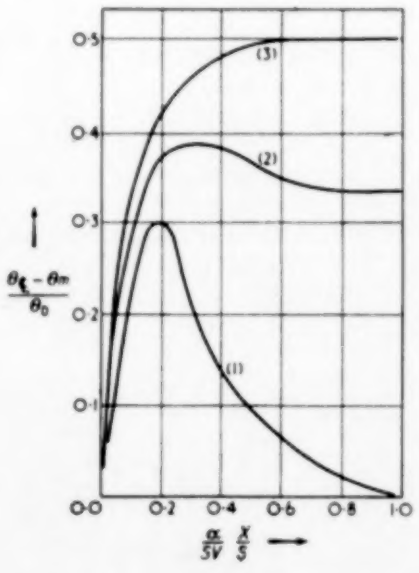


FIG. 4. Difference between axial and mean temperature. Laminar flow, uniform heat generation, isothermal wall:

(1) $\frac{As^2}{\alpha\theta_0} = 0$; (2) $\frac{As^2}{\alpha\theta_0} = 4$; (3) $\frac{As^2}{\alpha\theta_0} = 6$.

$$\frac{\theta}{\theta_0} =$$

$$\left(1{\cdot}476 - \frac{0{\cdot}292\,As^2}{a\theta_0}\right) R_0(w) \exp\left(-3{\cdot}66\,\frac{\alpha}{s\,V_m}\,\frac{x}{s}\right)$$

$$-\left(0{\cdot}808 + \frac{0{\cdot}051\,As^2}{a\theta_0}\right) R_1(w) \exp\left(-22{\cdot}8\,\frac{\alpha}{s\,V_m}\,\frac{x}{s}\right)$$

$$+\left(0{\cdot}588 - \frac{0{\cdot}019\,As^2}{a\theta_0}\right) R_2(w) \exp\left(-56{\cdot}5\,\frac{\alpha}{s\,V_m}\,\frac{x}{s}\right) \quad (30)$$

Fig. 8, is a plot of axial temperature ($w = 0$), from equation (30), using appropriate dimensionless groups. Fig. 4 expresses the difference between the axial temperature and the mean temperature (eq. (17)).

## 2. Temperature Mixing Between Concentric Streams

The rate of " mixing-out " of non-uniformities of temperature or of composition in a flowing stream is often important to the analysis of processes. The calculations that follow are equivalent to the rate of equalization of temperature due to the diffusion of heat alone. In most practical situations, the initial non-uniformity of temperature induces non-uniform velocities that expedite the temperature equalization. For this reason, the actual rate of temperature mixing should always be at least as great as indicated here.

Consider a stream of fluid entering a cylindrical tube of radius $S$. At $x = 0$, the stream temperature is $T_a$ from the axis ($r = 0$) to $r = a$ ($s > a$); it is $T_b$ from $r = a$ to $r = s$. The wall temperature remains constant at $T_s$, and the assumptions of eq. (1) apply here as well.

The differential equation is

$$V_x \frac{\partial\theta}{\partial x} = \frac{\alpha}{S^2}\left(\frac{\partial^2\theta}{\partial w^2} + \frac{1}{w}\frac{\partial\theta}{\partial w}\right) \quad (31)$$

with the boundary conditions

$$\text{At } x = 0,\ \theta = \theta_a = T_a - T_s,\ (a/s) > w > 0$$
$$\theta = \theta_b = T_b - T_s,\ 1 < w < (a/s) \quad (32)$$

$$\text{At } w = 1,\ \theta = 0 \quad (33)$$

### A. *Potential Flow*

$V_x$ is a constant, and (31) becomes

$$V_x \frac{\partial\theta}{\partial x} = \frac{\alpha}{s^2}\left(\frac{\partial^2\theta}{\partial w^2} + \frac{1}{w}\frac{\partial\theta}{\partial w}\right) \quad (34)$$

which has the solution

$$\theta = \sum_{n=1}^{\infty} N_n J_0(\beta_n w) \exp\left(-\beta_n^2\,\frac{\alpha}{s\,V}\,\frac{x}{s}\right) \quad (35)$$

where the $\beta_n$ are the positive roots of $J_0(\beta_n) = 0$. The $N_n$ are determined from eq. (32). Subject to certain restrictions on $f(w)$ that are satisfied here, when

$$f(w) = \sum_{n=1}^{\infty} N_n J_0(\beta_n w) \quad (36)$$

$$N_n = \frac{2}{[J_1(\beta_n)]^2}\int_0^1 w\, f(w)\, J_0(\beta_n w)\, dw \quad (37)$$

Here

$$N_n = \frac{2}{\beta_n [J_1(\beta_n)]^2}\left[\theta_a \int_0^{a/s} w\, J_0(\beta_n w)\, dw + \theta_b \int_{a/s}^1 w\, J_0(\beta_n w)\, dw\right] \quad (38)$$

$$N_n = \frac{2}{\beta_n [J_1(\beta_n)]^2}\left[\frac{a}{s}(\theta_a - \theta_b) J_1\left(\beta_n \frac{a}{s}\right) + \theta_b J_1(\beta_n)\right] \quad (39)$$

And finally,

$$\frac{\theta}{\theta_b} = \sum_{n=1}^{\infty} \frac{2}{\beta_n [J_1(\beta_n)]^2}\left[\frac{a}{s}\left(\frac{\theta_a - \theta_b}{\theta_b}\right) J_1\left(\beta_n \frac{a}{s}\right) + J_1(\beta_n)\right] J_0(\beta_n w) \exp\left(-\beta_n^2\,\frac{\alpha}{s\,V_m}\,\frac{x}{s}\right) \quad (40)$$

Fig. 5 indicates the approach of the temperature of the fluid to that of the isothermal wall when $(a/s)$ is 0·5 and $\left(\frac{\theta_a - \theta_b}{\theta_b}\right)$ is 0·5. The radial temperature distribution is plotted at $x = 0$ and at two values of the dimensionless distance downstream, $\left(\frac{\alpha}{s\,V_m}\,\frac{x}{s}\right)$.

### B. *Laminar Flow*

The problem is

$$2\,V_m(1 - w^2)\frac{\partial\theta}{\partial x} = \frac{\alpha}{s^2}\left(\frac{\partial^2\theta}{\partial w^2} + \frac{1}{w}\frac{\partial\theta}{\partial w}\right) \quad (41)$$

*Table* 1. *Graetz's* $R_n$ *Function* [4]

| $W$ | $R_0$ | $R_1$ | $R_2$ |
|---|---|---|---|
| 0·0 | 1 | 1 | 1 |
| 0·1 | 0·982 | 0·892 | 0·726 |
| 0·2 | 0·929 | 0·605 | 0·153 |
| 0·3 | 0·846 | 0·234 | − 0·315 |
| 0·4 | 0·738 | − 0·110 | − 0·392 |
| 0·5 | 0·615 | − 0·340 | − 0·142 |
| 0·6 | 0·483 | − 0·432 | 0·170 |
| 0·7 | 0·351 | − 0·398 | 0·332 |
| 0·8 | 0·224 | − 0·284 | 0·308 |
| 0·9 | 0·107 | 0·141 | 0·163 |
| 1·0 | 0 | 0 | 0 |

with boundary conditions of eqs. (32) and (33). The solution is

$$\theta = \sum_{n=0}^{\infty} N_n R(w, \beta_n) \exp\left(-\beta_n^2 \frac{\alpha}{s V_m} \frac{x}{s}\right) \qquad (42)$$

where $R(1, \beta_n) = 0$. The $N_n$ are from eq. (32):

$$f(w) = \sum_{n=0}^{\infty} N_n R_n(w) \qquad (43)$$

Multiply eq. (43) by $R_m w(1 - w^2)\, dw$, where $m$ need not be equal to $n$. Integrate from $w = 0$ to $w = 1$. For each $n$, using eq. (25) to (28),

$$\frac{N_n}{2\beta_n}\left[\left(\frac{\partial R}{\partial \beta}\right)_n \frac{d R_n}{dw}\right]_{w=1} = \theta_a \int_0^{a/s} R_n w(1 - w^2)\, dw + \theta_b \int_{a/s}^{1} R_n w(1 - w^2)\, dw \qquad (44)$$

$$N_n = -\frac{2}{\beta_n \left(\frac{\partial R}{\partial \beta}\right)_{n,w=1}} \left[\frac{a}{s}(\theta_a - \theta_b)\frac{(dR_n/dw)_{w=a/s}}{(dR_n/dw)_{w=1}} + \theta_b\right] \qquad (45)$$

$\left(\frac{dR_n}{dw}\right)_{w=a/s}$ is most conveniently calculated by graphical differentiation of $R_n$, or else by a graphical integration:

$$\left(\frac{dR_n}{dw}\right)_{w=a/s} = \frac{-\beta_n^2}{a/s} \int_0^{a/s} R_n w(1 - w^2)\, dw \qquad (46)$$

The first three terms of the solution to eq. (33) are

$$\left.\begin{aligned} \frac{\theta}{\theta_b} = 1{\cdot}476 \left[1 - \frac{a}{s}\left(\frac{\theta_a - \theta_b}{\theta_b}\right)\frac{\left(\frac{dR_0}{dw}\right)_{w=a/s}}{1{\cdot}01}\right] R_0(w) \exp\left(-3{\cdot}66 \frac{\alpha}{s V_m}\frac{x}{s}\right) \\ - 0{\cdot}808 \left[1 + \frac{a}{s}\left(\frac{\theta_a - \theta_b}{\theta_b}\right)\frac{(dR_1/dw)_{w=a/s}}{1{\cdot}33}\right] R_1(w) \exp\left(-22{\cdot}3 \frac{\alpha}{s V_m}\frac{x}{s}\right) \\ + 0{\cdot}588 \left[1 - \frac{a}{s}\left(\frac{\theta_a - \theta_b}{\theta_b}\right)\frac{(dR_2/dw)_{w=a/s}}{0{\cdot}78}\right] R_2(w) \exp\left(-56{\cdot}5 \frac{\alpha}{s V_m}\frac{x}{s}\right) \end{aligned}\right\} \qquad (47)$$

Fig. 6 expresses the temperature equalisation in laminar flow in a tube having an isothermal when $(a/s)$ is 0·5 and $\left(\frac{\theta_a - \theta_b}{\theta_b}\right)$ is 0·5 (the same conditions as for Fig. 5).

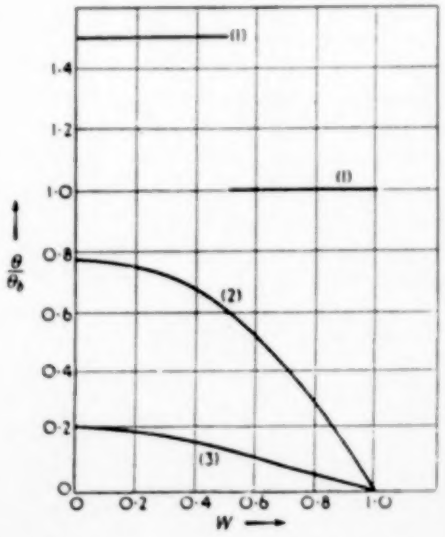


FIG. 5. Equalization of temperature. Potential flow, $(a/s) = 0{\cdot}5$, $\left(\frac{\theta_a - \theta_b}{\theta_b}\right) = 0{\cdot}5$.

(1) $\frac{\alpha}{sV}\frac{x}{s} = 0{\cdot}0$; (2) $\frac{\alpha}{sV}\frac{x}{s} = 0{\cdot}1$; (3) $\frac{\alpha}{sV}\frac{x}{s} = 0{\cdot}5$.



VOL. 5 1956

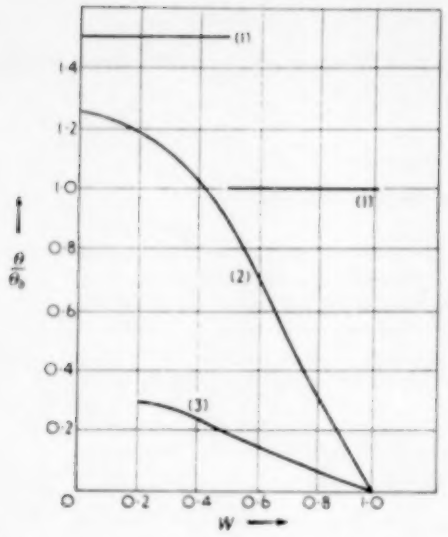


FIG. 6. Equalization of temperature. Laminar flow, $(a/s) = 0{\cdot}5$, $\left(\dfrac{\theta_a - \theta_b}{\theta_b}\right) = 0{\cdot}5$.

(1) $\dfrac{\alpha}{s\,V_m}\dfrac{x}{s} = 0{\cdot}0$ ; (2) $\dfrac{\alpha}{s\,V_m}\dfrac{x}{s} = 0{\cdot}1$ ; (3) $\dfrac{\alpha}{s\,V_m}\dfrac{x}{s} = 0{\cdot}5$.

## NOTATION

$A = q/\rho c$

$J_0, J_1$ = Bessel functions of the first kind and zero and first order

$N_n$ = coefficient of characteristic function in various equations

$R\,(w, \beta_n)$ = Graetz's function, defined by eq. (21)

$T, T_a, T_b, T_0, T_s$ = temperature, initial temperature at $r < a$, initial temperature at $a < r < s$, initial temperature, wall temperature

$V_m, V_x$ = mean velocity, local axial velocity

$a$ = radial coordinate at discontinuity of initial temperature

$c$ = heat capacity

$q$ = heat generation per unit volume and time

$r$ = radial coordinate

$s$ = tube radius

$w = (r/s)$

$x$ = axial coordinate

$\alpha$ = thermal diffusivity

$\beta_n$ = a zero of $J_0$ or of $R_n$

$\rho$ = density

$\theta, \theta c = T - T_s$, $\theta$ at $w = 0$

$\tau$ = time

## REFERENCES

[1] DREW, T. B.; *Tr. A. I. Ch. E.* 1931 **26** 49.

[2] GRAETZ, L.; *Z. Math. Physik.* 1880 **25** 316.

[3] JAKOB, M.; *Heat Transfer*, Vol. 1, John Wiley, 1949.

[4] SCHENK, J. and DUMORE, J. M.; *Appl. Sci. Res.* 1953 **A4** 39.

Chemical Engineering Science, 1956, Vol. 5, pp. 20 to 33. Pergamon Press Ltd.

# The simultaneous transfer of heat and mass between water and moist coal gas

G. S. Cribb and E. T. Nelson

Fulham Research Laboratory, North Thames Gas Board

**Abstract**—The Graphical Method of Mickley [3] for the counter current contacting of moist air with water is modified to apply to the system moist coal gas–water, over the range of saturation temperatures 32°F to 180°F. Over this range the Lewis Number $h_G/k_G s$ cannot be considered constant and the log mean partial pressure of the non-diffusing gas varies widely from unity.

A driving force is derived, which incorporates these variables for use in conjunction with the gas film mass transfer coefficient. This necessitates the use of two equilibrium lines as in the method of Lewis and White [5].

Although no suitable data are available for truly counter current flow for the system considered, the method has been applied to test data on a cross flow water-tube condenser. The results are compared with those obtained by the well known method of Colburn and Hougen [1].

**Résumé**—Les auteurs ont transformé la méthode graphique de Mickley valable pour l'échange entre de l'eau et de l'air humide circulant à contre-courant afin de l'appliquer au système eau-tas de houille, au-dessus de l'intervalle des températures de saturation (32°F-180°F). Au-delà de ce domaine, on ne peut pas considérer le nombre de Lewis $h_G/K_G S$ comme constant et la moyenne logarithmique de la pression partielle du gaz diffusant s'écarte largement de l'unité.

Les auteurs déduisent une équation de la force motrice qui comprend variables et en même temps tient compte du coefficient de transfert massique du film gazeux. Cela nécessite l'emploi de deux lignes d'équilibre comme dans la méthode de Lewis et White.

Quoique dans le système envisagé, il ne soit pas possible d'avoir des données valables pour un écoulement réellement à contre-courant, ils ont vérifié par cette méthode les valeurs relatives à un condenseur à tube d'eau avec circulation externe à angle droit. Ils ont comparé leurs résultats aux résultats obtenus par la méthode bien connue de Colburn et Hougen.

## 1. Introduction

Since Colburn and Hougen [1] first published their paper on the "Design of Cooler Condensers for Mixtures of Vapours and Non-Condensing Gases," several less rigorous but simpler methods have been proposed. Colburn [2] in a recent paper stressed the need for such methods, based preferably on the terminal conditions only, and suggested that the most hopeful direction for investigation was the method proposed by Mickley [3].

By extending the method of Mickley to a system other than air-water having high vapour concentrations, a graphical method is developed which is as rigorous as that of Colburn and Hougen. Moreover, the method does not assume that the relative rates of heat and mass transfer are such that the gas remains saturated throughout the apparatus, an assumption which is shown to be invalid.

The method may also be employed to determine values for individual film coefficients from performance data on actual plant.

## 2. The Development of a Graphical Method for the Design of Plant Involving the Simultaneous Transfer of Heat and Mass

If in countercurrent operation of contacting moist gas with water, a small section of transfer area $dA$ is considered; five basic differential equations for heat and mass transfer may be written down.

The mass balance relating to the transfer of the water between the gas and liquid phase is given by

$$G\,dH_G = dL \qquad (1)$$

The complete heat balance over the section,

expressed as changes in enthalpy based on gas and liquid water at $t_0$ (32°F), is given by

$$G\,di_G = L\,c_L\,dt_L + dL\,c_L\,(t_L - t_0) \qquad (2a)$$

The enthalpy change of the gas comprises four terms

$$G\,di_G = G\,s\,dt_G + G\,dH_G\,\lambda_i + G\,dH_G\,c_V\,(t_G - t_i) + G\,dH_G\,c_L\,(t_i - t_0) \qquad (2b)$$

where $G\,s\,dt_G$ is the sensible heat change in the bulk of the gas.

$G\,dH_G\,\lambda_i$ is the latent heat of the mass of water transferred across the interface at temperature $t_i$.

$G\,dH_G\,c_V\,(t_G - t_i)$ is the sensible heat change in the water vapour in passing between the bulk of the gas and the interface.

$G\,dH_G\,c_L\,(t_i - t_0)$ is the sensible heat or enthalpy of the water transferred above 32°F.

The three remaining basic equations are as follows :—

The rate equation for sensible heat transfer across the gas film

$$-G\,s\,dt_G = h_G\,(t_G - t_i)\,dA \qquad (3)$$

The rate equation for mass transfer across the gas film

$$-G\,dH_G = k_G\,(H_G - H_i)\,dA \qquad (4)$$

The rate equation for total heat transfer across the liquid film

$$L\,c_L\,dt_L = h_L\,(t_L - t_i)\,dA \qquad (5)$$

The difference between $d\,L\,c_L\,(t_L - t_0)$ in eq. (2a) and $G\,dH_G\,c_L\,(t_i - t_0)$ in eq. (2b) is $G\,dH_G\,c_L\,(t_i - t_L)$ the heat given up by the condensate in cooling down to the bulk liquid temperature $t_L$. This quantity is small compared with $G\,dH_G\,\lambda_i$ and may be neglected. The significance of the quantity $G\,dH_G\,c_V\,(t_G - t_i)$ is discussed below.

The total sensible heat flux at a point in the gas film is given by

$$q = h_G\,dt/dz + \frac{G\,dH_G}{dA}\,c_V\,(t - t_i) \qquad (6)$$

where $z$ is the fractional distance through the gas film corresponding to temperature. Colburn and Drew [4] integrated this expression across the gas film to give

$$q = h_G\,(t_G - t_i)\,\frac{a}{1 - e^{-a}} \qquad (7)$$

where

$$a = -G\,dH_G\,c_V/h_G dA = \frac{k_G\,c_v}{h_G}\,(H_G - H_i) \qquad (8)$$

For moist coal gas up to a saturation temperature of 180°F, $a$ lies between 0 and 1, and under these conditions $a/1 - e^{-a}$ approximates to $1 + 0{\cdot}54a$. Thus the contribution to the sensible heat flux by the diffusing vapour approximates to $0{\cdot}54\ G\,dH_G\,c_V\,(t_G - t_i)$ or $G\,dH_G\,(t_G - t_i)/4$. This term is usually very small compared with $G\,dH_G\,\lambda_i$ and may safely be ignored.

The heat balance for the total heat transfer across the interface is therefore given by equation (9),

$$G\,di_G \simeq G\,s\,dt_G + G\,dH_G\,\lambda_i \simeq L\,c_L\,dt_L \qquad (9)$$

$L\,c_L\,dt_L$ is a closer approximation to the total heat transferred across the interface than $G\,di_G$.

In order to avoid laborious trial and error calculations employing the above equations, methods have been developed for combining the heat and mass transfer driving forces across the gas film into a single potential difference. For the system air-water, a fortuitious relationship exists over the range of cooling tower operation. The ratio $h_G/k_G s$ (the Lewis Number $b$) approximates to unity under these conditions, and eqs. (3) and (4) may be combined as follows

$$-G\,(s dt_G + \lambda_0\,dH_G) = k_G\,[(st_G + \lambda_0\,H_G) - (st_i + \lambda_0\,H_i)]\,dA \qquad (10)$$

Assuming $s$ is constant, the left-hand side of the equation is equal to $-G\,di_G$, and the right-hand side approximates to the difference in enthalpy between the moist air and that in equilibrium with water at the interface temperature ($t_i$). This equation forms the basis of the graphical method of Mickley [3] for the air-water system.

For cases where the Lewis Number is not equal to unity but may be considered constant,

Lewis and White [5] have proposed a "modified enthalpy method." In the gas industry, gas coolers handle highly saturated gas over a wide range of temperature. Under such conditions the humid heat, on the basis of unit volume of dry gas and consequently the corresponding Lewis Number, vary by as much as 100%. Any method therefore that assumes constant humid heat is not applicable. Furthermore, humidity as a potential for mass transfer is a valid approximation, only when $p$ the partial pressure of the diffusing vapour is small compared with $P - p$, the partial pressure of the non-diffusing gas.

At 180°F the vapour pressure of water is 15·29 in. Hg. Thus for saturated gas at 180°F and 30 in. Hg. total pressure, the partial pressure of the water vapour exceeds that of the gas, and humidity difference cannot be used as an approximate driving force. The expression for humidity driving force is $H_i - H_G = \left[\frac{p_i}{P - p_i} - \frac{p_G}{P - p_G}\right]$. The true driving force or potential difference for mass transfer, under conditions of steady state diffusion of one gas through a second stagnant gas, is given by Sherwood and Pigford [6] as $\ln \frac{P - p_G}{P - p_i}$. This may be written as $\ln\left(\frac{P}{P - p_i}\right) - \ln\left(\frac{P}{P - p_G}\right)$ Comparing the two expressions for driving force, the true potential for mass transfer is the humidity multiplied by a factor $\alpha$.

$$\alpha = \frac{\ln\left(\frac{p}{P-p}\right)}{\frac{p}{P-p}} = \frac{\ln\left(1 + \frac{p}{P-p}\right)}{\frac{p}{P-p}} \qquad (11)$$

Equation (11) is of the form $\alpha = \frac{\ln(1+x)}{x}$, and if the right-hand side of the equation is expanded and terms of $x^2$ and greater powers ignored, then $\alpha = 1$. Values of $\alpha$ are tabulated below for saturation temperatures from 32°F to 180°F.

| °F | 32 | 40 | 60 | 80 | 100 | 120 | 140 | 160 | 180 |
|---|---|---|---|---|---|---|---|---|---|
| $\alpha$ | 0·997 | 0·996 | 0·991 | 0·982 | 0·969 | 0·925 | 0·895 | 0·819 | 0·686 |

Humidity as a driving force therefore is a very good approximation up to saturation temperatures of 90°F, but the error at higher temperatures may be illustrated as follows. Humidity may conveniently be expressed in the gas industry as pounds of water per 1,000 cu. ft. of gas at S.T.P. (60°F and 30 inches saturated). To simplify the units of humidity and humid heat, this quantity of gas will be termed a Standard Gas Volume, abbreviated to S.G.V.

Consider saturated gas at 180°F in contact with water at 160°F.
From Table 111 in Spiers 5th edn. [7], humidity driving force between saturated gas at 180°F and gas in equilibrium with water at 160°F is equal to

$$49{\cdot}19 - 22{\cdot}39 = 26{\cdot}80 \text{ lbs./S.G.V.}$$

True driving force = (0·686 × 49·19) − (0·819 × 22·39) = 15·31 lbs./(S.G.V.). The error is therefore 75%.

The rate equation for mass transfer is more correctly expresesd as

$$-G\,dH_G = k_G\,(\alpha_G H_G - \alpha_i H_i)\,dA \qquad (12)$$

Thus the mass transfer coefficient $k_G$ used in conjunction with $\alpha H$ as a driving force, is equivalent to the $k_G p_{BM}$ used in conjunction with partial pressure as a driving force. The

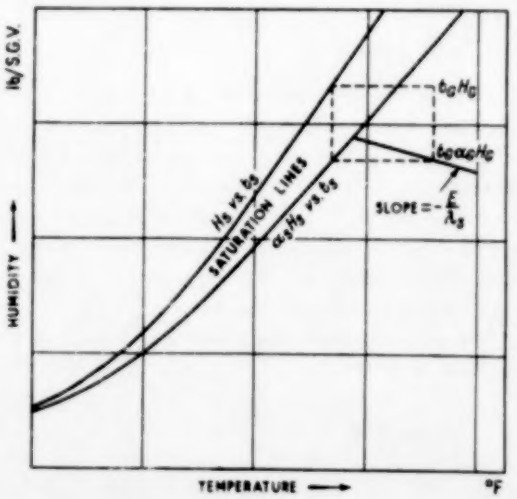


Fig. 1.



VOL. 5 1956

latter form is that normally encountered in mass transfer problems [6].

The true potential $\alpha H$ is a unique function of humidity $H$ and may be added to the humidity temperature diagram, more familiarly known as a psychrometric chart (Fig. 1).

Equations (3), (9) and (12) may be combined to give the following expression

$$-Gd_{iG} = [h_G(t_G - t_i) + k_G \lambda_i (\alpha_G H_G - \alpha_i H_i)]\, dA \quad (13)$$

In order to combine the driving forces for heat and mass transfer, one further relationship is required in addition to the five basic differential equations. This is the relationship between $h_G$ and $k_G$, and it is assumed, with theoretical justification, that a constant value for the ratio $h_G/k_G$ may be assumed throughout the apparatus. CHILTON and COLBURN [8] have demonstrated that for a variety of flow conditions the ratio $h_G/k_G c$ is substantially constant. The heat capacity $c$ is expressed on the basis of the total number of moles. The molar heat capacities of coal gas and water vapour are 7·7 B.Th.U/lb. mole and 8·0 B.Th.U/lb. mole respectively. Thus the variation in $c$ is small over the whole range of humidity.

$$E = h_G/k_G = a \text{ constant} \quad (14)$$

Equation (13) may therefore be re-written as follows :

$$-G\, di_G = k_G\{[E(t_G - t_0) + \lambda_i \alpha_G H_G] - [E(t_i - t_0) + \lambda_i \alpha_i H_i]\}\, dA \quad (15)$$

Applying the equation to saturated gas and introducing $\lambda_S$

$$-G\, di_G = k_G\{[E(t_S - t_0) + \lambda_S \alpha_S H_S] + (\lambda_i - \lambda_S)\alpha_S H_S - [E(t_i - t_0) + \lambda_i \alpha_i H_i]\}dA \quad (16)$$

Thus the driving force is the difference between two potentials, plus a small deviation $(\lambda_i - \lambda_S)\alpha_S H_S$.

It will be shown later, by reference to an example based on actual test data, that this deviation is small, and it will be ignored in the further development of the method.

The form of the uncorrected enthalpy transfer potential

$$\theta = E(t_S - t_0) + \lambda_S \alpha_S H_S \quad (17)$$

is such that if $E$ and $\lambda_S$ are constants, points of equal potential are connected by a straight line of slope $-E/\lambda_S$ on a plot of $\alpha H$ against temperature. With reference to Fig. 1, the condition of unsaturated gas may be represented by a point $(t_G, \alpha_G H_G)$, to the right of the saturation line on the ordinate through $(t_G, H_G)$. This point may be related to a saturation temperature $t_S$, on the saturation line $\alpha_S H_S$ vs. $t_S$, by means of a line of slope $-E/\lambda_S$. The enthalpy transfer potential $\theta_G$ of the unsaturated gas $(t_G, H_G)$ is therefore equal to $\theta_S$ that of saturated gas at a temperature $t_S$.

Humidity determination by means of a wet and dry bulb hygrometer involves the ratio of the heat and mass transfer coefficients. If $t_G$ and $t_W$ are the dry and wet bulb temperatures, as recorded on the hygrometer, then the humidity $H_G$ of the gas is given by the relationship

$$h_G(t_G - t_W) = k_G \lambda_W (H_W - H_G) \quad (18)$$

or

$$\frac{H_W - H_G}{t_W - t_G} = -\frac{E}{\lambda_W} \quad (19)$$

For the temperature range over which $E$ is determined, $\alpha$ is approximately equal to 1, and if the wet bulb relationship is to be extended to temperatures above 90°F, then $(H_W - H_G)$ should be replaced by $(\alpha_W H_W - \alpha_G H_G)$. Lines of ' constant transfer potential ' are therefore lines of ' constant wet bulb temperature ' if the value of $E$ is the same for both the apparatus under consideration and the wet and dry bulb hygrometer. In packed towers where, if wetting is incomplete, the area available for heat transfer exceeds that available for mass transfer, then $E$ varies if the coefficients are expressed on the basis of unit volume of packing. However, at high liquor rates, HENSEL and TREYBAL [9] found that the ratio of coefficients agreed with the psychrometric ratio for air-water used in conjunction with the wet and dry bulb thermometer. The rate equation for

total heat transfer in the gas film may therefore be written as

$$-G\,di_G = k_G\,(\theta_G - \theta_i)\,dA \tag{20}$$

or

$$A = \frac{G}{k_G}\int \frac{di_G}{(\theta_G - \theta_i)} \tag{21}$$

The two remaining relationships required for a graphical solution of problems involving the simultaneous transfer of heat and mass are given by the combination of equation (20) with the other rate equations.

Combining (5), (9) and (20)

$$\frac{(\theta_G - \theta_i)}{(t_L - t_i)} = -\frac{h_L}{k_G} \tag{22}$$

Combining (3) and (20)

$$\frac{di_G}{dt_G} = \frac{k_G s\,(\theta_G - \theta_i)}{h_G\,(t_G - t_i)} \tag{23}$$

The significance of these equations will be explained with reference to Fig. 2, a plot of the enthalpy of moist gas at saturation ($i_S$) and the transfer potential at saturation ($\theta_S$) against the saturation temperature. Line $\overline{AB}$ is the operating line representing equation (2) and having a slope of $L/G$. The line of constant enthalpy or isenthalp $\overline{AC}$ represents the enthalpy of moist gas at the hot end of the apparatus.

Points $A$ and $C$ correspond to the water and gas temperatures respectively. The line of constant potential $\overline{A'C'}$ represents the transfer potential corresponding to the terminal condition of the moist gas. $(t_{S1})_\theta$ and thus $\theta_{G1}$ is obtained from $(i_{G1}, t_{G1})$ by a "constant wet bulb temperature line" on the pyschrometric chart.

The point of intersection $D$, of a line of slope $-h_L/k_G$ through $A'$, with the potential saturation line, gives the conditions at the interface.

Line $\overline{C'D}$ has a slope of $(\theta_G - \theta_i)/(t_G - t_i)$. Equation (20) may be re-arranged as follows

$$\frac{1}{b}\frac{b\,dt_G}{di_G} = \frac{(t_G - t_i)}{(\theta_G - \theta_i)} \tag{24}$$

If the isenthalp $\overline{FG}$ is the enthalpy of the gas after a small change $di_G$ then the intercept $\overline{GJ}$ cut off by the intersection of a line parallel to $\overline{C'D}$ with $\overline{FG}$, is equivalent to $1/b\,dt_G$. Thus the correct gas temperature, after the first increment of transfer, is given by point $E$ where $\overline{EG} = b\,\overline{JG}$. Line $\overline{CE}$ is the instantaneous direction of the gas path and the required value of $b$ is that corresponding to $(i_{G1}, t_{G1})$.

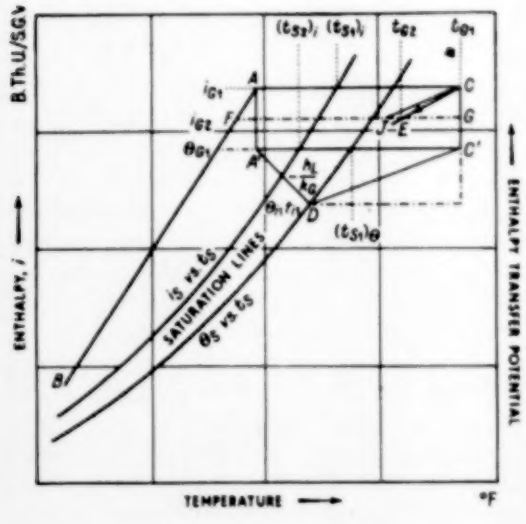


Fig. 2.

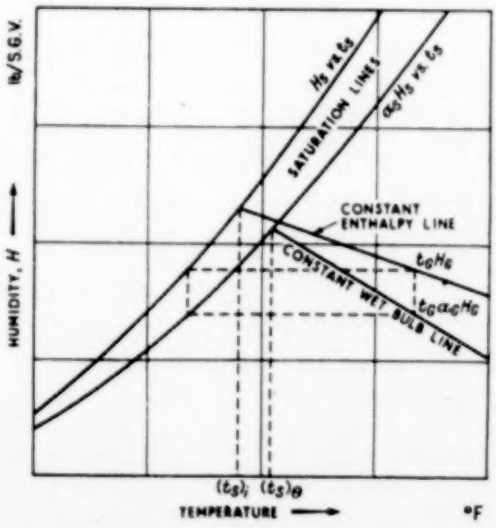


Fig. 3.

The representation of enthalpy on the psychrometric chart by a straight line relationship is an approximation, and the percentage deviation from the true value may also be plotted on the chart as a series of curves. From a knowledge therefore of the enthalpy and the temperature of the gas; the humidity, and thus the transfer potential, can be obtained as shown in Fig. 3. This diagram illustrates the connection between the saturation temperature on a constant enthalpy basis $(t_S)_i$ and the wet bulb temperature of the gas $(t_S)_\theta$. This conversion has to be carried out for each increment of enthalpy. For saturated gas the two saturation temperatures are of course identical.

The procedure for the graphical method is therefore as follows:

1. Determine the overall enthalpy changes in the gas and the liquid.
2. From these data, plot the operating line $\overline{AB}$ on the enthalpy-temperature chart (Fig. 2).
3. Plot $\theta_S$ vs. $t_S$ on the same chart.
4. Sub-divide the operating line into ten equal increments ($i_{G1}$, $i_{G2}$ . . . . . $i_{G11}$)
5. Determine the value of $(t_{S1})_\theta$ from $(t_{S1})_i$ (Fig. 3) and hence the value of $\theta_{G1}$ (Fig. 2).
6. Construct a tie-line of slope $-h_L/k_G$ and locate $\theta_{i1}$, $t_{i1}$ (Fig. 2).
7. Join point ($\theta_{G1}$, $t_{G1}$) with point ($\theta_{i1}$, $t_{i1}$) and construct a line parallel to this line through $i_{G1}$, $t_{G1}$, to intersect a line parallel to the abscissa with ordinate $i_{G2}$. Locate point $t_{G2}$ on this line by the method indicated (Fig. 2).
8. Repeat steps 5, 6 and 7 for the remaining increments.
9. Tabulate the values of $\dfrac{1}{(\theta_G - \theta_i)}$ and apply Simpson's Rule to obtain $\int di_G/(\theta_G - \theta_i)$ the number of individual gas film transfer units required.

The transfer area required is then given by eq. (21)

$$A = \frac{G}{k_G} \int \frac{di_G}{(\theta_G - \theta_i)}$$

The reverse procedure to determining $A$ from individual coefficients, is to determine the coefficients from tests on actual plant of known transfer area. The problem then arises as to what value to assume for the tie-line slope. MICKLEY claims that this value may be found from a single test, by adjusting the slope until the humidity of the outlet gas agrees with the observed value. The disadvantages of this method are as follows:

1. The locus of the gas condition is dependent on the method of selecting the increments.
2. Small errors in the outlet gas condition correspond to large variations in tie-line slope.
3. If the gas becomes saturated at any point it is almost certain to leave the unit in a saturated condition irrespective of tie-line slope.

An alternative method is to eliminate the liquid film resistance for a given set of flow conditions by adjusting the water temperature so that it is constant throughout the apparatus. Under these conditions, the loss of sensible heat from the gas is balanced by the gain in latent heat, and thus the method is only applicable to direct contact apparatus such as packed towers. Furthermore, the method requires adiabatic conditions and the measurement of small driving forces. It is in fact suitable only for experimental plant and not for checking the design of plant under operating conditions.

A third method is suggested by expressing the overall coefficient for enthalpy transfer in terms of $k_G$ and $h_L$.

$$G\,di_G = K_G(\theta_G - \theta_L)\,dA$$
$$= k_G(\theta_G - \theta_i)\,dA = h_L(t_i - t_L)\,dA$$

Now $(t_i - t_L) = \dfrac{1}{m}(\theta_i - \theta_L)$ where $m$ is the slope of a chord on the saturation line ($\theta_S$ vs. $t_S$)

$$\therefore \frac{1}{K_G} = \frac{(\theta_G - \theta_L)\,dA}{G\,di_G} = \frac{1}{k_G} + \frac{m}{h_L} \qquad (25)$$

Equation (25) is identical with the expression for the overall coefficient in gas absorption,

where $m$ is the slope of the equilibrium line. For the system under consideration, $m$ increases rapidly with temperature, thus there is a corresponding decrease in the value of $K_G$. This is a particular case of the general axiom, that if the tie-line slope is assumed is too steep, the value of $k_G$ so determined will decrease with temperature. If therefore the unit can be divided into two sections of equal area, the tie-line slope can be adjusted until the calculated values for $k_G$ in the two halves are equal. For a multipass tubular condenser this is possible if the interpass water temperatures are recorded. The water velocity must however be such that thermosyphoning, as described by Pollard [10] is avoided. In direct contact apparatus, where it is not possible to measure intermediate temperatures, the humidity of the gas could be determined by aspirating a sample through a wet and dry bulb hygrometer. This third method of ascertaining the correct tie-line slope should therefore be more applicable to test data on full scale plant obtained under working conditions.

The graphical method which has been developed requires a knowledge of the enthalpy and the transfer potential of moist gas and the relationship between these two properties. This relationship is obtained from the psychrometric chart, the construction of which is described below.

## 8. Construction of a Psychrometric Chart for Moist Coal Gas

The psychrometric chart is based on a plot of humidity vs. temperature, and these data may be obtained for coal gas from Spiers 5th edn., Table 111. A convenient unit for gas industry purposes, is pounds of water vapour per 1,000 cu. ft. of gas at S.T.P., abbreviated to lbs./-S.G.V. When the humidity saturation line has been constructed, the plot of $\alpha_S H_S$ may be added using the appropriate values in Table 1 for $\alpha$.

As stated previously, lines of "constant transfer potential" are straight lines on the psychrometric chart of slope $-E/\lambda_W$. $E$ is

*Table* 1.

| 1 | 2 | 3 | 4 | 5 | 6 | 7 | 8 | 9 | 10 | 11 | 12 | 13 |
|---|---|---|---|---|---|---|---|---|---|---|---|---|
| $t_S$ °F | $H_S$ lbs./ (S.G.V.) | $\alpha_S$ | $c_G (t_S - t_0)$ B.Th.U./ (S.G.V.) | $\lambda_0 H_S$ B.Th.U./ (S.G.V.) | $c_V H_S (t_S - t_0)$ B.Th.U./ (S.G.V.) | $i_S$ B.Th.U./ (S.G.V.) | $E_1 (t_S - t_0)$ B.Th.U./ (S.G.V.) | $E_2 (t_S - t_0)$ B.Th.U./ (S.G.V.) | $\lambda_S \alpha_S H_S$ B.Th.U./ (S.G.V.) | $\theta_{S1}$ B.Th.U./ (S.G.V.) | $\theta_{S2}$ B.Th.U./ (S.G.V.) | $c_G + 0{\cdot}45 H_S$ B.Th.U./ (S.G.V.) |
| 40 | 0·390 | 0·996 | 160 | 420 | 1·40 | 581 | 222 | 146 | 416 | 638 | 562 | 20·18 |
| 50 | 0·573 | 0·994 | 360 | 617 | 4·64 | 982 | 499 | 329 | 607 | 1,106 | 936 | 20·26 |
| 60 | 0·829 | 0·991 | 560 | 892 | 10·48 | 1,462 | 776 | 512 | 871 | 1,647 | 1,383 | 20·37 |
| 70 | 1·183 | 0·987 | 760 | 1,278 | 21·8 | 2,055 | 1,053 | 695 | 1,231 | 2,284 | 1,926 | 20·53 |
| 80 | 1·669 | 0·982 | 960 | 1,796 | 36·0 | 2,792 | 1,330 | 878 | 1,720 | 3,050 | 2,598 | 20·76 |
| 90 | 2·332 | 0·976 | 1,160 | 2,509 | 60·9 | 3,730 | 1,607 | 1,061 | 2,375 | 3,982 | 3,436 | 21·05 |
| 100 | 3·234 | 0·969 | 1,360 | 3,480 | 98·8 | 4,939 | 1,884 | 1,244 | 3,250 | 5,134 | 4,494 | 21·45 |
| 110 | 4·440 | 0·957 | 1,560 | 4,777 | 156 | 6,493 | 2,161 | 1,427 | 4,386 | 6,547 | 5,818 | 22·00 |
| 120 | 6·093 | 0·940 | 1,760 | 6,556 | 242 | 8,558 | 2,438 | 1,610 | 5,879 | 8,317 | 7,489 | 22·74 |
| 130 | 8·347 | 0·916 | 1,960 | 8,981 | 368 | 11,310 | 2,715 | 1,793 | 7,800 | 10,515 | 9,593 | 23·76 |
| 140 | 11·47 | 0·890 | 2,160 | 12,340 | 556 | 15,060 | 2,992 | 1,976 | 10,350 | 13,340 | 12,330 | 25·15 |
| 150 | 15·89 | 0·857 | 2,360 | 17,100 | 844 | 20,300 | 3,269 | 2,159 | 13,720 | 16,990 | 15,880 | 27·15 |
| 160 | 22·39 | 0·819 | 2,560 | 24,090 | 1,290 | 27,940 | 3,546 | 2,342 | 18,330 | 21,880 | 20,670 | 30·05 |
| 170 | 32·40 | 0·764 | 2,760 | 34,860 | 2,011 | 39,630 | 3,821 | 2,525 | 24,610 | 28,480 | 27,140 | 34·58 |
| 180 | 49·19 | 0·686 | 2,960 | 52,920 | 3,275 | 59,150 | 4,101 | 2,710 | 33,410 | 37,510 | 36,120 | 42·12 |

$E_1$ = 27·7 B.Th.U/(S.G.V.) (°F). $E_2$ = 18·8 B.Th.U/(S.G.V.) (°F.)

expressed as B.Th.U./(S.G.V.)(°F) and $\lambda_W$ as B.Th.U./lb. The slope is therefore (lbs. $H_2O$/S.G.V.)/(°F). Lines of constant wet bulb temperature also have the slope of $-E\lambda/_W$, where $E$ is the experimentally determined constant for the wet and dry bulb hygrometer.

In the gas industry, the standard method of measuring the dew point of gas employs the G.L.C.C. hygrometer described in the Gas Examiners' General Directions [11]. The instrument factor for this hygrometer at 30 in. Hg. and 32°F is given as 0·42, i.e.

$$p_W - p = 0{\cdot}42\,(t - t_W) \qquad (26)$$

where $p$ is the partial pressure of the water vapour in mm in this instance. Expressing the water vapour content as lbs. $H_2O$/S.G.V.

$$(H_W - H_G) = \frac{0{\cdot}42 \times 18}{762 \times 0{\cdot}385}(t_G - t_W) \qquad (27)$$

or $$H_W - H_G = 0{\cdot}0258\,(t_G - t_W)$$

$$\therefore \quad h_G/k_G\,\lambda_0 = 0{\cdot}0258$$

$$h_G/k_G = 27{\cdot}7 \text{ B.Th.U./(S.G.V.)(°F)} \qquad (28)$$

As $\alpha H$ is the correct potential for humidity, the wet bulb lines terminate on this saturation line. If it is desired to use values for the rates other than 27·7 B.Th.U./(S.G.V.)(°F), then constant transfer potential lines and wet bulb lines are no longer coincident.

The enthalpy of moist gas may be expressed in the form

$$i_G = c_G\,(t_G - t_0) + c_V\,H_G\,(t_G - t_0) + \lambda_0\,H_G \qquad (29)$$

The three terms are the sensible heat of the dry gas, the sensible heat of the water vapour, and the latent heat of the water vapour, all related to the reference temperature $t_0$ (32°F). A constant value of 20 B.Th.U./(S.G.V.)(°F) is assumed for the specific heat of dry gas ($c_G$) over the range considered, based on the composition of Fulham mixed gas averaged over a year. The enthalpy at saturation

$$i_S = c_G\,(t_S - t_0) + c_V\,H_G\,(t_S - t_0) + \lambda_0\,H_S$$

In order to obtain a straight line plot on the humidity chart, a term "apparent enthalpy" is introduced, defined as

$$i_G' = c_G\,(t_G - t_0) + c_V\,H_S\,(t_S - t_0) + \lambda_0\,H_G \qquad (30)$$

$$\therefore\ i_G' - i_S = c_G\,(t_G - t_S) + \lambda_0\,(H_G - H_S) \qquad (31)$$

A line of "constant apparent enthalpy" ($i_G' - i_S = 0$) is thus a straight line of slope $-c_G/\lambda_0$ terminating at the saturation line ($H_S$ vs. $t_S$) on the psychrometric chart. The deviation between the true enthalpy and the apparent enthalpy is therefore given by

$$i_G - i_G' = c_V\,H_G\,(t_G - t_0) - c_V\,H_S\,(t_S - t_0)$$

The form taken by equation (32) is indicated in Fig. 4.

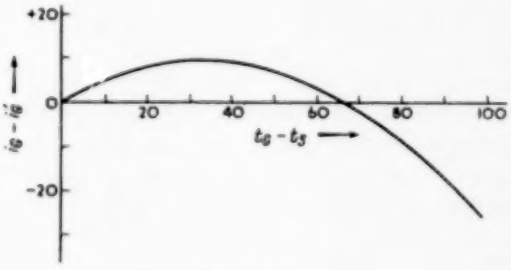


FIG. 4.

As $c_G$ and $\lambda_0$ are both constants, all lines of constant apparent enthalpy have the same slope on the psychrometric chart, namely

$$-\frac{20}{1076}\,(= -0{\cdot}0186) \qquad \text{B.Th.U./(S.G.V.)(°F)},$$

thus interpolation is a simple process. The difference between the true and apparent enthalpy is recorded for convenience on the chart as a series of curves of percentage deviation. It will be observed from Fig. 4 that it is possible to have three points where the deviation has the same absolute value, two being positive and one negative.

Two psychrometric charts, illustrated by Figs. 5 and 6, have been constructed in the manner described, covering different temperatures ranges. In calculating the enthalpy of moist gas a value of 0·45 B.Th.U./lb. for $c_V$ has been assumed throughout. This does not take into account the variations in specific heat with

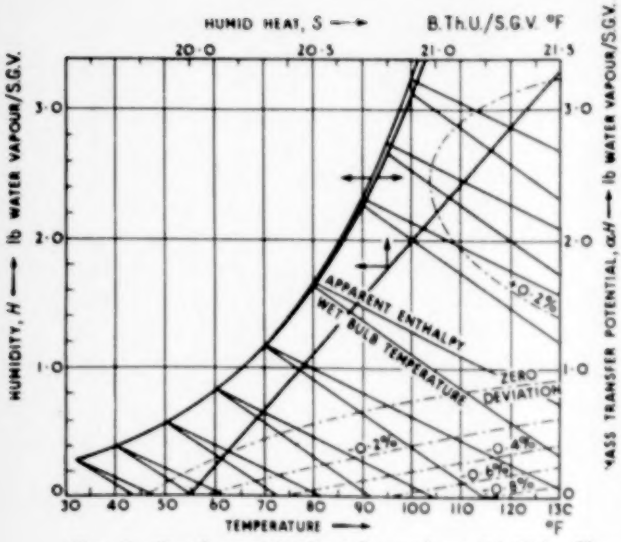


Fig. 5. Psychrometric chart for coal gas (at 30 in. Hg. pressure).

temperature and partial pressure, but these variations are within the accuracy of the charts. The most severe limitation of the charts is that they apply to a single total pressure, and other charts must be prepared for pressures other than 30 in. of mercury.

The data used in the construction of the charts and that required for the graphical method are summarized in Table 1.

## 4. An Example of the Use of the Charts

*Example* 1—Consider moist gas at 120°F with a dew-point of 60°F, entering a washer cooler. What is the maximum theoretical temperature to which the cooling water will rise?

The theoretical maximum temperature for the water is that at which the moist gas and the water are in equilibrium. Assuming that the ratio $E$ for the washer-cooler is equal to that for the wet and dry bulb hygrometer, then the wet bulb temperature is the criterion.

From the chart the wet bulb temperature for gas at 120°F with a dew-point of 60°F is 83·0°F. If enthalpy were considered as the driving force then the limiting temperature would be that given by a constant enthalpy line, namely 78·8°F.

## 5. Application of the Graphical Method to Condenser Design

Pollard [12] describes a test on a cross-flow water-tube condenser, and compares the area calculated by the method of Colburn and Hougen [1] with the known area. Although the gas and water flown in such a condenser are not truly countercurrent, the example does provide an opportunity of comparing the proposed graphical method with the laborious

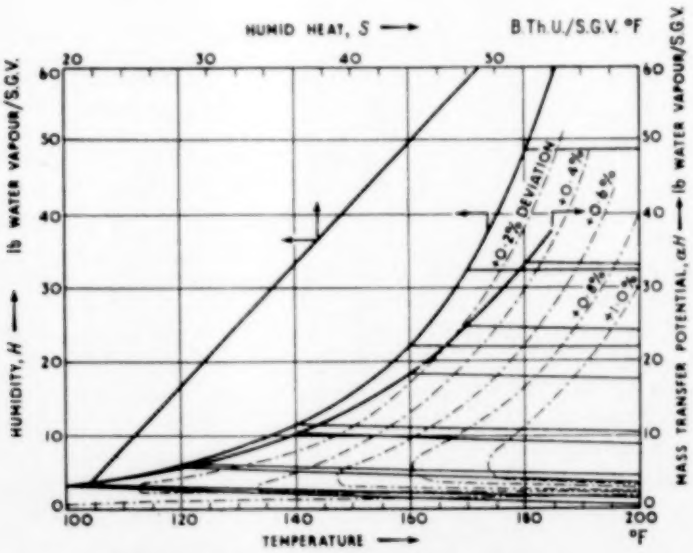


Fig. 6. Psychrometric chart for coal gas (at 30 in. Hg. pressure).

trial and error method of COLBURN and HOUGEN.

*Example 2.—Cross Tube Flow Cooler.*

Gas Rate = 4,000 cu. ft./hr. at S.T.P. = 4 S.G.V./hr.
Cooling Range = 160°F to 53°F.
Saturation Temperature of Inlet Gas = 156·5°F.
Water Rate = 2,000 lbs./hr.
Water Temperature Range = 44·5° to 91·5° = 47°F.
Enthalpy of Inlet Gas = 25,000 B.Th.U./S.G.V.
Enthalpy of Outlet Gas = 1,100 B.Th.U./S.G.V.

Slope of Operating Line $= \frac{23{,}900}{47} = 509$ B.Th.U./(S.G.V.)(°F). The values for the individual film coefficients used by POLLARD are calculated values and allowance is made for varying conditions of gas and water flow. The proposed graphical method requires that mean values of the individual coefficients be used. The relationship between $h_G$, $k_G$ and $h_L$ and the nomenclature used by POLLARD are as follows :

$$h_G = h_S, \quad k_G = \frac{K \cdot p_{gF}}{2{\cdot}60} \quad \text{and} \quad h_L = h_0$$

The mean values for the individual coefficients based on those calculated by POLLARD are :

$$h_G = 10 \text{ B.Th.U/(ft}^2\text{)(hr.)(°F).}$$

$$k_G = 1{\cdot}42 \frac{\text{lb. moles}}{\text{hr.}}/(\text{ft}^2)\left(\frac{\text{atm.}}{\text{atm.}}\right)$$

$$= 0{\cdot}546 \frac{\text{lbs.}}{\text{hr.}}/(\text{ft}^2)\ (\text{lbs./(S.G.V.)})$$

$$h_L = 80 \text{ B.Th.U./(ft}^2\text{) (hr.) (°F).}$$

$$\therefore \quad E = h_G/k_G = 18{\cdot}3 \text{ B.Th.U./(S.G.V.) (°F).}$$

and $\quad h_L/k_G = 147$ B.Th.U./(S.G.V.) (°F).

It will be observed that the value of $E$ calculated by the $j$ factor method of CHILTON and COLBURN is approximately two thirds of the value obtained from the wet and dry bulb hygrometer. In order to obtain an exact comparison between the COLBURN and HOUGEN method and the graphical method, an enthalpy transfer potential based on $E = 18{\cdot}3$ B.Th.U./(S.G.V.)(°F) will be used. This function appears in Table 1, as column 12.

It will also be assumed that the gas rapidly approaches saturation and remains in this condition throughout the condenser. This simplifies the problem considerably, as the enthalpy of the gas and its enthalpy transfer potential are functions of the same saturation temperature and the use of the psychrometric chart is obviated, once the terminal conditions have been established. The validity of this assumption which is inherent in the COLBURN and HOUGEN method, will be discussed later.

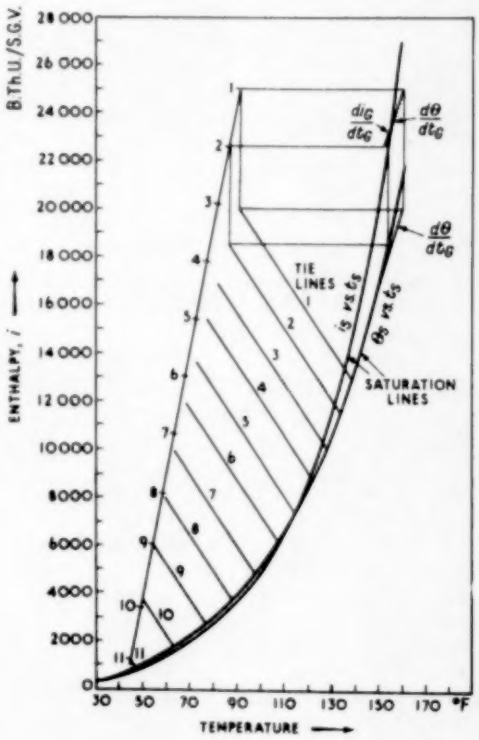


FIG. 7.

Fig. 7 is the graphical solution of the problem with tie-lines drawn in at ten equal increments of gas enthalpy. The values of gas enthalpy, water temperature and transfer potential of the gas and the interface are given in Table 2.

The value $1/\theta_G - \theta_i$ for each tie-line is given in Table 3 and $di_G \times 10^{-3} = 2{\cdot}390$ B.Th.U./S.G.V. By Simpson's Rule $\int \frac{di_G}{(\theta_G - \theta_i)} = \frac{2{\cdot}39}{3} \times 10{\cdot}61 = 8{\cdot}45$ Transfer units

$$A = 8{\cdot}45 \times \frac{4}{0{\cdot}546} = 61{\cdot}9 \text{ sq. ft.}$$

*Table 2.*

| $t_L$ °F | $i_G \times 10^{-3}$ B.Th.U./ S.G.V. | $\theta_G \times 10^{-3}$ B.Th.U./ S.G.V. | $\theta_i \times 10^{-3}$ B.Th.U./ S.G.V. | $(\theta_G - \theta_i) \times 10^{-3}$ B.Th.U./ S.G.V. | $\alpha_S H_S (\lambda_i - \lambda_S) \times 10^{-3}$ B.Th.U./ S.G.V. | $\frac{1}{(\theta_G - \theta_i) + \alpha_S H_S (\lambda_i - \lambda_S) \times 10^{-3}}$ B.Th.U./ S.G.V. |
|---|---|---|---|---|---|---|
| 91·5 | 25·00 | 18·90 | 11·95 | 6·95 | 0·164 | 0·1405 |
| 86·8 | 22·61 | 17·35 | 10·47 | 6·88 | 0·166 | 0·1419 |
| 82·1 | 20·22 | 15·90 | 9·12 | 6·78 | 0·164 | 0·1440 |
| 77·4 | 17·83 | 14·25 | 7·73 | 6·52 | 0·164 | 0·1496 |
| 72·7 | 15·44 | 12·50 | 6·42 | 6·08 | 0·154 | 0·1604 |
| 68·0 | 13·05 | 10·90 | 5·29 | 5·61 | 0·140 | 0·1739 |
| 63·3 | 10·66 | 9·07 | 4·17 | 4·90 | 0·121 | 0·1992 |
| 58·6 | 8·27 | 7·25 | 3·12 | 4·12 | 0·097 | 0·2371 |
| 53·9 | 5·88 | 5·29 | 2·21 | 3·08 | 0·068 | 0·3188 |
| 49·2 | 3·49 | 3·25 | 1·43 | 1·82 | 0·037 | 0·5380 |
| 44·5 | 1·10 | 1·05 | 0·78 | 0·27 | 0·004 | 3·651 |

The value $1/\theta_G - \theta_i$ for each tie-line is given in Table 3 and $di_G = 10^{-3} \times 2{\cdot}390$ B.Th.U./S.G.V.

*Table 3. Value of the tie-line slope.*

| $t_L$ | − 147 B.Th.U./(S.G.V.)(°F) | | ∞ | | − 80 B.Th.U./(S.G.V.)(°F) | |
|---|---|---|---|---|---|---|
| | $\theta_G - \theta_i$ | $1/\theta_G - \theta_i$ | $\theta_G - \theta_i$ | $1/\theta_G - \theta_i$ | $\theta_G - \theta_i$ | $1/\theta_G - \theta_i$ |
| 91·5 | 6·95 | 0·1439 | 15·31 | 0·0653 | 4·40 | 0·2278 |
| 86·8 | 6·88 | 0·1453 | 14·22 | 0·0703 | 4·40 | 0·2278 |
| 82·1 | 6·78 | 0·1497 | 13·13 | 0·0761 | 4·40 | 0·2273 |
| 77·4 | 6·52 | 0·1534 | 11·85 | 0·0844 | 4·33 | 0·2309 |
| 72·7 | 6·08 | 0·1645 | 10·41 | 0·0962 | 4·11 | 0·2433 |
| 68·0 | 5·61 | 0·1783 | 9·10 | 0·1099 | 3·90 | 0·2564 |
| 63·3 | 4·90 | 0·2041 | 7·55 | 0·1325 | 3·54 | 0·2825 |
| 58·6 | 4·12 | 0·2427 | 5·96 | 0·1678 | 3·07 | 0·3257 |
| 53·9 | 3·08 | 0·3247 | 4·21 | 0·2375 | 2·39 | 0·4184 |
| 49·2 | 1·82 | 0·5495 | 2·36 | 0·4237 | 1·46 | 0·6849 |
| 44·5 | 0·27 | 3·704 | 0·85 | 2·857 | 0·24 | 4·167 |
| $N_T$ | 8·45 | | 5·90 | | 10·88 | |
| $N_H$ | 3·50 | | 2·10 | | 5·05 | |
| $N_H/N_T$ | 0·414 | | 0·356 | | 0·464 | |

$N_T$ = Number of enthalpy transfer units corresponding to total area.
$N_H$ = Number of enthalpy transfer units correpsonding to half the area (91·5°F to 53·9°F).

This compares with 61·4 × 1·6 sq. ft. calculated by Pollard. His addition of 1·6 sq. ft. for the range 160°F to 156·5°F is not valid because it assumes that no latent heat is transferred in this range. Referring to Fig. 7, the assumption is that the initial gas path is one of constant humidity ($dH = 0$). The initial slope of $di_G/dt_G$ by graphical construction gives an enthalpy of 23,200 B.Th.U./S.G.V. at 156·5°F, a decrease of 1,800 B.Th.U./S.G.V. The amount of superheat in gas at 160°F saturated at 156·5°F is only 100 B.Th.U./S.G.V. thus the correction should be $\frac{100}{1800} \times 1{\cdot}6$ or approximately 0·1 sq. ft. of

the 1·6 sq. ft. observed. The area therefore of 61·9 sq. ft. calculated by the proposed graphical method agrees with that calculated by the method of COLBURN and HOUGEN (61·5 sq. ft.) to within 1%.

It has been stated previously that the true driving force is given by the expression

$$(\theta_G - \theta_i) + (\lambda_i - \lambda_S)\,\alpha_S\,H_S$$

The magnitude of the deviation, the second term in the expression, appears at the sixth column in Table 2. The last column gives value of $1/[(\theta_G - \theta_i) + (\lambda_i - \lambda_S)\,\alpha_S\,H_S]$. By Simpson's Rule $\int \frac{di_G}{(\theta_G - \theta_i) + (\lambda_i - \lambda_S)\,\alpha_S\,H_S} = \frac{2{\cdot}39}{3} \times 10{\cdot}40 = 8{\cdot}28$.

$$A = 8{\cdot}28 \times \frac{4}{0{\cdot}546} = 60{\cdot}7 \text{ sq. ft.}$$

The effect therefore of omitting the deviation is to obtain an area 2% in excess of that obtained by using the true driving force. For design purposes the error is in the right direction, but when determining coefficients allowance should be made for the reduction in driving force.

In order to check whether the ratio $h_L/k_G$ assumed corresponds to the observed facts, a knowledge of the water temperature at the junction of the third and fourth passes (corresponding to half the transfer area) is required. Unfortunately POLLARD does not give these data for the test considered, but from the profiles given in Fig. 1 of his paper, one may assume it is approximately 53·9°F. This temperature is selected for convenience in demonstrating the method, as it corresponds to eight out of the ten increments of gas enthalpy. Values of $(\theta_G - \theta_i)$ have been obtained from Fig. 7 for two other tie-line slopes, and the number of transfer units corresponding to eight and ten increments calculated. The results are summarized in Table 3.

The reasons for selecting the two other values for the tie-line slopes are as follows. Infinite slope implies zero liquid film coefficient and $t_i = t_L$. The number of transfer units may be calculated for this case without graphical construction of the tie lines. The latter value of $-80$ B.Th.U./(S.G.V.)(°F) is assumed to be in the region of the correct value.

The effect of plotting the ratio $N_H/N_T$ against the reciprocal of the tie-line slope is shown in Fig. 8. The fact that the three points are colinear is fortuitous as this relationship cannot be established from equation (25). Assuming $k_G$ is a constant, the ratio $N_H/N_T$ should equal one half, if the tie-line slope is correct. If therefore 53·9°F was the correct mid-point temperature the correct tie-line slope obtained by extrapolation would be $-60$ B.Th.U./(S.G.V.)(°F). Normally the plot obtained will not be a straight line and the correct tie-line slope should be obtained by interpolation rather than extrapolation.

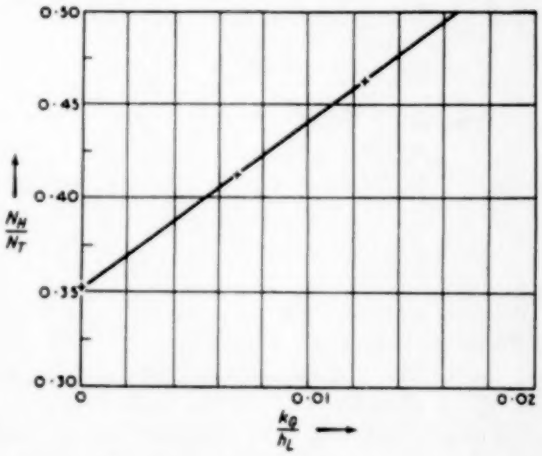


FIG. 8. Correct slope of $h_L/k_G$ by extrapolation $= -60$ B.Th.U./(S.G.V.)(°F).

It is appreciated that $k_G$ cannot be a constant throughout the condenser due to the large change in humidity of the gas and thus in the true mass flow of the mixture. In this example the calculated value of $k_G$ at the hot end is 1·28 times the value at S.T.P. If $h_L$ remains substantially constant, the effect of the increased value of $k_G$ is to decrease the tie-line slope and hence the value of $(\theta_G - \theta_i)$. The total heat flux however depends on the product $k_G\,(\theta_G - \theta_i)$ and the two factors compensate one another. The compensation would be exact if the equilibrium line were of infinite slope. This is not so, but the slope

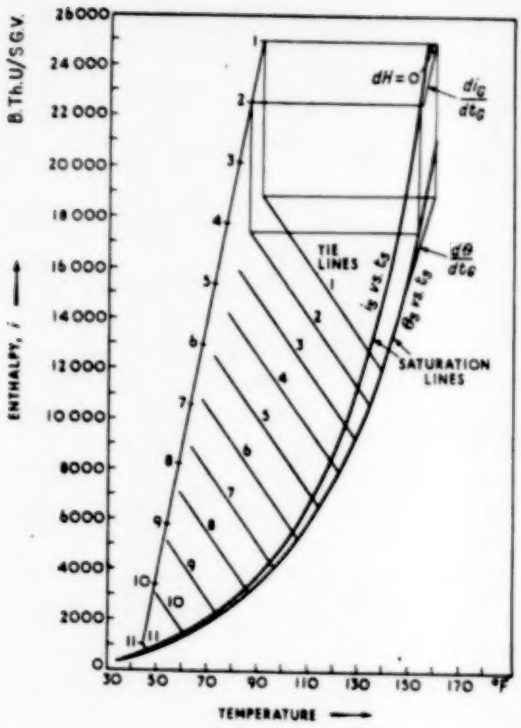


FIG. 9.

increases with humidity as does the mass flow, and the residual error is small.

Fig. 9 is the graphical solution of the problem using an enthalpy transfer potential based on 27·7 B.Th.U./(S.G.V.)(°F) and the same values for $k_G$ and $h_L$. The resulting number of transfer units is 7·70 corresponding to an area of 56·4 sq. ft. The area is smaller, because the assumed transfer potential implies a heat transfer coefficient ($h_G$) equal to 15·0 B.Th.U./ft.$^2$ hr. °F as against 10·0 B.Th.U./ft$^2$ hr °F.

It will be observed from Fig. 9 that the effect of taking $E$ equal to 27·7 B.Th.U./(S.G.V.)(°F) is that the gas approaches saturation more rapidly. The construction indicates, in fact, that the gas becomes supersaturated, i.e. fog formation occurs. Under these conditions the basic differential equations no longer holds and all methods, including that of COLBURN and HOUGEN, become approximations. If the true value of $E$ is as high as 27·7 B.Th.U./(S.G.V.)(°F), then the ratio $b/\alpha$ will exceed unity over the whole range considered. Consequently the rate of mass transfer will be less than that required to keep the gas saturated, and fogging will occur with gas that is initially saturated. Water condensing in the bulk of the gas reduces the total quantity of heat to be transferred across the interface, and a smaller area is required.

Even when the ratio $b/\alpha$ is less than unity, fog formation is still possible, because on a curve of rapidly increasing slope such as the saturation line, the slope of a chord is inevitably much less than the slope of the curve at the upper extremity of the chord. Insufficient importance has been attached to the formation of fog in cooler-condensers, and care should be taken to see that coefficients determined under fogging conditions are not applied to the design of plant in which such conditions do not exist.

Although the method has been described with specific reference to moist coal gas, it can be applied to any other system for which the requisite data are available or may be calculated. Furthermore the integral $\int di_G/\theta_G - \theta_i$ may be evaluated by the other methods described in the literature on simultaneous heat and mass transfer.

**Acknowledgements**—The authors wish to express their indebtedness to Mr. G. F. EDWARDS for preparing the diagrams and assisting in the calculations and to the Gas Council and the North Thames Gas Board for permission to publish this paper.

## NOMENCLATURE

$A$ = area of transfer surface [ft$^2$]
$E$ = ratio of transfer coefficients $h_G/k_G$ [B.Th.U./(S.G.V.)(°F)]
$G$ = gas flow [S.G.V./hr]
$H$ = humidity [lbs/S.G.V.]
$K$ = overall coefficient of enthalpy transfer [lbs./(hr.)(ft$^2$)($\Delta\theta$)]
$L$ = mass flow of liquid [lbs./hr]
$N$ = number of gas film enthalpy transfer units
$P$ = total pressure [in. of mercury]
$b$ = Lewis Number $h_G/k_G s$
$c$ = heat capacity [B.Th.U./(S.G.V.)(°F)] or [B.Th.U./(lb.)(°F)]
$h$ = heat transfer coefficient [B.Th.U./(ft$^2$)(°F)]
$i$ = enthalpy [B.Th.U./S.G.V.]
$i'$ = apparent enthalpy [B.Th.U./S.G.V.]

$k$ = mass transfer coefficient [lbs./(ft$^2$)(hr.)($\Delta x$H)]
or enthalpy transfer coefficient [B.Th.U./(ft$^2$)(hr)($\Delta\theta$)]
$m$ = slope of saturation line $d\theta_S/dt_S$ [B.Th.U./(S.G.V.)(°F)]
$p$ = partial pressure of diffusing vapour (in. of mercury]
$q$ = heat flux [B.Th.U./(hr)(ft$^2$)]
$s$ = humid heat $c_G + 0{\cdot}45\,H$ [B.Th.U./(S.G.V.)(°F)]
$t$ = temperature [°F]
$\alpha$ = humidity correction factor
$z$ = fractional distance thourgh the gas film
$\theta$ = enthalpy transfer potential [B.Th.U./(S.G.V.)(°F)]
$\lambda$ = latent heat [B.Th.U./lb.]

*Subscripts*

$G$ = gas or gas film coefficient
$i$ = interface
$L$ = liquid or liquid film coefficient
$S$ = saturation
$V$ = vapour phase
$W$ = wet bulb conditions
$O$ = reference conditions (32°F)

## References


[1] Colburn, A. P. and Hougen, O. A.; *Industr. Engng. Chem.* 1934 **26** 1178.

[2] Colburn, A. P.; *Proceedings of The General Discussion on Heat Transfer*, p. 1. Inst. of Mech. Eng., 1951.

[3] Mickley, H. S.; *Chem. Engng. Prog.* 1949 **45** 739.

[4] Colburn, A. P. and Drew, T. B.; *Trans. Amer. Inst. Chem. Eng.* 1937 **33** 197.

[5] Lewis, J. G. and White, R. R.; *Industr. Engng. Chem.* 1953 **45** 486.

[6] Sherwood, T. K. and Pigford, R. L.; *Absorption and Extraction 2nd edn.* (McGraw-Hill) 1952, p. 6.

[7] *Technical Data on Fuel*, 5th edn., 141, 1952.

[8] Chilton, T. H. and Colburn, A. P.; *Industr. Engng. Chem.* 1934 **26** 1183.

[9] Hensel, S. L. and Treybal, R. E.; *Chem. Engng. Prog.* 1952 **48** 362.

[10] Pollard, R.; *The Gas World* – Coking Section 1954 **139** 1st May.

[11] *Gas Examiners' General Directions*, 31, H.M.S.O. 1950.

[12] Pollard, R.; *Man. and Dist. Jun. Assoc. of Gas Engineers*, 18th April, 1953.

Chemical Engineering Science, 1956, Vol. 5, pp. 34 to 40. Pergamon Press Ltd.

# The separation of common gases by thermal diffusion

W. J. THOMAS and S. B. WATKINS
Chemical Engineering Department, King's College, University of London

(*Received* 24 *July*, 1955 ; *revised version* 12 *November*, 1955)

**Asbtract**—The separation of common gases in pilot plant thermal diffusion columns has been investigated. The effects of the variables temperature, concentration, flow conditions, and column dimensions have been obtained experimentally.

Results show that the equations deduced for isotopes apply to common gases in certain limited cases : that turbulence reduces enrichment, but that it is offset to some extent by a probable effective reduction in annulus width. Continuous operation of columns demonstrates a marked adverse effect of increase in withdrawal rates, which have to be greater than those normally used for isotope separation, if the method is to have industrial importance. Consequently, the column separation performance factors $H$ and $K$, normally assumed independent of the small withdrawal rates for the case of isotopes, are no longer so for common gases. It is apparent that, for the separation of common gases, pilot plant design data is essential, and that a semi-empirical approach is necessary in the absence of theory relating the withdrawal effects.

**Résumé**—Les auteurs ont étudié la séparation des gaz usuels dans une installation pilote de colonnes de diffusion. Ils ont étudié expérimentalement l'influence des variables : température, concentration, conditions d'écoulement, dimensions de la colonne.

Les résultats montrent que les équations valables pour les isotopes s'appliquent aux gaz usuels dans certains cas limites : à savoir que la turbulence réduit l'enrichissement, effet compensé dans une certaine mesure par une réduction efficace probable de la largeur annulaire.

Les opérations continues mettent én évidence un effet notable antagoniste de l'augmentation de la vitesse de soutirage : pour que la méthode ait une importance industrielle, cette vitesse de soutirage doit être supérieure aux vitesses normalement utilisées pour la séparation des isotopes. Par suite, les facteurs H et K d'efficacité de fonctionnement des colonnes qu'on suppose habituellement indépendants des petites vitesses de soutirage dans les cas des isotopes ne le sont plus dans les cas des gaz usuels.

Il est évident que, pour la séparation des gaz usuels, il est nécessaire de disposer de données d'installations pilotes et de procéder semi-empiriquement en l'absence de théorie relative aux effets de soutirage.

## INTRODUCTION

WHEN a gas mixture is passed through an annulus across which there is a temperature difference, a separation of the components of the mixture occurs by thermal diffusion. The effect was anticipated by CHAPMAN [1] and ENSKOG [2], and considerable experimental work by IBBS [3] substantiated the theory.

The effect is considerably enhanced by the convective flow of the gases on the walls of a vertical separation column. This was demonstrated experimentally by CLUSIUS and DICKEL [4], who also proposed a preliminary analysis of the hydrodynamics of such columns. These columns have received considerable attention for the purpose of isotope separation.

The theoretical hydrodynamics of the process has been examined by CLUSIUS and DICKEL [4], JENSEN [5], STEINWEDEL [6], and WALDMAN [7] of the German school, and by FURRY [8, 9], ONSAGER [8], and JONES [8, 9] of the American school. The principal references mentioned contain a large number of additional references to isotope separation. The important features of the design of columns for such separations are the similarity of the molecules concerned, and the exceedingly small withdrawal rates used.

There is little information on the application

of the existing theories, which were specifically derived for isotopes, to the design of columns for the separation of industrial gases.

The following results of a pilot plant investigation of the separation of mixtures of hydrogen, carbon monoxide, carbon dioxide, and nitrogen by thermal diffusion, give an indication of the complexity of the design problem.

## General Principles

For "total reflux" or "discontinuous" operation, the net differential transport of the heavy component in a binary mixture is given by the differential equation

$$\tau = H \cdot c\,(1 - c) - K \cdot dc/dz \qquad (1)$$

The re-mixing effects opposing the separation by thermal diffusion are represented by the term $K \cdot dc/dz$. Furry further defined the individual re-mixing effects.

(i) convective re-mixing, $k_c$
(ii) re-mixing due to back diffusion along the column, $k_d$
(iii) re-mixing due to asymmetrical effects, $k_p$

Then

$$K = k_c + k_d + k_p$$

Under total reflux conditions the net differential transport of the heavy component $\tau$, is zero. Hence between appropriate limits,

$$N = \frac{L}{(K/H)} = \ln_e \frac{c_z\,(1 - c_0)}{c_0\,(1 - c_z)}$$

where $K/H = \frac{1}{2}A$, and corresponds to the "ideal separation length" proposed by the German school. Then $N$ becomes the number of ideal separation lengths corresponding to a column height $L$, under given conditions of concentration and temperature. In the following work, the results are calculated with common logarithms, so that $N' = N/2{\cdot}303$.

According to the theory, $H$ and $K$ are constants for any apparatus, their values being determined by the properties of the gas mixtures, and the dimensions of the separating columns. For simplified conditions, which apply to the annular columns in the following experimental work, Furry proposed the use of the "plane parallel case." The properties of the gas mixtures are taken at the arithmetic mean temperature of the annulus. The expressions for the constants proposed by Furry are then as follows.

$$H = \frac{\alpha \cdot \rho^2 \cdot g \cdot w^3 \cdot B}{96\eta} \left[\frac{\Delta T}{\overline{T}}\right]^2 \qquad (3)$$

$$\left.\begin{aligned} k_c &= \frac{\rho^3 \cdot g^2 \cdot w^7 \cdot B}{2304 \cdot \eta^2 \cdot D} \left[\frac{\Delta T}{\overline{T}}\right]^2 \\ k_d &= 2 \cdot w \cdot B \cdot \rho \cdot D \\ k_p &= 2 \left[\frac{B}{w}\right]^2 \left[\frac{\partial T}{\Delta T}\right]^2 \cdot k_c \end{aligned}\right\} \qquad (4)$$

These expressions are developed on the assumption that no convective turbulence exists in the annuli. For the truly plane case, Furry suggests that turbulence occurs when $Re \geq 25$, and for safe working $Re \leq 10$.

$$Re_c = \frac{w^3 \cdot g \cdot \rho^2}{48 \cdot \eta^2} \frac{\Delta T}{\overline{T}} \qquad (5)$$

It will be evident from the equations that transport is aided by large values of $w$ and $B$, but at the expense of increase in re-mixing effects, and decreases in separation. This is characteristic of thermal diffusion columns, necessitating a compromise which can be made eventually only on a basis of experimental work.

For continuous operation, of a column where a definite amount of concentrated material is withdrawn continuously, the differential equations of Steinwedel or Furry may be used. The integrated Steinwedel equation has been preferred for this work.

$$L = \frac{I}{(2A) \times 2\Gamma} \cdot \log_{10} \frac{\left[c_z - \frac{1+\gamma}{2} + \Gamma\right]\left[c_0 - \frac{1+\gamma}{2} - \Gamma\right]}{\left[c_z - \frac{1+\gamma}{2} - \Gamma\right]\left[c_0 - \frac{1+\gamma}{2} + \Gamma\right]} \qquad (6)$$

where

$$\gamma = \sigma H \text{ and } \Gamma = \sqrt{\left(\frac{1+\gamma}{2}\right)^2 - \gamma c_z}$$

To design a thermal diffusion column for separating a certain mixture, it would be necessary to establish :

(i) that existing hydrodynamic equations

satisfactorily correlate experimental results.

(ii) the values of column transport coefficients for different sizes of columns under different conditions, and to show the effects of these variables on $H$ and $K$.

(iii) to what extent conditions approach turbulence without being too harmful to the separation.

(iv) how the constants or coefficients $H$ and $K$, once determined, can be used for scaling up plant.

## PROPOSED METHOD FOR DETERMINING THE EXPERIMENTAL VALUES OF THE COLUMN TRANSPORT FACTOR $H$ UNDER GIVEN CONDITIONS

A theoretical plot of the total reflux conditions in a column can be represented as in Fig. 1 (eq. 2). For the pilot plant column of length $L$, the ideal separation length $\frac{1}{2}A$ or $K/H$ would be fixed by the physical conditions and the dimensions of the

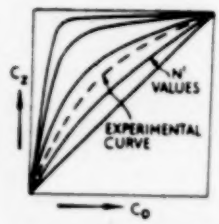


FIG. 1.
Constant $T$ and $\Delta T$.

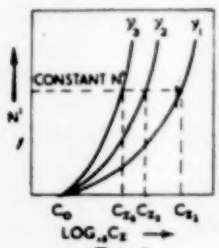


FIG. 2.
Constant $T$. $\Delta T$ and $C_0$.

apparatus. Accordingly, $N$ and $N'$ will have practical values for the set conditions. The value of $N'$ can be established by plotting $c_z$ versus $c_0$ from the experimental results of total reflux operation. As $L$ for the column is fixed, $N'$ yields an experimental value for $K/H$. If now an experimental value for $H$ could be obtained for the same column, then an experimental value of $K$ could be deduced.

The STEINWEDEL equation for continuous operation can be represented graphically as in Fig. 2 with constant initial concentration of heavy component $c_0$. For a practical column with fixed initial concentration $c_0$, the end-concentration $c_z$ corresponding to a series of withdrawal rates $\sigma_0$ can be determined experimentally. Under constant temperature conditions, a curve similar to that shown in Fig. 3 could be obtained from the results.

The $K/H$ and $N'$ values for the column are available from total reflux experiments. Choosing a value of $\sigma$ within the experimental range, say $\sigma_1$, the experimental end concentration corresponding to $c_0$ would be $c_z$ from Fig. 3. From Fig. 2, $N'$ and $c_0$ being fixed, the value of $\gamma$ could be determined which gives the correct $c_z$, viz. $c_{z_1}$. Suppose the value of $\gamma$ is $\gamma_1$, then $\gamma_1 = \sigma_1/H$ or

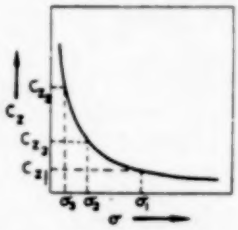


FIG. 3. Constant $T$, $\Delta T$, $C_0$ and $L'$.

$H = \sigma_1/\gamma_1$. In this way the value of $H$ corresponding to the experimental condition is determined.

Having obtained $(K/H)_{\text{expt.}}$ and $H_{\text{expt.}}$, and by deduction $K_{\text{expt.}}$, their values can be compared with theoretically calculated values. Such a comparison should indicate to what extent design could be fundamental for the case of common gases.

## DESCRIPTION ON THE PILOT PLANTS

Two plants were built. The first consisted of a single column 15 ft. high, gas heated, and the second of three 6 ft. electrically heated columns. The columns differed in their diameters and annuli widths. The dimensions are given in Table 1. Line diagrams of the columns, in Figs. 4 and 5, describe the construction. High water rates were maintained on the outside of the outer pipe for cooling, and the upper distribution ring was swathed in muslin to reduce splashing.

Needle valves on the separate heating-gas lines of the 15 ft. column permitted good control, and a reasonably uniform temperature along the length of the column.

The electrical heating of the 6 ft. columns was controlled through external resisters. The heaters were of nichrome wire threaded with recessed porcelain beads.



VOL. 5 1956

Connections were at the top only, and the wire and beads were plaited before inserting into the central tube. Temperature measurements on the periphery of the inner tube were not taken, so that it is not known to what

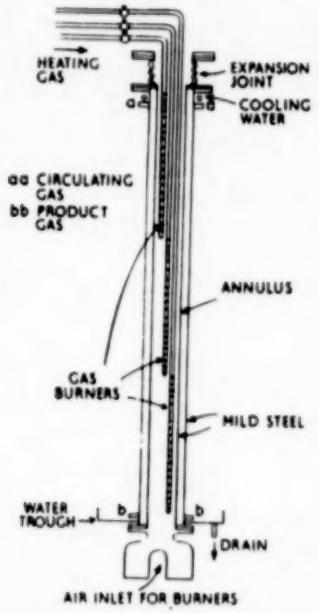


FIG. 4. 15 ft. column.

extent temperature asymmetry interfered with the separation. The effect would not be important for the two larger 6 ft. columns. The inner tubes of the 6 ft.

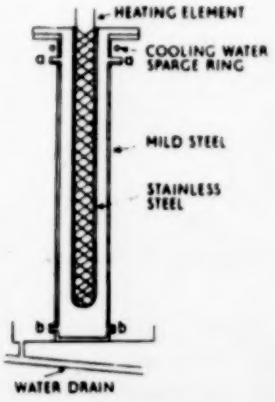


FIG. 5. 6 ft. column: aa—Circulating gas connections; bb—Product gas connections.

columns were of stainless steel, and it is now realized that for the smallest column the preferred material would be copper, as, with its much higher thermal conductivity, asymmetrical temperature effects would be minimized. Diametrical asymmetry was minimized by fitting a centralizing spider to the outside of the inner tube. The material used in the construction of the top flanges and the outer tubes was heavy gauge mild steel to obviate buckling under heat stress.

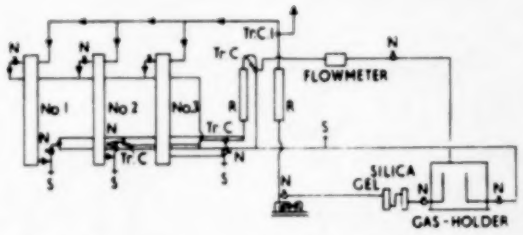


FIG. 6. Thermal diffusion pilot plant: *N* – needle valves *S* – sample cocks; *Tr.C* – three-way cocks.

A line diagram of one of the pilot plants is shown in Fig. 6. The columns could be operated in parallel or singly, and a re-arrangement was made later to operate in multistage.

Photographs (7 and 8) showing some detail and a general view of the plant are given in Figs. 7 and 8 respectively.

"Rotameters" were used to measure gas rate. They were calibrated for each mixture over the concentration range being measured, by means of a soapfilm bubble flow-meter.

Gas analysis was by means of a katharometer, and by direct Orsat. Small samples were taken, or the sampling spread over a period to cause least disturbance of the conditions.

For all cases, gas was circulated around the tops of the column at a relatively high rate (approx. 20 l/min.).

Continuous operation necessitated a balanced operation as the system was sensitive to small volume and pressure changes.

## EXPERIMENTAL RESULTS

These were obtained for the following mixtures. $H_2/CO_2$, $H_2/CO$, $CO/CO_2$, and $O_2/N_2$ in the three 6 ft. columns, and for $H_2/CO$ mixtures in the 15 ft. column.

The results cover both the "total reflux" or "discontinuous operation," and "continuous operation" having a finite fixed withdrawal rate.

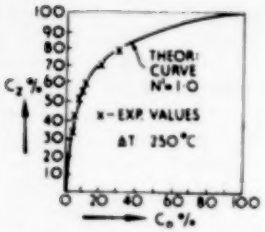


Fig. 9. Total reflux $H_2$-CO. 15 ft. column.

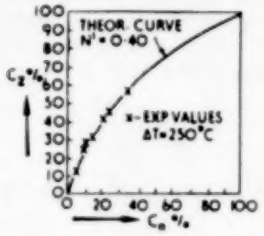


Fig. 10. Total reflux $H_2$-$CO_2$. Column 2.

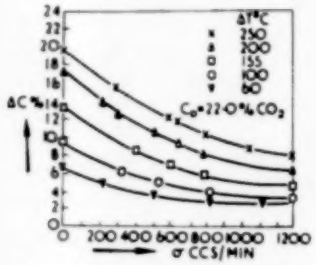


Fig. 11. Continuous operation $H_2$-$CO_2$. Column 2.

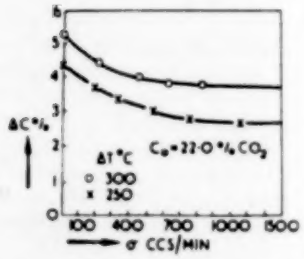


Fig. 12. Continuous operation $H_2$-$CO_2$. Column 1.

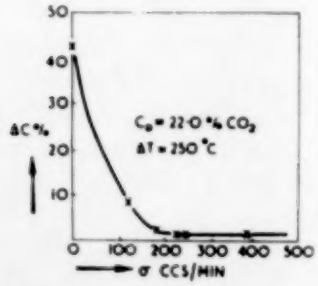


Fig. 13. Continuous operation $H_2$-$CO_2$. Column 3.

*Table* 1. *Column dimensions.*

| | | *Columns* | | | |
|---|---|---|---|---|---|
| | | 1 | 2 | 3 | 15 ft. |
| $2\pi$ | in. | $1^{11}/_{32}$ | $^{45}/_{64}$ | $^{6}/_{32}$ | $^{27}/_{32}$ |
| | cm. | 3·38 | 1·80 | 0·48 | 2·15 |
| Inner tube o/d | in. | $1^{11}/_{16}$ | $1^{11}/_{16}$ | $1^{21}/_{32}$ | $4^{17}/_{32}$ |
| Outer tube i/d | in. | $4^{3}/_{32}$ | $3^{3}/_{32}$ | $2^{1}/_{32}$ | $6^{7}/_{32}$ |
| $B = \pi\left[\frac{D_1 + D_2}{2}\right]$ | cm. | 23·05 | 19·10 | 14·60 | 42·80 |
| $L$ | ft. | 6 | 6 | 6 | 15 |

These are recorded in Tables 2—9 inclusive. Certain of these results are plotted in Figs. 9—13 inclusive. The corresponding tables and figures are as follows:—Table 2(*b*), Fig. 9; Table 2(*a*), Fig. 10; Table 5, Figs. 11, 12 and 13.

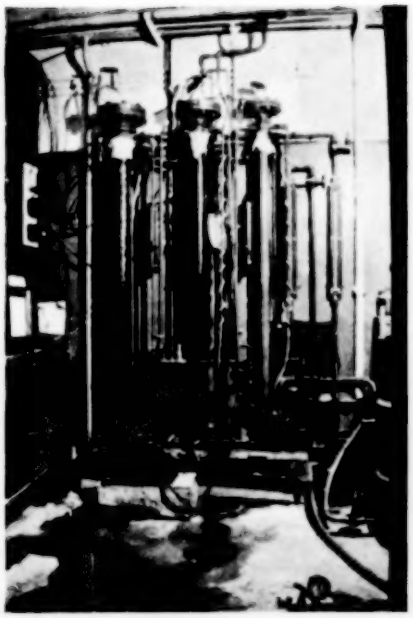

FIG. 7. A general view on the 6 ft. thermal diffusion columns.

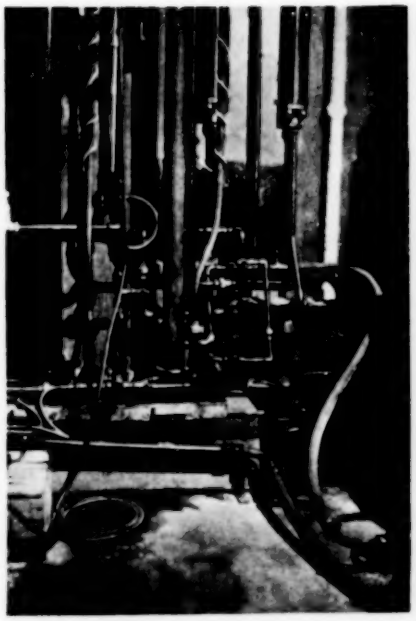

FIG. 8. A detail view around the main blower of the thermal diffusion plant.

*Table* 2 (*a*). *Discontinuous or total reflux operation* $H_2/CO_2$ *mixtures.* $c$ = %$CO_2$ *by volume in the mixture.*

| *Col. No.* | $2 \cdot w$ *cm* | $c_0$ | $c_z$ | $T_h$°C | $\Delta T$ | $[K/H]_{expt.}$ | $N'$ |
|---|---|---|---|---|---|---|---|
| 1 | 3·58 | 22·0 | 26·4 | 270 | 250 | 774 | 0·105 |
| | 3·58 | 22·0 | 27·5 | 320 | 300 | 615 | 0·129 |
| 2 | 1·80 | 22·0 | 29·0 | 80 | 60 | 505 | 0·157 |
| | 1·80 | 22·0 | 31·8 | 120 | 100 | 368 | 0·216 |
| | 1·80 | 22·0 | 35·5 | 175 | 155 | 276 | 0·288 |
| | 1·80 | 22·0 | 39·0 | 220 | 200 | 227 | 0·350 |
| | 1·80 | 22·0 | 41·2 | 270 | 250 | 205 | 0·388 |
| | 1·80 | 5·2 | 12·0 | 270 | 250 | 200 | 0·400 |
| | 1·80 | 10·0 | 23·2 | 270 | 250 | 183 | 0·434 |
| Fig. 10 | 1·88 | 12·5 | 27·0 | 270 | 250 | 192 | 0·412 |
| | 1·80 | 16·0 | 32·1 | 270 | 250 | 202 | 0·394 |
| | 1·80 | 22·0 | 40·8 | 270 | 250 | 190 | 0·388 |
| | 1·80 | 25·2 | 45·1 | 270 | 250 | 190 | 0·388 |
| | 1·80 | 35·2 | 56·0 | 270 | 250 | 216 | 0·367 |
| 3 | 0·48 | 22·0 | 63·0 | 270 | 250 | 102 | 0·790 |

*Table* 2 (*b*). $H_2/CO$. $c$ = % *CO by volume in the mixture.*

| *Col. No.* | $2 \cdot w$ *cm* | $c_0$ | $c_z$ | $T_h$°C | $\Delta T$ | $[K/H]_{expt.}$ | $N'$ |
|---|---|---|---|---|---|---|---|
| 1 | 3·58 | 15·0 | 18·6 | 270 | 250 | 735 | 0·110 |
| | 3·58 | 15·0 | 20·1 | 320 | 300 | 516 | 0·154 |
| 2 | 1·80 | 15·0 | 22·7 | 120 | 100 | 360 | 0·221 |
| | 1·80 | 15·0 | 27·0 | 220 | 200 | 247 | 0·322 |
| | 1·80 | 15·0 | 29·1 | 270 | 250 | 217 | 0·366 |
| | 1·80 | 15·0 | 30·8 | 320 | 300 | 198 | 0·401 |
| 3 | 0·48 | 15·0 | 30·6 | 270 | 250 | 200 | 0·398 |
| | 0,48 | 15·0 | 31·6 | 320 | 300 | 190 | 0·418 |
| | 0·48 | 15·0 | 32·5 | 375 | 355 | 184 | 0·434 |
| 15 ft. | 2·15 | 5·0 | 35·0 | 215 | 200 | 202 | 1·0 |
| | 2·15 | 6·2 | 43·3 | 215 | 200 | 191 | 1·06 |
| | 2·15 | 9·3 | 53·8 | 215 | 200 | 193 | 1·05 |
| Fig. 9 | 2·15 | 10·4 | 54·0 | 215 | 200 | 192 | 1·058 |
| | 2·15 | 13·5 | 60·5 | 215 | 200 | 194 | 1·046 |
| | 2·15 | 21·0 | 67·0 | 215 | 200 | 230 | 0·882 |

*Table* 3. *Discontinuous operation.* $H_2/CO$ (*water-gas*) 15 *ft. column.*

| | $c_0$ | | $c_z$ | |
|---|---|---|---|---|
| $CO_2$ | 2·60 | } 61·8 | 3·30 | } 89·6 |
| CO | 47·30 | | 66·30 | |
| $N_2$ | 11·90 | | 20·00 | |
| $H_2$ | 38·20 | | 10·40 | |

*Table 4 (a). Discontinuous operation. $O_2/N_2$.*

| Col. No. | $2 \cdot \pi$ | $c_0$ | $c_z$ | $T_h$°C | $\Delta T$ | $[K/H]_{expt.}$ | $N'$ |
|---|---|---|---|---|---|---|---|
| 2 | 1·80 | 21·0 | 22·4 | 270 | 250 | 2310 | 0·035 |
| 3 | 0·48 | 21·0 %$O_2$ | 26·6 | 320 | 300 | 398 | 0·135 |

*Table 4 (b). Discontinuous operation. $CO/CO_2$.*

| Col. No. | $2 \cdot \pi$ | $c_0$ | $c_z$ | $T_h$°C | $\Delta T$ | $[K/H]_{expt.}$ | $N'$ |
|---|---|---|---|---|---|---|---|
| 2 | 1·80 | 32·0 | 33·5 | 270 | 250 | 2700 | 0·030 |
| 3 | 0·48 | 32·0 %$CO_2$ | 46·2 | 270 | 250 | 308 | 0·262 |

*Table 3. Continuous operation $H_2/CO_2$. $c$ = % by volume. Withdrawal rate = $\sigma$ cc/min.*

$T_c = 20$°C, $c_0 = 22{\cdot}0$%, $CO_2$ $T_h = 270$°C, Column 2, Fig. 11.

| | | | | | | | | |
|---|---|---|---|---|---|---|---|---|
| $c_z$ | 41·2 | 38·4 | 36·1 | 34·2 | 33·6 | 32·0 | 30·8 | 29·7 |
| $\sigma$ | 0·0 | 220 | 400 | 580 | 640 | 860 | 1030 | 1280 |

$T_c = 20$°C, $c_0 = 22{\cdot}0$% $CO_2$, $T_h = 220$°C, Column 2, Fig. 11

| | | | | | | | |
|---|---|---|---|---|---|---|---|
| $c_z$ | 39·0 | 35·8 | 34·6 | 32·8 | 31·6 | 30·2 | 28·6 |
| $\sigma$ | 0·0 | 220 | 320 | 480 | 640 | 860 | 1280 |

$T_c = 20$°C, $c_0 = 22{\cdot}0$% $CO_2$, $T_h = 175$°C, Column 2, Fig. 11

| | | | | | |
|---|---|---|---|---|---|
| $c_z$ | 33·6 | 31·0 | 29·4 | 28·0 | 26·4 |
| $\sigma$ | 0·0 | 380 | 580 | 860 | 1300 |

$T_c = 20$°C, $c_0 = 22{\cdot}0$% $CO_2$, $T_h = 120$°C, Column 2, Fig. 11

| | | | | | |
|---|---|---|---|---|---|
| $c_z$ | 31·8 | 28·4 | 27·4 | 26·3 | 25·2 |
| $\sigma$ | 0·0 | 310 | 520 | 800 | 1280 |

$T_c = 20$°C, $c_0 = 22{\cdot}0$% $CO_2$, $T_h = 80$°C, Column 2, Fig. 11

| | | | | | |
|---|---|---|---|---|---|
| $c_z$ | 29·0 | 26·8 | 25·6 | 24·8 | 24·3 |
| $\sigma$ | 0·0 | 220 | 480 | 820 | 1120 |

$T_c = 20$°C, $c_0 = 22{\cdot}0$% $CO_2$, $T_h = 270$°C, Column 1, Fig. 12

| | | | | | | |
|---|---|---|---|---|---|---|
| $c_z$ | 26·4 | 25·9 | 25·6 | 25·3 | 25·2 | 25·2 |
| $\sigma$ | 0·0 | 220 | 350 | 510 | 730 | 1120 |

$T_c = 20$°C, $c_0 = 22{\cdot}0$% $CO_2$, $T_h = 320$°C, Column 1, Fig. 12

| | | | | | |
|---|---|---|---|---|---|
| $c_z$ | 27·5 | 26·5 | 26·3 | 26·1 | 26·0 |
| $\sigma$ | 0·0 | 330 | 450 | 620 | 940 |

$T_c = 20$°C, $c_0 = 22{\cdot}0$% $CO_2$, $T_h = 270$°C, Column 3, Fig. 13

| | | | | | | |
|---|---|---|---|---|---|---|
| $c_z$ | 63·5 | 33·5 | 26·0 | 24·2 | 24·0 | 23·6 |
| $\sigma$ | 0·0 | 110 | 170 | 230 | 250 | 400 |

*Table 6. Continuous operation $H_2/CO$. $c$ = % by volume.*

$T_c$ = 20°C, $T_h$ = 320°C, $c_0$ = 15·0% CO, Column 2

| $c_z$ | 30·8 | 28·7 | 27·7 | 27·0 | 25·7 | 24·6 | 23·3 | 22·1 | 21·3 | |
|---|---|---|---|---|---|---|---|---|---|---|
| $\sigma$ | 0·0 | 220 | 360 | 460 | 660 | 860 | 1120 | 1420 | 1700 | |

$T_c$ = 20°C, $T_h$ = 270°C, $c_0$ = 15·0% CO, Column 2

| $c_z$ | 29·1 | 26·4 | 25·3 | 24·6 | 23·7 | 22·9 | 22·4 | 21·9 | 21·1 | 20·0 |
|---|---|---|---|---|---|---|---|---|---|---|
| $\sigma$ | 0·0 | 240 | 360 | 480 | 630 | 786 | 880 | 1000 | 1230 | 1640 |

$T_c$ = 20°C, $T_h$ = 220°C, $c_0$ = 15·0% CO, Column 2

| $c_z$ | 27·0 | 24·7 | 23·7 | 22·5 | 21·2 | 20·6 | 28·2 | 19·2 | 18·8 | 18·7 |
|---|---|---|---|---|---|---|---|---|---|---|
| $\sigma$ | 0·0 | 200 | 330 | 500 | 740 | 880 | 1000 | 1420 | 1700 | 1800 |

$T_c$ = 20°C, $T_h$ = 170°C, $c_0$ = 15·0% CO, Column 2

| $c_z$ | 22·7 | 21·3 | 20·4 | 19·2 | 18·5 | 17·7 | 17·5 | 17·3 | |
|---|---|---|---|---|---|---|---|---|---|
| $\sigma$ | 0·0 | 240 | 400 | 620 | 810 | 1120 | 1260 | 1600 | |

$T_c$ = 20°C, $T_h$ = 270°C, $c_0$ = 15·0% CO, Column 1

| $c_z$ | 18·5 | 17·9 | 17·4 | 17·0 | 16·9 | 16·7 | |
|---|---|---|---|---|---|---|---|
| $\sigma$ | 0·0 | 120 | 200 | 270 | 500 | 1020 | |

$T_c$ = 20°C, $T_h$ = 320°C, $c_0$ = 15·0% CO, Column 1

| $c_z$ | 20·1 | 18·6 | 17·9 | 17·7 | 17·7 | |
|---|---|---|---|---|---|---|
| $\sigma$ | 0·0 | 220 | 400 | 670 | 1200 | |

$T_c$ = 20°C, $T_h$ = 270°C, $c_0$ = 15·0% CO, Column 3

| $c_z$ | 30·6 | 15·8 | 15·7 | 15·7 | 15·7 | |
|---|---|---|---|---|---|---|
| $\sigma$ | 0·0 | 28 | 50 | 100 | 200 | |

$T_c$ = 20°C, $T_h$ = 320°C, $c_0$ = 15·0% CO, Column 3

| $c_z$ | 31·8 | 19·6 | 17·2 | 17·6 | 16·8 | |
|---|---|---|---|---|---|---|
| $\sigma$ | 0·0 | 28 | 45 | 100 | 135 | |

$T_c$ = 20°C, $T_h$ = 375°C, $c_0$ = 15·0% CO, Colum 3

| $c_z$ | 32·7 | 18·8 | 17·6 | 17·2 | |
|---|---|---|---|---|---|
| $\sigma$ | 0·0 | 50 | 100 | 175 | |

*Table 7. Continuous operation $O_2/N_2$*

Column 2 : $T_c$ = 20°C, $T_h$ = 270°C, $c_0$ = 21·0% $O_2$

| $c_z$ | 22·4 | 21·6 | 21·5 | 21·4 | 21·4 | |
|---|---|---|---|---|---|---|
| $\sigma$ | 0·0 | 200 | 250 | 320 | 580 | |

Column 3 : $T_c$ = 20°C, $T_h$ = 320°C, $c_0$ = 21·0% $O_2$

| $c_z$ | 26·6 | 21·2 | 21·1 | 21·1 | |
|---|---|---|---|---|---|
| $\sigma$ | 0·0 | 60 | 100 | 170 | |

*Continuous Operation* $CO/CO_2$

Column 2 : $T_c$ = 20°C, $T_h$ = 270°C, $c_0$ = 32·0% $CO_2$

| $c_z$ | 33·5 | 33·1 | 33·0 | 33·1 | 33·0 | 32·9 | 33·0 | 32·8 | 32·8 |
|---|---|---|---|---|---|---|---|---|---|
| $\sigma$ | 0·0 | 220 | 220 | 260 | 310 | 380 | 440 | 640 | 800 |

Column 3 : $T_c$ = 20°C, $T_h$ = 270°C, $c_0$ = 32·0% $CO_2$

| $c_z$ | 46·2 | 33·8 | 33·0 | 32·6 | 32·6 | |
|---|---|---|---|---|---|---|
| $\sigma$ | 0·0 | 75 | 105 | 200 | 400 | |

*Table 8. Continuous operation $H_2/CO$. 15 ft. column. $T_c = 20°C$. $T_h = 270°C$.*

| | | | | | | | | | |
|---|---|---|---|---|---|---|---|---|---|
| | | | | $c_0 = 5{\cdot}0\%$ CO | | | | | |
| $c_z$ | 7·1 | 7·8 | 9·0 | 13·1 | 15·7 | 16·5 | 35·0 | | |
| $\sigma$ | 6200 | 4300 | 2900 | 1400 | 800 | 700 | 0·0 | | |
| | | | | $c_0 = 7{\cdot}6\%$ CO | | | | | |
| $c_z$ | 11·2 | 13·4 | 16·1 | 16·5 | 18·3 | 20·9 | 22·5 | 48·0 | |
| $\sigma$ | 5300 | 3400 | 2400 | 2360 | 1400 | 1000 | 600 | 0·0 | |
| | | | | $c_0 = 9{\cdot}7\%$ CO | | | | | |
| $c_z$ | 15·9 | 17·7 | 21·7 | 23·5 | 25·8 | 26·4 | 33·3 | 39·4 | 54·7 |
| $\sigma$ | 4600 | 3200 | 2360 | 1500 | 1060 | 900 | 470 | 340 | 0·0 |
| | | | | $c_0 = 14{\cdot}1\%$ CO | | | | | |
| $c_z$ | 18·9 | 22·7 | 28·1 | 31·9 | 34·6 | 41·6 | 41·9 | 61·0 | |
| $\sigma$ | 8000 | 4500 | 2180 | 1700 | 900 | 400 | 180 | 0·0 | |

*Table 9. Power consumption. 6 ft. columns.*

| | |
|---|---|
| | $H_2/CO_2$: $c_0 = 22{\cdot}0\%$ $CO_2$; $T_c = 20°C$; $T_h = 270°C$ |
| Column 1 | 5 amps, 155 volts across the heater, i.e. 775 watts.<br>On the outer pipe surface: 0·12 watt/sq. cm. or 0·775 watt./sq. in. |
| Column 2 | 6·2 amps, 82 volts, i.e. 500 watts. 0·10 watt/sq. cm. or 0·635 watt/sq. in. |
| Column 3 | 620 watts, 0·17 watt/sq. cm. or 1·10 watt/sq. in. |

*Analysis of experimental results*

The results are re-expressed below in suitable units for intrepretation. The values of $D$, the diffusivity for various mixtures at different temperatures were obtained from the semi-empirical equation of GILLILAND [10]. Densities of mixtures were obtained at appropriate mean temperatures, and the arithmetic mean of the concentrations at the ends of the columns were used to establish a mean density. For the sake of simplicity such a procedure was considered adequate at this stage. The viscosities of gas mixtures were taken as being proportional to concentration for the same reason. Over the concentration ranges being considered the errors introduced should be small.

*The values of $K/H$ from experimental data, and a consideration of turbulence in the columns*

From the results of total reflux operation of the columns, it would be useful to determine how the 'ideal separation length' (on the JENSEN basis), or the ratio $K/H$ (on the FURRY basis), is affected by temperature and concentration for any mixture. The theoretical values of $K/H$ and $Re_c$ for the experimental conditions have been evaluated from the following equations, and are given in Table 10 for the separation of a $H_2/CO_2$ mixture in Column 2.

$$\frac{K}{H} = \frac{0{\cdot}84}{\alpha} \cdot \frac{\overline{T}}{\Delta T}\left[\frac{\Delta x^4}{\Delta x_0^3} + 2\frac{\Delta x_0^3}{\Delta x^2}\right] \qquad \text{(JENSEN)}$$

$$\Delta x_0^3 = 425\left[\frac{\eta D}{g\rho}\right]\frac{\overline{T}}{\Delta T} \qquad \text{(JENSEN)}$$

$$Re_c = \frac{w^3 \cdot g \cdot \rho^2}{48 \cdot \eta^2} \cdot \frac{\Delta T}{\overline{T}}$$

In order to obtain the values for $[K/H]_{theor.}$, it is necessary to choose a value for $\alpha$. This is extremely difficult as WALDMAN [11] gives values varying from 0·17 to 0·41, with concentration changes from 0·96 to 0·031 mol. fraction of $CO_2$ in $H_2/CO_2$ mixtures at 20°C. A mean value of $\alpha$ of 0·25 was taken as being reasonable over the concentration range required. WINTER [12] gives values of $\alpha$ at two temperatures, but while it

*Table* 10. *Total reflux or discontinuous operation* $H_2/CO_2$. $c_0 = 22{\cdot}0\%$ $CO_2$, *Column* 2.

| $c_{e\ \text{expt.}}$ | $T_h°C$ | $\Delta T$ | $[K/H]_{\text{expt.}}$ | $[K/H]_{\text{theor.}}$ | $Re_{\text{calc.}}$ |
|---|---|---|---|---|---|
| 29·0 | 80 | 60 | 505 | 570 | 47·4 |
| 31·8 | 120 | 100 | 368 | 492 | 66·5 |
| 35·6 | 195 | 175 | 276 | 386 | 82·5 |
| 39·0 | 220 | 200 | 227 | 329 | 83·5 |
| 41·2 | 270 | 250 | 205 | 287 | 86·0 |

demonstrated that $\alpha$ is temperature dependent, no correlation is possible. NIER [13] obtained a relationship $\alpha \propto T^{-\frac{1}{2}}$ for Neon isotopes at low temperatures. On the basis of present information, it is unsafe to take such a relationship. A plot of $K/H$ versus $\bar{T}/\Delta T$ gives similar curves for the experimental and theoretical case. As to the condition of the convective flow, it would appear that in every case except Column 3, turbulence exists, i.e. $Re_c > 25$. This is shown in Table 11.

*Table* 11. *Total reflux or discontinuous operation.* $H_2/CO_2$. $T_c = 20°C$. $c = \%\ CO_2$.

| *Col. No.* | $c_0$ | $c_{e\ \text{expt.}}$ | $T_h°c$ | $Re_c$ |
|---|---|---|---|---|
| 2 | 22·0 | 29·0 | 80 | 47·4 |
| | – | 31·8 | 120 | 66·5 |
| | – | 35·6 | 195 | 82·8 |
| | – | 39·0 | 220 | 83·5 |
| | – | 41·2 | 270 | 86·0 |
| 1 | 22·0 | 30·0 | 270 | 112·5 |
| 2 | 22·0 | 42·0 | 270 | 88·6 |
| | 40·0 | 60·0 | – | 160·0 |
| | 5·0 | 12·0 | – | 21·0 |
| 3 | 22·0 | 60·0 | 270 | 1·86 |

It will be observed that, despite the fact that convective conditions are turbulent, the experimental values all lie on the appropriate equilibrium curves. This suggests that the separation is not interfered with to the extent which would be expected due to re-mixing. This applies to $Re_c$ values as large as 160. An explanation would be that the temperature gradient is reduced in a central region between the hot and cold walls, due to a higher heat transfer rate in the central turbulent core, so that the existing gradient occurs across a reduced width. A smaller effective annulus width would result in an increased separation, which would then tend to counteract loss of separation due to the re-mixing effects of turbulence.

The results for the total reflux operation with $H_2$/CO mixtures are given in Table 12.

For the 15 ft. column the $N'$ value is reasonably constant at constant temperature over a wide range of concentrations. An interesting feature of the calculations is that, for columns 2 and 3, flow conditions are substantially streamline. It would then be expected that $[K/H]_{\text{expt.}}$ would deviate less from $[K/H]_{\text{theor.}}$ and it should be useful to obtain values of $\alpha$ from the JENSEN expression for $K/H$, but using $[K/H]_{\text{expt.}}$ values. Table 12 summarizes the flow conditions and the $\alpha$ values obtained.

WALDMAN [11] has collected the results of IBBS, GREW and HIRST [14] for $H_2/N_2$. As nitrogen is almost identical with CO in its thermal diffusion effect, these values are of interest for comparison. They are given in Table 13.

$\gamma N_2 = 0{\cdot}20$ and $\alpha = 0{\cdot}33$ from these collected values, whereas from Column 2 (Table 12), $\alpha = 0{\cdot}143$. If the WALDMAN value is correct an assumption of $\alpha = 0{\cdot}33$ for substitution in the JENSEN equation to calculate $[K/H]$ would give $[K/H)$ values different from those obtained experimentally. The $\alpha$ values obtained for the 15 ft. column are of the same order as those quoted by WALDMAN, despite the fact that turbulent conditions exist.

*Table* 12. *Total reflux or discontinuous operation.*

Column 2, $H_2/CO$ ; $c_0 = 15\%$ CO ; $T_c = 20°C$

| $T_h$°C | 120 | 220 | 270 | 320 |
|---|---|---|---|---|
| $c_e$ expt. | 22·7 | 27·0 | 29·1 | 3·08 |
| $[K/H]_{expt.}$ | 360 | 247 | 217 | 198 |
| $N'$ | 0·221 | 0·322 | 0·366 | 0·401 |
| $Re_c$ | 17·9 | 19·1 | 23·5 | 23·8 |
| $\alpha$ | 0·143 | 0·110 | 0·114 | 0·107 |

Column 3 : $H_2/CO$ ; $c_0 = 15\%$ CO ; $T_c = 20°C$

| $T_h$°C | 270 | 320 |
|---|---|---|
| $c_e$ expt. | 30·6 | 31·8 |
| $[K/H]_{expt.}$ | 200 | 190 |
| $N'$ | 0·398 | 0·420 |
| $Re_c$ | 0·46 | – |
| $\alpha$ | 0·358 | 0·360 |

15 ft. Column : $H_2/CO$ ; $T_c = 15°C$ ; $T_h = 215°C$

| $c_0$ | 5·0 | 6·2 | 9·3 | 10·4 | 13·5 | 21·0 |
|---|---|---|---|---|---|---|
| $c_e$ expt. | 35·0 | 43·3 | 53·8 | 54·0 | 60·5 | 67·0 |
| $[K/H]_{expt.}$ | 195 | 187 | 188 | 197 | 202 | 224 |
| $Re_c$ | 39·2 | 50·0 | 61·8 | 67·6 | 79·0 | 96·0 |
| $N'$ | 1·01 | 1·063 | 1·056 | 1·005 | 0·981 | 0·883 |
| $\alpha$ | 0·312 | 0·360 | 0·406 | 0·393 | 0·464 | 0·412 |

*Table* 13. *Collected values for $H_2/N_2$ mixtures.*

| $\gamma N_2$ | 0·025 | 0·05 | 0·075 | 0·15 | 0·25 | 0·35 | 0·55 | 0·65 | 0·75 | 0·85 |
|---|---|---|---|---|---|---|---|---|---|---|
| $\alpha_{20°C}$ | 0·47 | 0·47 | 0·42 | 0·40 | 0·32 | 0·32 | 0·27 | 0·24 | 0·23 | 0·21 |

The conclusions that can be drawn appear to be as follows,

(i) the JENSEN type of equation for $[K/H]$ applies.

(ii) It is impossible to predict with certainty from theoretical equations, the value of $[K/H]$ as $\alpha$ is concentration – and temperature – dependent, and the turbulence has an effect which cannot be correlated by existing equations.

(iii) It is reassuring to find that, with fixed temperature conditions as for the 15 ft. column (Table 12), the $[K/H]$ value remains reasonably constant over a wide range of $Re_c$ values, although it is understood that the factors influencing enrichment must be changing. Hence, it can be assumed that the only values of $[K/H]$ of use for design are those determined experimentally, and which are relative to the conditions of the experiment.

## THE VALUE OF $H$ FROM EXPERIMENTAL DATA

The induction method used for obtaining experimental values of $H$ has been described. The physical data required for calculation of the values were evaluated at the appropriate arithmetic mean concentration relative to each experimental run. The conditions and experimental values of $H$ are given in Table 14.

It should be noted that, in the tables, $\sigma$ the withdrawal rate is given in cc/min as directly measured. For the calculation of $H$ from experimental data, $H = \sigma'/\gamma$, the mass flow $\sigma'$ g/sec, being calculated from the volume flow under the appropriate conditions.

## THE VALUES OF $K$ OBTAINED DIRECTLY FROM THE EXPERIMENTAL DATA

From total reflux or discontinuous operation, values of $[K/H]_{expt.}$ have been obtained for the columns.



VOL. 5 1956

*Table* 14. *Column* 2 $c_0 = 22{\cdot}0\%$ $CO_2$, $\alpha = 0{\cdot}25$.

| | | | | |
|---|---|---|---|---|
| $\bar{T} = 50°C$, $\Delta T = 60$, $[K/H]_{expt.} = 505$, $Re_c = 474$ | | | | |
| $c_z$ | 26·9 | 27·4 | 28·6 | |
| $H_{expt.}$ | 0·00118 | 0·0024 | 0·0024 | |
| $\sigma$ | 210 | 150 | 40 | |
| $\bar{T} = 70°C$, $\Delta T = 100$, $[K/H]_{expt.} = 368$, $Re_c = 66{\cdot}5$ | | | | |
| $c_z$ | 26·9 | 28·85 | 30·60 | |
| $H_{expt.}$ | 0·0033 | 0·0020 | 0·0011 | |
| $\sigma$ | 630 | 250 | 70 | |
| $\bar{T} = 97{\cdot}5°C$, $\Delta T = 155$, $[K/H]_{expt.} = 276$, $Re_c = 82{\cdot}8$ | | | | |
| $c_z$ | 28·85 | 30·90 | 33·10 | 35·18 |
| $H_{expt.}$ | 0·0035 | 0·0030 | 0·0025 | 0·0016 |
| $\sigma$ | 670 | 390 | 160 | 20 |
| $\bar{T} = 120°C$, $\Delta T = 200$, $[K/H]_{expt.} = 227$, $Re_c = 83{\cdot}5$ | | | | |
| $c_z$ | 29·8 | 32·4 | 35·50 | 38·00 |
| $H_{expt.}$ | 0·0046 | 0·0039 | 0·0037 | 0·0043 |
| $\sigma$ | 920 | 520 | 250 | 60 |
| $\bar{T} = 145°C$, $\Delta T = 250$, $[K/H]_{expt.} = 205$, $Re_c = 86{\cdot}0$ | | | | |
| $c_z$ | 29·9 | 33·5 | 36·75 | 39·80 |
| $H_{expt.}$ | 0·0052 | 0·0042 | 0·0050 | 0·0069 |
| $\sigma$ | 1220 | 640 | 350 | 100 |

The values of $H_{expt.}$ are obtained as shown for the same experimental conditions. Hence $K_{expt.}$ values are directly obtainable. These are given below in Table 15.

*Table* 15. *Column* 2, $c_0 = 22{\cdot}0\%$ $CO_2$, $\alpha = 0{\cdot}25$.

| | | | | |
|---|---|---|---|---|
| $\bar{T} = 50°C$, $\Delta T = 60$, $[K/H]_{expt.} = 505$, $Re_c = 474$ | | | | |
| $c_z$ | 26·9 | 27·4 | 28·6 | |
| $K_{expt.}$ | 0·57 | 0·61 | 0·326 | |
| $\sigma$ | 210 | 150 | 40 | |
| $\bar{T} = 70°C$, $\Delta T = 100$, $[K/H]_{expt.} = 368$, $Re_c = 66{\cdot}5$ | | | | |
| $c_z$ | 26·9 | 28·85 | 30·60 | |
| $K_{expt.}$ | 1·225 | 0·728 | 0·408 | |
| $\sigma$ | 630 | 250 | 70 | |
| $\bar{T} = 97{\cdot}5°C$, $\Delta T = 155$, $[K/H]_{expt.} = 276$, $Re_c = 82{\cdot}8$ | | | | |
| $c_z$ | 28·85 | 30·90 | 33·10 | 35·18 |
| $K_{expt.}$ | 0·960 | 0·836 | 0·687 | 0·427 |
| $\sigma$ | 670 | 390 | 160 | 20 |
| $\bar{T} = 120°C$, $\Delta T = 200$ $[K/H]_{expt.} = 227$, $Re_c = 83{\cdot}5$ | | | | |
| $c_z$ | 29·80 | 32·40 | 35·50 | 38·00 |
| $K_{expt.}$ | 1·040 | 0·878 | 0·845 | 1·015 |
| $\sigma$ | 920 | 520 | 250 | 60 |
| $\bar{T} = 145°C$, $\Delta T = 250$, $[K/H]_{expt.} = 205$, $Re_c = 86{\cdot}0$ | | | | |
| $c_z$ | 29·90 | 33·50 | 36·75 | 39·80 |
| $K_{expt.}$ | 1·055 | 0·865 | 0·995 | 1·420 |
| $\sigma$ | 1220 | 640 | 350 | 100 |

### Theoretical Values of $H$

These values have been calculated from the Furry equation for the experimental conditions in Column 2 with $H_2/CO_2$ and $H_2/CO$ mixtures as shown below in Tables 16 and 17.

$$H = \frac{\alpha \cdot \rho^2 \cdot g \cdot w^3 \cdot B}{96\,\eta} \left[\frac{\Delta T}{\bar{T}}\right]^2 \qquad \text{(Furry)}$$

The physical properties of the mixtures such as $\rho$ and $\eta$, were evaluated at the arithmetic mean concentration over the column for experimental conditions.

As $H$ is proportional to $\alpha$, any change in $\alpha$ due to concentration or temperature will be reflected in $H$. From Waldman, it would seem that $\alpha = 0{\cdot}25$ is a good average figure to use over the concentration range of the experimental case for $H_2/CO_2$ mixture. The values of $H_{theor.}$ would then have to be used in the knowledge of its variation with concentration and temperature. The former can be related to $\alpha$ reasonably well, but the temperature effect is not certain.

*Table* 16.

*Column* 2, $c_0 = 22{\cdot}0\%$ $CO_2$, $H_2/CO_2$, $\alpha_{20°C} = 0{\cdot}25$.

| $c_m$ | 26·9 | 27·5 | 28·8 | 30·5 | 31·6 |
|---|---|---|---|---|---|
| $T_h°C$ | 80 | 120 | 175 | 220 | 270 |
| $\Delta T$ | 60 | 100 | 155 | 200 | 250 |
| $H_{theor.} \times 10^4$ | 24 | 54 | 134 | 135 | 174 |

Similar values of $H$ are calculated for Column 2 on $H_2/CO$ mixtures on the basis of $\alpha = 0{\cdot}33$ from Waldman's collected figures. These are recorded in Table 17.

*Table* 17.

*Column* 2, $H_2/CO$, $c_0 = 15{\cdot}0\%$ $CO$, $\alpha_{20°C} = 0{\cdot}33$.

| $c_m$ | 18·85 | 21·0 | 22·05 | 22·90 |
|---|---|---|---|---|
| $T_h°C$ | 120 | 220 | 270 | 320 |
| $\Delta T$ | 100 | 200 | 250 | 300 |
| $H \cdot_{theor.} \times 10^4$ | 19·8 | 49·8 | 56·8 | 71·4 |

*Table* 18. *Total reflux operation. Column* 2 : $H_2/CO_2$ ; $c_0 = 22{\cdot}0\%\ CO_2$.

| | | | | | | | |
|---|---|---|---|---|---|---|---|
| $c_t$ expt. | 29·0 | 31·8 | 34·6 | 39·0 | 41·2 | 60·0 | 12·0 |
| $T_h$°C | 80 | 120 | 195 | 220 | 270 | 270 | 270 |
| $\Delta T$ | 60 | 100 | 175 | 200 | 250 | 250 | 250 |
| $k_c$ | 1·82 | 3·65 | 6·95 | 5·90 | 6·54 | 18·50 | 0·45 |
| $k_d \times 10^4$ | 97 | 105 | 121 | 124 | 184 | 204 | 49 |
| $Re_c$ | 47·4 | 66·5 | 82·8 | 83·5 | 86·0 | 160 | 21 |
| $\frac{Re_c}{[k_c/k_d]^{\frac{1}{2}}}$ | 3·46 | 3·56 | 3·46 | 3·84 | 3·90 | 5·80 | 2·20 |
| $K$ | 1·83 | 3·66 | 6·96 | 5·91 | 6·55 | 18·52 | 0·455 |

THEORETICAL VALUES OF $k_c$, $k_d$ AND $K$

These have been evaluated from the FURRY equations below, using the experimental data on Column 2 for $H_2/CO_2$ and $H_2/CO$ mixtures, under total reflux.

$$k_c = \frac{\rho^3 \cdot g_c^2 \cdot w^7 \cdot B}{2304 \cdot \eta^2 \cdot D}\left[\frac{\Delta T}{T}\right]^2 \qquad \text{(FURRY)}$$

$$k_d = 2 \cdot \pi \cdot B \cdot \rho \cdot D$$

$$K = k_c + k_d \qquad \text{(neglecting } k_p\text{)}$$

The values are given in Tables 18 and 19 below.

*Table* 19. *Total reflux operation* : *Column* 2 : $H_2/CO$ ; $c_0 = 15{\cdot}0\%\ CO$

| | | | | |
|---|---|---|---|---|
| $c_t$ expt. | 22·7 | 27·0 | 29·1 | 30·8 |
| $T_h$°C | 120 | 220 | 270 | 320 |
| $\Delta T$ | 100 | 200 | 250 | 300 |
| $k_c$ | 0·40 | 0·554 | 0·592 | 0·593 |
| $k_d \times 10^4$ | 70 | 100 | 107 | 112 |
| $Re_c$ | 17·9 | 19·1 | 23·5 | 23·8 |
| $\frac{Re_c}{[k_c/k_d]^{\frac{1}{2}}}$ | 2·37 | 2·55 | 3·16 | 3·27 |
| $K$ | 0·407 | 0·564 | 0·593 | 0·593 |

It is seen that $k_c$ the re-mixing effect due to convection is much greater than $k_d$ the longitudinal back-diffusion. For isotopes, FURRY showed that in the streamline range $Re_c/[k_c/k_d]^{\frac{1}{2}}$ is reasonably constant at 2·0. Both $K_c$ and $k_d$ increase with $Re_c$. As given in Table 18, when conditions are streamline $Re_c/[k_c/k_d)^{\frac{1}{2}}$ approaches the value for isotopes. The deviation produced by turbulence is apparent, but there is no attempt at a correlation. Similar conclusions apply to the results in Table 19.

A COMPARISON OF THE EXPERIMENTAL AND CALCULATED VALUES OF $K$ AND $H$

The individual $K$ and $H$ values have been given in the preceding tables. These are now brought together, and their ratios considered in the following Tables 20 and 21 ; in this way a comparison can readily be made.

## DISCUSSION

It will be apparent from Tables 20 and 21, that the values of $H$ and $K$ are affected very considerably by the withdrawal rate $\sigma$. This problem does not occur in the design of columns for isotope separation, as the withdrawal rates are so small, that they do not interfere with the conditions in the annulus to the same extent. The considerable interference evidence with common gases is due to the effect of convective turbulence $Re_c$, and turbulence produced by the mass flow resulting from continuous withdrawal, i.e. $Re$. The convective turbulence $Re_c$, as indicated for the total reflux operation, may not be so adverse in effect, being counter-balanced by an effective reduction in annulus width leading to enrichment. The optimum value of $Re_c$, and its relationship to the critical $Re_c$ of 25, will depend on each case, and has not been ascertained.

Both for $H_2/CO_2$ and $H_2/CO$ there is an increase in $H_{expt.}$ and $K_{expt.}$ with increase in $\sigma$, depending on the $\Delta T$ values. However, no correlation has been attempted.

It is apparent, that in the design of columns for separating common gases, pilot plant information is essential. The values of $H$ and $K$ must be available for the conditions anticipated for full-scale operation. Values of $\alpha$ would have to



VOL. 5 1956

*Table* 20. *Column* 2. $H_2/CO_2$; $c_0 = 22{\cdot}0\%\ CO_2$; $z = 0{\cdot}25$.

| $c_z$ | $H_{\text{expt.}}$ | $H_{\text{theor.}}$ | $\frac{H\text{ theor.}}{H_{\text{expt.}}}$ | $K_{\text{theor.}}$ | $K_{\text{expt.}}$ | $\frac{K\text{ theor.}}{K_{\text{expt.}}}$ | $\alpha$ |
|---|---|---|---|---|---|---|---|
| $\bar{T} = 50°C$, $\Delta T = 60$, $[K/H]_{\text{expt.}} = 505$, $Re_c = 47{\cdot}4$ | | | | | | | |
| 26·9 | 0·00113 | 0·0024 | 2·13 | 1·83 | 0·57 | 3·21 | 210 |
| 27·4 | 0·00121 | 0·0024 | 1·97 | 1·83 | 0·61 | 3·00 | 150 |
| 28·6 | 0·00065 | 0·0024 | 3·70 | 1·83 | 0·326 | 5·61 | 40 |
| $\bar{T} = 70°C$, $\Delta T = 100$, $[K/H]_{\text{expt.}} = 368$, $Re_c = 66{\cdot}5$ | | | | | | | |
| 26·9 | 0·0038 | 0·0054 | 1·64 | 3·66 | 1·225 | 2·98 | 630 |
| 28·85 | 0·0020 | 0·0054 | 2·70 | 3·66 | 0·728 | 5·03 | 250 |
| 30·60 | 0·0011 | 0·0054 | 4·90 | 3·66 | 0·408 | 8·98 | 70 |
| $\bar{T} = 97{\cdot}5°C$, $\Delta T = 155$, $[H/K]_{\text{expt.}} = 276$, $Re_c = 82{\cdot}8$ | | | | | | | |
| 28·85 | 0·0035 | 0·0134 | 3·83 | 6·96 | 0·960 | 7·25 | 670 |
| 30·90 | 0·0030 | 0·0134 | 4·47 | 6·96 | 0·836 | 8·33 | 390 |
| 33·10 | 0·0025 | 0·0134 | 5·36 | 6·96 | 0·687 | 10·10 | 160 |
| 35·18 | 0·0016 | 0·0134 | 8·38 | 6·96 | 0·427 | 16·30 | 20 |
| $\bar{T} = 120°C$, $\Delta T = 200$, $[K/H]_{\text{expt.}} = 227$, $Re_c = 83{\cdot}5$ | | | | | | | |
| 29·80 | 0·0046 | 0·0185 | 2·94 | 5·91 | 1·040 | 5·68 | 920 |
| 32·40 | 0·0039 | 0·0185 | 3·46 | 5·91 | 0·878 | 6·74 | 520 |
| 35·50 | 0·0037 | 0·0185 | 3·65 | 5·91 | 0·845 | 7·00 | 250 |
| 38·00 | 0·0045 | 0·0185 | 3·00 | 5·91 | 1·015 | 5·82 | 60 |
| $\bar{T} = 145°C$, $\Delta T = 250$, $[K/H]_{\text{expt.}} = 205$, $Re_c = 86{\cdot}0$ | | | | | | | |
| 29·90 | 0·0052 | 0·0174 | 3·35 | 6·55 | 1·055 | 6·21 | 1220 |
| 33·50 | 0·0042 | 0·0174 | 4·14 | 6·55 | 0·865 | 7·58 | 640 |
| 36·75 | 0·0050 | 0·0174 | 3·48 | 6·55 | 0·995 | 6·60 | 350 |
| 39·80 | 0·0069 | 0·0174 | 2·52 | 6·55 | 1·420 | 4·60 | 100 |

be available for the mixtures being studied, and the influence of temperature, concentration, and pressure on these values established. It is suggested that the ratios $K_{\text{theor.}}/K_{\text{expt.}}$, and $H_{\text{theor.}}/H_{\text{expt.}}$ for different temperatures, pressures, and columns dimensions, coupled with a knowledge of the flow conditions, such as $Re_c$ and $Re$, could be used for design.

*Table* 21. *Column* 2. $H_2/CO_2$; $c_0 = 15{\cdot}0\%\ CO$.

| $c_z$ | $H_{\text{expt.}}$ | $H_{\text{theor.}}$ | $\frac{H\text{ theor.}}{H_{\text{expt.}}}$ | $K_{\text{theor.}}$ | $K_{\text{theor.}}$ | $\frac{K\text{ theor.}}{K_{\text{expt.}}}$ | $\alpha$ |
|---|---|---|---|---|---|---|---|
| $\bar{T} = 70°C$, $\Delta T = 100$, $[K/H]_{\text{expt.}} = 360$, $Re_c = 17{\cdot}9$ | | | | | | | |
| 20·45 | 0·00156 | 0·00198 | 1·27 | 0·407 | 0·560 | 0·725 | 380 |
| 21·85 | 0·00115 | 0·00198 | 1·72 | 0·407 | 0·414 | 0·984 | 140 |
| $\bar{T} = 120°C$, $\Delta T = 200$, $[K/H]_{\text{expt.}} = 247$, $Re_c = 19{\cdot}1$ | | | | | | | |
| 22·4 | 0·0021 | 0·00198 | 2·38 | 0·407 | 0·518 | 1·09 | 540 |
| 24·85 | 0·00146 | 0·00198 | 3·41 | 0·407 | 0·360 | 1·57 | 190 |
| $\bar{T} = 145°C$, $\Delta T = 250$, $[K/H]_{\text{expt.}} = 217$, $Re_c = 23{\cdot}5$ | | | | | | | |
| 22·05 | 0·00294 | 0·00198 | 1·93 | 0·407 | 0·636 | 0·93 | 780 |
| 26·00 | 0·00196 | 0·00198 | 2·90 | 0·407 | 0·425 | 1·42 | 260 |
| 28·85 | 0·00075 | 0·00198 | 7·58 | 0·407 | 0·168 | 3·70 | 20 |

*Comments on the operation of Columns* 1 *and* 3

According to FURRY

$$H \propto w^3 \cdot B \quad k_c \propto w^7 \cdot B \quad k_d \propto w \cdot B$$

It is evident from these relationships that, for design, a compromise must be arrived at which will give a reasonable transport and enrichment.

Column 1 has a large annulus, and consequently gives high transport and low separation. This was demonstrated.

Column 3 has a small annulus, and the reverse effect is true.

Column 2 was taken as the compromise.

Column 3 is of greater interest than Column 1, as it gives high enrichment. From the results for the total reflux operation of Column 3, the gas mixture being $H_2/CO_2$ (Table 2), it can be shown that $Re = 1{\cdot}86$, $k_c = 0{\cdot}00063$, and $k_d = 0{\cdot}00315$. In this case, streamline conditions exist, and unlike the other columns, back-diffusion is greater than convective re-mixing. The asymmetrical term $k_p$ could not be calculated as the peripheral temperature variation of the inner tube could not be measured. The inner tube was centralized. The conditions could have been improved if a copper instead of a stainless steel inner tube had been used. The value of $k_p$ must have been appreciable in this case, as an enrichment up to 93·0% of $CO_2$ in $H_2$ at equilibrium was obtained, whereas according to the other conditions, a near 100% separation should have been possible.

To this effect of $k_p$ in column 3, would be added the effect of withdrawal rate, which would have a disastrous effect on the separation. Such columns could therefore be used only under carefully controlled conditions, and in a cascade system.

## CONCLUSIONS

(i) The hydrodynamic equations, for discontinuous operation of thermal diffusion columns, as deduced for isotopes, apply to common gases.

(ii) The adverse re-mixing effect of convective turbulence in the annulus is masked by what is probably a reduction in effective annulus width, resulting in increased separation which offsets loss of enrichment due to re-mixing.

(iii) There is a lack of reliable information on the large effects of concentration and temperature on $\alpha$ values for various mixtures of common gases. This makes design of columns from first principles unreliable.

(iv) From the results of continuous operation, it has been demonstrated that the values of $H$ and $K$ are dependent on withdrawal rates to such an extent that the theoretical approach to design as used for isotope separation is unreliable.

(v) Pilot-plant data are essential for mixtures of different gases to obtain column dimensions and optimum flow conditions for any desired separation.

## NOTATION

$L$ = heated length of column
$\frac{1}{2}A$ or $K/H$ = ideal separation length
$B$ = mean circumference of concentric tubes
$2w$ = annulus width
$c_0$ = initial concentration of heavy componen
$c_2$ = final concentration of heavy component
$c$ = intermediate concentrations
$c_e$ = equilibrium concentration of heavy component
$D_{1,2}$ = coefficient of natural diffusion
$D_T$ = coefficient of thermal diffusion (true)
$k_T$ = thermal diffusion coefficient
$\alpha$ = thermal diffusion constant
$\tau$ = net differential transport
$H$ = transport coefficient
Remixing coefficients
$k_c$ = convective
$k_d$ = back-diffusion
$k_p$ = asymmetrical
$K$ = total
$N$ = number of ideal separation lengths in height $L$
$N' = N/2{\cdot}303$
$Re_c$ = Reynold's Number (convective)
$Re$ = Reynold's Number of mass flow due to withdrawal
$T_c°K$ = temperature of the cold wall
$T_h°K$ = temperature of the hot wall
$\bar{T}°K$ = arithmetic mean temperature across annulus
$\rho$ = gas density
$\eta$ = gas viscosity
$\sigma$ = withdrawal rate, ccs/min
$\sigma'$ = withdrawal rate, grs/sec
$n = \sigma'/H$ = column factor
$\Delta r_0$ = column factor (vide JENSEN [3] for definition
$g$ = acceleration of gravity

## References


[1] Chapman ; *Proc. Roy. Soc.*, A, 1917, **93**, 1 ; *The Mathematical Theory of Nonuniform Gases*, 1939, Cambridge University Press.

[2] Enskog ; *Diss. Upsala*, 1917 ; *Philos. Mag. J. Sci.*, 1929 **7** 1.

[3] Ibbs ; *Proc. Roy. Soc.* 1921, **A 99** 385 ; *Proc. Roy. Soc.* A 1923 **107** 470

[4] Clusius and Dickel ; *Z. Phys. Chem.* 1940 **44** 397.

[5] Jensen ; *Angew. Chemie.* 1941 **54** 27-88.

[6] Steinwedel ; *Die Chemie* 1942 **55** 152.

[7] Wadlmann ; *Z. Phys.* 1939 **114** 53.

[8] Furry, Onsager and Jones ; *Phys. Rev.* 1939 **55** 1083.

[9] Jones and Furry ; *Reviews of Modern Physics*, 1946 **18**, No. 2, 151.

[10] Gilliland ; *Ind. Eng. Chem.* 1934 **26** 516.

[11] Waldmann ; *Naturwissenschaften* 1943 **31** 204 and 1944 **32** 223.

[12] Winter ; *Trans. Faraday Soc.* 1949 **45** 1091 and 1950 **46** 80.

[13] Nier ; *Phys. Rev.* 1939 **56** 1009 and 1940 **57** 30.

[14] Ibbs, Grew and Hirst ; *Proc. Roy. Soc.* 1929 **41** 456.

Chemical Engineering Science, 1956, Vol. 5, pp. 50 to 58. Pergamon Press Ltd.

# Heat transfer to boiling water-methylethylketone mixtures

A. S. Vos and S. J. D. van Stralen

Laboratory of Physics and Meteorology, Agricultural University, Wageningen, The Netherlands

**Abstract**—An apparatus has been designed for determination of heat transfer to boiling mixtures of water-methylethylketone under atmospheric pressure, using the central portion of a horizontal platinum heating wire at the same time as a resistance thermometer, according to the method of McAdams [5].

A hysteresis effect observed in mixtures containing an excess of methylethylketone was avoided by keeping the annealed wire immersed in the liquid for a sufficiently long time at room temperature. The reference value of the resistance thermometer was aso measured with immersed wire at the boiling temperature of the liquid.

The entire region of heat transfer up to the maximum of nucleate boiling was measured for some mixtures including the pure components (0, 4·2, 20, 52, 88·5, and 100% wt of methylethylketone). With increasing concentration of methylethylketone a gradual shift of the curves to lower heat transfer occurred, except for the 4·2% and 20% mixtures, where a noticeably high maximum heat flux of 2·5 and 2·0 times that of water was found. Since it was also observed with heating wires of different metals and alloys, this peculiar behaviour can be considered to be a characteristic property of the liquid mixtures themselves.

**Résumé**—Pour déterminer le coefficient de transmission thermique des mélanges d'eau et de méthyl-ethyl-cétone bouillant sous la pression atmosphérique, les auteurs ont conçu un appareil utilisant la partie centrale horizontale d'un fil de platine servant d'élément chauffant ainsi que de thermomètre à résistance selon la méthode de McAdams.

Ils ont évité l'hystéresis, observée pour les mélanges contenant un excès de methyl ethyl cétone en immergeant le fil recuit dans le liquide pendant un temps suffisant à la température ambiante.

De même, ils ont pris comme résistance de référence, celle du fil immergé dans le liquide bouillant. Pour des mélanges de composants purs (0, 4.2, 20, 52, 88.5 et 100% de methyl éthyl cétone), ils ont mesué les diverses valeurs du transfert jusqu'au maximum " nucleate boiling."

Pour une augmentation de la concentration de m.e.c., il se produit un déplacement graduel des courbes vers un transfert plus petit, excepté pour les mélanges à 4,2 et 20% pour lesquels il y a un maximum notable du flux de chaleur, 2,5 et 2 fois celui de l'eau. Puisque ce comportement particulier a été observé avec d'autres fils chauffants, en métaux et alliages divers, il s'agit bien d'une propriété caractéristique des mélanges liquides eux-mêmes.

## Method and Apparatus

The rate of heat flow $q$ from a heated wire to a boiling liquid is a function of $\Theta = t - T$, the difference in temperature between the heating surface and the bulk liquid :

$$q = q(\Theta) \tag{1}$$

The method described by McAdams [5] has in principle been used to determine the heat transfer curves (1) for mixtures of water and methylethylketone of different composition under atmospheric pressure. A horizontal platinum wire (of diameter $D$) was provided with thin potential leads, and thereby the central portion of the wire could be used as a heating surface and at the same time as a resistance thermometer.

The heat flux $\frac{q}{A}$ and the temperature difference $\Theta$ were directly calculated from measurements of the potential drop $E$ across the test section, which had a length $L$, and of the current $I$, since the specific resistance of platinum is known as a function of temperature [1]. For these measurements D.C. was used. One has :

$$\frac{q}{A}\,(\text{cal sec}^{-1}\,\text{cm}^{-2}) = 0{\cdot}07604\,\frac{EI}{LD}$$

(volts amperes $\text{cm}^{-2}$), and (2)

$$\Theta = \psi(T) \left(\frac{E}{IR_T} - 1\right) \qquad (3)$$

Here $A$ denotes the area of the test section, $R_T$ the resistance of that section at the boiling temperature of the liquid in ohms, and $\psi(T)$ a multiplication factor which for small or moderate temperature differences (i.e. in the ranges of convection and nucleate boiling) is found to be equal to :

$$\psi(T) = \frac{1 + BT - CT^2}{B - 2CT} \qquad (4)$$

Physically pure (99·99%) platinum wires, obtained from Drijfhout's Edelmetaalbedrijven, Amsterdam, have been used, for which $B$ is taken as $3{\cdot}9788 \times 10^{-3}$, and $C$ is taken as $5{\cdot}88 \times 10^{-7}$ if $T$ is expressed in degrees centigrade. The diameter of the heating wires was 0·020 and of the potential leads 0·005 cm.

The chemically pure methylethylketone (M.E.K.) was obtained from Brocades-Stheeman & Pharmacia, Meppel, and distilled water was used. The important data pertaining to these mixtures were taken from literature [4], i.e.

B.P. of methylethylketone : 79·56°C.
Region of demixing : from 18·2 to 84·3% wt of M.E.K.
B.P. in the region of demixing : 73·62°C.
Composition of azeotrope : 88·6% wt of M.E.K.
B.P. of azeotropic composition : 73·56°C.

The test section of the heating wire was connected in series with a constant resistance of manganine. The potential drop across this resistance was directly proportional to the heating current. This voltage and that across the test section were recorded on a synchro-printing 12-record fast speed Brown ElectroniK potentiometer, with scale range from − 0·5 to 2·5 mV, after reduction to suitable values by application of tapped shunts. The reference value $R_T$ was determined by passing a small current through the circuit while the wire was immersed in the boiling liquid. An anticorrosion circuit [5] was used by keeping the base of the boiling vessel at a tension 2 V lower than the negative end of the wire.

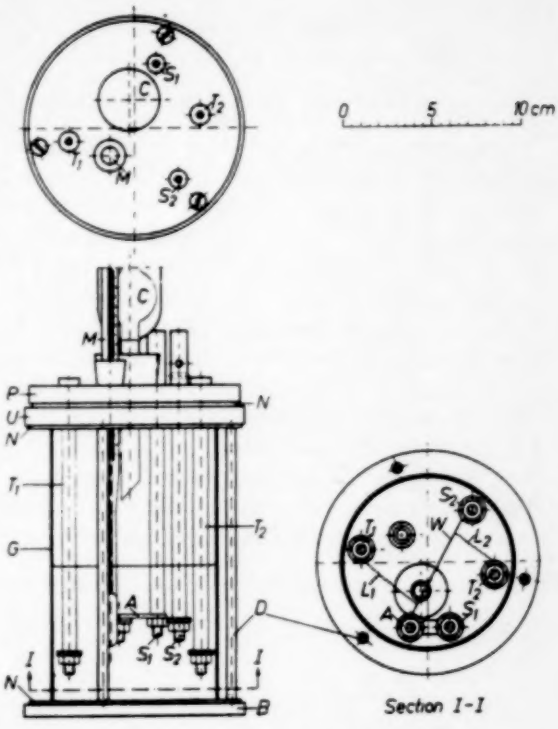


FIG. 1. Diagram of boiling vessel.
A = revolving arm ; B = nickel coated brass base ; C = total reflux condenser ; D = draw bars ; G = glass cylinder ; M = calibrated thermometer ; N = neoprene packing ; $L_1$ and $L_2$ = potential leads ; P = pertinax cover ; $S_1$, $S_2$, $T_1$ and $T_2$ = nickel coated brass bars ; W = heating wire.

The boiling vessel (Fig. 1) consisted of a glass cylinder with ground endfaces. A nickel-coated brass cover ring and base were fastened by draw bars to the glass cylinder, and neoprene rings were used for packing. A pertinax cover was provided with four nickel-plated brass bars. One of the bars was fitted with a revolving arm, which made it possible to use wires of various length. The wire was stretched between this arm and the opposite bar, while the potential leads were attached to the other bars. A total reflux condenser was mounted on the cover plate, and the boiling vessel was only half filled with the mixture. The liquid was then heated from below by a Bunsen flame until gentle boiling took place. This insured a uniform temperature throughout the liquid.

## Results with Platinum Heating Wires

A curve giving heat flux $\frac{q}{A}$ as a function of temperature difference $\theta$ was determined by successively increasing the heating current, starting with a low value of $I$, as well as by decreasing the current starting with a high value of $I$. Two different curves were obtained, especially with mixtures in which the concentration of M.E.K. was high (Fig. 2 – curve 2). This hysteresis effect was, however, removed (curve 3) when the wire, after annealing, was kept immersed in the liquid at room temperature for a sufficiently long period $\tau$ (for which 18 h was taken), before the observations were made. This procedure was adopted in all further experiments, even in case of pure water (curve 1).

Figs. 3 and 4 show heat flux $\frac{q}{A}$, and coefficient of heat transfer $h = \frac{q}{A\theta}$ respectively, as functions of temperature difference $\theta$. With the same wire, which had a length $L = 4{\cdot}88$ and a diameter $D = 0{\cdot}0198$ cm, we successively determined the curves for : (a) water, (b) M.E.K. (3 ×), (c) water, (d) the azeotropic mixture containing 88·5% wt of M.E.K. (3 ×), and (e) a mixture containing 52% wt of M.E.K. The heating wire burned out after these determinations. and the mixtures (g) and (h), containing 20% and 4·2% wt of M.E.K. respectively, were investigated, using other heating wires.

In the cases (a) to (d) inclusive, increasing current was first applied, and the current was reduced before the maximum heat transfer in nucleate boiling was reached. After these measurements, an entire curve was determined for increasing current only, until maximum nucleate heat transfer was obtained. Since the

VOL. 5 1956

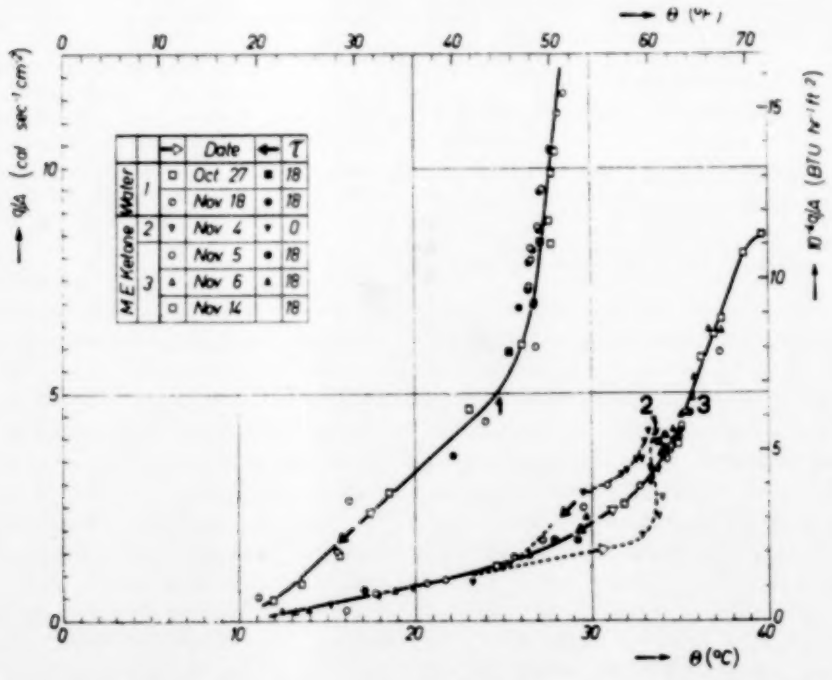


Fig. 2. Effect of immersion of platinum wire on heat transfer for convection and nucleate boiling to water and to methylethylketone.

The curves represent heat flux as a function of temperature difference between heating surface and liquid.

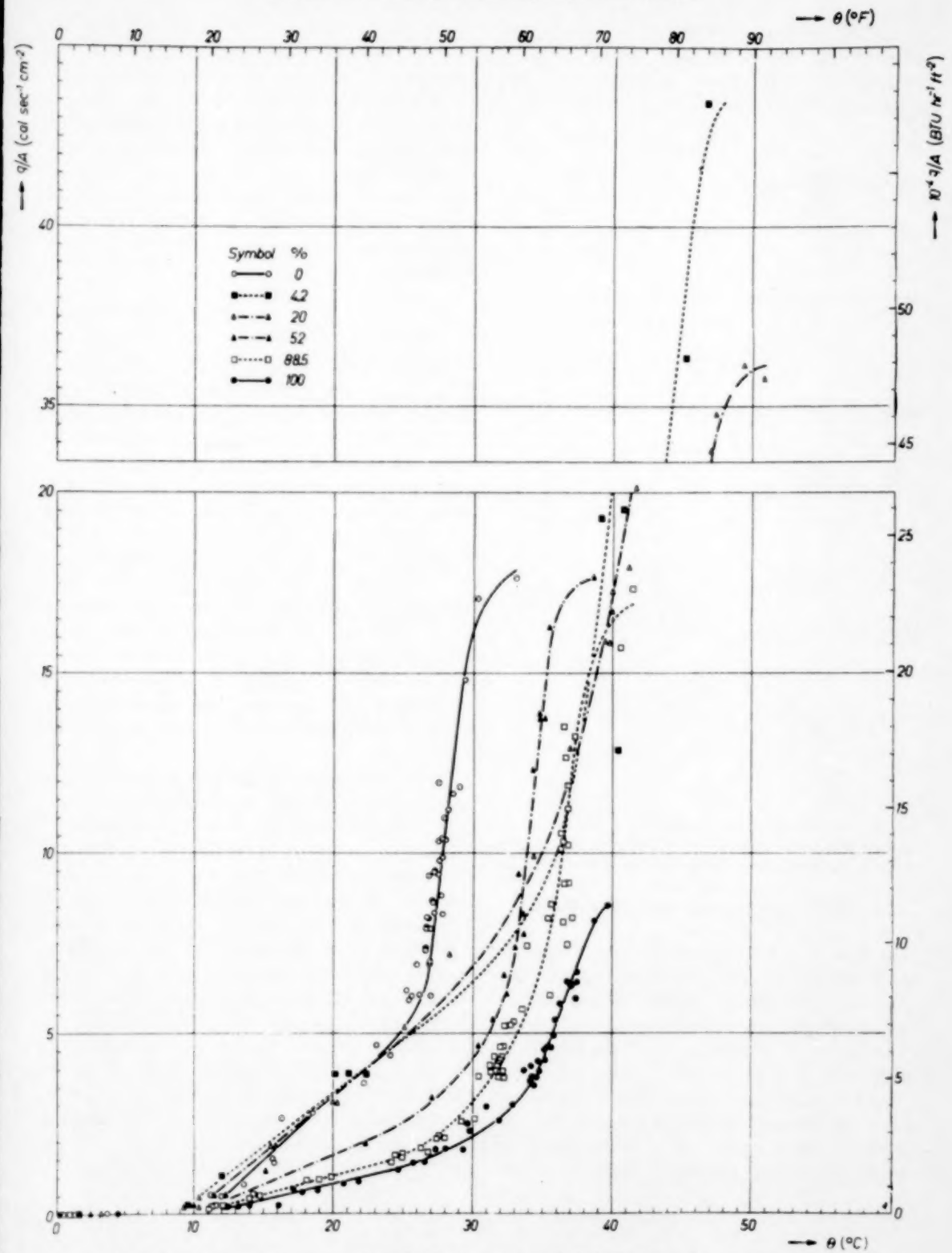


Fig. 3. Heat flux for convection and nucleate boiling to water-methylethylketone mixtures as a function of temperature difference between heating surface and liquid. % denotes % wt of M.E.K.

results obtained with increasing and decreasing current were found to tally satisfactorily, a determination with increasing current only was made in the experiments (e), (g) and (h).

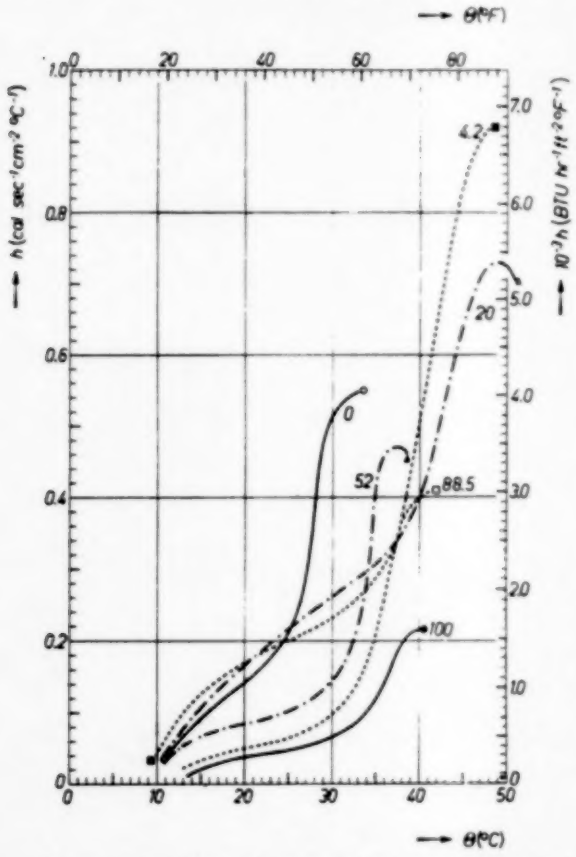


FIG. 4. Coefficient of heat transfer for convection and nucleate boiling to water-methylethylketone mixtures as a function of temperature difference between heating surface and liquid.
The figures at the curves denote % wt of M.E.K.

In Figs. 2 and 3, all curves show a region in which convection seems to be rather inefficient (" micro "-convection). Similar phenomena have been described by other investigators [3; 6; 7]. At a temperature difference $\theta$ of about 10°C a stronger convection sets in.

A gradual decrease of heat transfer occurs with increasing concentration of M.E.K., if this concentration exceeds 52% wt. The nucleate boiling maxima of heat flux and of coefficient of heat transfer in the 52% and 88·5% wt of M.E.K. do not exceed the corresponding value in water. On the contrary, however, in the 4·2% and 20% wt of M.E.K., the maxima exceed the value in water by not less than 150% and 100% in heat flux, and 70% and 35% in coefficient of heat transfer, respectively. It may be useful to observe that, for these mixtures, the size of vapour bubbles leaving the heating surface is definitely smaller than for the other compositions investigated.

## Results with Heating Wires of Different Metals and Alloys

With the object of ascertaining that the peculiar behaviour of the heat transfer in the 4·2% and 20% mixtures is really a property of the liquid mixture itself, and not a property of the special combination of heating surface and mixture, wires consisting of other metals have been used. These investigations have been carried out with A.C. and the maximum heat flux in the region of nucleate boiling only has been determined.

The results are shown in Fig. 5. For these experiments, 20% and 28% wt of M.E.K. were used. The ratio of the maximum heat flux in these mixtures to that in water is also shown (Fig. 5 – curves 1 to 10). An increase similar to that with platinum wires was observed in all cases, although the numerical value of the ratio varied.

With a nichrome V (80 Ni ; 20 Cr) wire of a diameter $D = 0{\cdot}08$ cm, which had been oxidized in air, the very high heat flux of 75 cal $sec^{-1}$ $cm^{-2}$ in case of a 4·2% wt of M.E.K. was found. The maximum heat transfer to water was also considerably higher than with the other wires used, viz. 40 cal $sec^{-1}$ $cm^{-2}$ (Fig. 5 – curve 11). Farber and Scorah [2] determined the heat transfer to boiling water with wires of a diameter of 0·1 cm, which were oxidized at red heat in boiling water. They found maxima of 47 cal $sec^{-1}$ $cm^{-2}$ for chromel A (80 Ni ; 20 Cr), and an average of 72 cal $sec^{-1}$ $cm^{-2}$ for chromel C (57 Ni ; 14-18 Cr ; 23-28 Fe) respectively, at atmospheric pressure. Unfortunately chromel C was not at our disposal, but it seems not unreasonable to expect that the 4·2% mixture would show a still considerably

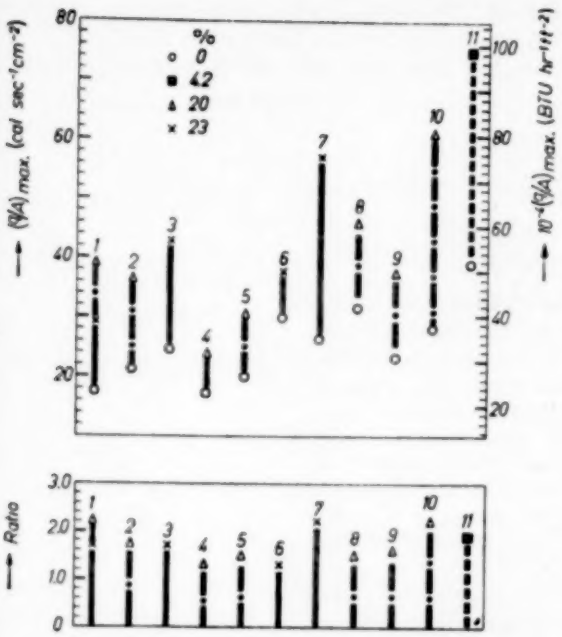


FIG. 5. Maximum heat flux for nucleate boiling of different wires to 4·2%, 20% and 23% wt of methylethylketone mixtures in comparison with maximum heat flux to water. 1. Pt (D = 0·02 cm); 2. Ag (0·02); 3. Cu (0·025); 4. Ni (0·02); 5. oxidized Ni (0·02); 6. Fe (0·025); 7. W (0·041); 8. constantan (0·02); 9. nichrome V (0·02); 10. oxidized nichrome V (0·02); 11. oxidized nichrome V (0·08).

higher maximum heat flux with this oxidized alloy.

From the results obtained with different heating wires, it is concluded that high maximum heat transfer in nucleate boiling occurring in certain mixtures of water and methylethylketone is a characteristic property of the mixtures themselves. The question whether for mixtures in general an increase of the maximum nucleate boiling heat flux as compared with the pure components must be expected, and at which concentration this should occur, will be considered in a subsequent publication [8].

**Acknowledgement**—The cooperation of one of the authors (VAN STRALEN) was made possible by a stipendium from the "Marshall-gelden ten behoeve van de Landbouwhogeschool."

Some preliminary investigations were carried out by Mr. L. VAN DEN BERG, who received financial support from the "Stichting voor Fundamenteel Onderzoek der Materie" (F.O.M.) and the "Organisatie voor Zuiver Wetenschappelijk Onderzoek" (Z.W.O.).

## NOTATION

$A$ = Area of surface of test section, cm²
$B, C$ = Constants in temperature equation, °C⁻¹, °C⁻²
$D$ = Diameter of test section, cm
$E$ = Potential drop across test section, V
$h = \frac{q}{A\theta}$ = Coefficient of heat transfer in test section, cal sec⁻¹ cm⁻² °C⁻¹
$I$ = Electrical current strength through test section, A
$L$ = Length of test section, cm
$q$ = Heat transfer rate in test section, cal sec⁻¹
$\frac{q}{A}$ = Heat flux in test section, cal sec⁻¹ cm⁻²
$R_T$ = Electrical resistance of test section at boiling temperature of liquid, Ω
$t$ = Temperature of test section, °C
$T$ = Boiling point of liquid at atmospheric pressure, °C
$\theta = t - T$ = Temperature difference between test section and boiling liquid, °C
$\psi(T)$ = Multiplication factor in temperature difference equation, °C
$\tau$ = Time of immersion of wire in liquid at room temperature, h

## REFERENCES

[1] BURGESS, G. K. and CHATELIER, H. LE; *The Measurement of High Temperatures*. John Wiley & Sons, New York, 3rd ed., 1912, 197, 493-495.

[2] FARBER, E. A. and SCORAH, R. L.; Heat transfer to water boiling under pressure. *Trans. Amer. Inst. Mech. Eng.* 1948 **70** 369-384.

[3] GRAAF, J. G. A. DE, and HELD, E. F. M. VAN DER; The relation between the heat transfer and the convection phenomena in enclosed plane air layers, *Appl. Sci. Res.* 1953 **A3** 393-409.

[4] MARSHALL, A.; The vapour pressures of binary mixtures, *J. Chem. Soc.* 1906 **90** 1350-1386.

[5] MCADAMS, W. H., ADDOMS, J. N., RINALDO, P. M. and DAY, R. S.; Heat transfer from single horizontal wires to boiling water, *Chem. Eng. Progr.* 1948 **44** 639-646.

[6] Saunders, O. A. and Fishenden, M.; loc. cit. McAdams, W. H.: *Heat Transmission*, McGraw-Hill, New York, 2nd ed., 1942, 239-240.

[7] Sutton, O. G.; On the stability of the fluid heated from below, *Proc. Roy. Soc.* 1951 **A204** 297-309.

[8] Wijk, W. R. van, Vos, A. S. and Stralen, S. J. D. van; Heat transfer to boiling binary liquid mixtures, *Chem. Eng. Sci.* to be published.

## Book review

**Ullmanns Encyklopaedie der Technischen Chemie** (3rd Edition), Vol. 5, 854 pp. 237 illustrations. DM 108 £9 9s. 0d. (18 vols.). Urban & Schwarzenberg, Munich.

The volumes of this monumental third edition of *Ullmann's Encyclopaedia* are being published in quick succession. So far the first volume of the general introduction to chemical engineering has appeared (the second volume is eagerly awaited), as well as three of the ten volumes which cover, in alphabetical arrangement, the whole field of applied chemistry including its theoretical foundations.

The approach, in this volume which ranges from calcium carbide to di-isosyanate, is as comprehensive and lucid as in the previous volumes. References to pertinent literature and patents have been included up to 1953. The uniformly high standard of accuracy and modernity is remarkable, and the treatment seems to the reviewer free from any noticeable blemishes or errors. For those with sufficient knowledge of German this encyclopaedia is of great value.

J.H.

## Announcement

### CHEMICAL ENGINEERING CONFERENCE

An International Conference with the theme "Chemical Engineering in the Coal Industry" is being sponsored this summer by the National Coal Board. It will be held from 26th to 29th June, 1956, at the new laboratories of the Board's Coal Research Establishment at Stoke Orchard, near Cheltenham, Gloucestershire.

The Conference will comprise four technical sessions: "The Physical and Chemical Pre-treatment of Coal," "Fluid Bed Carbonisation," "Briquette Carbonisation" and "Liquid By-Products." Delegates will receive and discuss seven papers given by English, French, German Dutch and American scientists and chemical engineers which will deal with the fundamentals and with the practical aspects of these subjects. English, French and German will be the working languages of the Conference.